AD 273338

ASD TR 7-888(II)

ASD INTERIM REPORT 7-888(II)
December 1961

ERRATA-28 May 1962

The following corrections are to be made in ASD Interim Report 7-888(II), entitled Development of Ultrasonic Welding Equipment for Refractory Metals, and dated December 1961. The Report covers work done in ASD Project No. 7-888 under Contract AF 33(600)-43026 for the Fabrication Branch, Manufacturing Technology Laboratory, AFSC, Aeronautical Systems Division, United States Air Force, Wright-Patterson Air Force Base, Ohio.

Page 29

In Table 6, under "Surface Preparation", opposite Inconel X-750 and René 41, "at %" should be changed to read "wt %".

Page 40

The picture below should be substituted for that of Figure 6A.

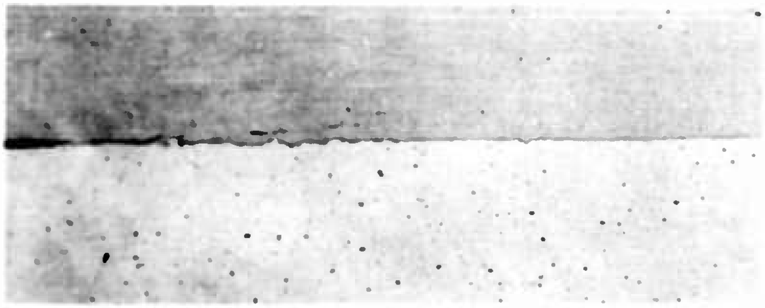

Page 41

Captions for Figures 6G and 6H should be inverted to read, respectively:

"G. Mo-0.5 Ti (0.032-inch)
Cb(D-31) (0.025-inch)"

"H. Inconel X-750 (0.040-inch)
Mo.-0.5 Ti (0.032-inch)"

ASD TR 7-888(II)

ASD INTERIM REPORT 7-888(II)
December 1961

ERRATA-28 May 1962

(Concluded)

Page 60

Beginning with "Dr. Robert E. Maringer," Lines 2 and 3 of Paragraph 2 should be changed to read:

> . . ."Dr. Robert E. Maringer, Battelle Memorial Institute, Professor B. J. Lazan, Head (etc.) . . ."

Page 92

In the third sentence under the column stub "Fabrication" in row "Type 4," the word "Life" should be substituted for the work "Piece," so as to read: "Life is slightly longer than types 2 and 3."

Under "Fabrication" in the second sentence in row "Type 6," the word "center" should be inserted between "stressed" and "disk," so as to read: "Highly stressed center disk area eliminated."

* * * * *

ASD TR 7-888(II)

ASD INTERIM REPORT 7-888(II)
December 1961

Development of ULTRASONIC WELDING EQUIPMENT for REFRACTORY METALS

J. Byron Jones
Nicholas Maropis
Carmine F. DePrisco
John G. Thomas
Janet Devine

AEROPROJECTS INCORPORATED
West Chester, Pennsylvania

Contract: AF 33(600)-43026
ASD Project No. 7-888

Interim Technical Progress Report
1 June 1961 to 15 December 1961

The previously demonstrated feasibility of ultrasonically welding thin sheets of Cb(D-31), Inconel X-750, Mo-0.5Ti, PH15-7Mo, René 41 and tungsten was extended to heavier gages of these materials. Measurements of the acoustical energy required to join these materials confirm values previously estimated by an equation devised during the course of earlier fundamental research. Salient problems associated with high power ultrasonic transducer-coupling systems for welding machines were considered and solutions to such problems were formulated. Thus, the ultrasonic welding of both mono- and bi-metal combinations in gages up to 0.10 inch is considered feasible and the development of the requisite equipment can be accomplished in a reasonable length of time.

FABRICATION BRANCH
MANUFACTURING TECHNOLOGY LABORATORY

AFSC Aeronautical Systems Division
United States Air Force
Wright-Patterson Air Force Base, Ohio

NOTICES

extended to heavier gages of these materials. Measurements of the acoustical energy required to join these materials confirm values previously estimated by an equation devised during the course of earlier fundamental research work. Salient problems associated with high power ultrasonic transducer-coupling systems for welding machines were considered and solutions to such problems were formulated. Thus, the ultrasonic welding of both mono- and bi-metal combinations in gages up to 0.10 inch is considered feasible and the development of the requisite equipment can be accomplished in a reasonable length of time.		extended to heavier gages of these materials. Measurements of the acoustical energy required to join these materials confirm values previously estimated by an equation devised during the course of earlier fundamental research work. Salient problems associated with high power ultrasonic transducer-coupling systems for welding machines were considered and solutions to such problems were formulated. Thus, the ultrasonic welding of both mono- and bi-metal combinations in gages up to 0.10 inch is considered feasible and the development of the requisite equipment can be accomplished in a reasonable length of time.	
extended to heavier gages of these materials. Measurements of the acoustical energy required to join these materials confirm values previously estimated by an equation devised during the course of earlier fundamental research work. Salient problems associated with high power ultrasonic transducer-coupling systems for welding machines were considered and solutions to such problems were formulated. Thus, the ultrasonic welding of both mono- and bi-metal combinations in gages up to 0.10 inch is considered feasible and the development of the requisite equipment can be accomplished in a reasonable lenght of time.		extended to heavier gages of these materials. Measurements of the acoustical energy required to join these materials confirm values previously estimated by an equation devised during the course of earlier fundamental research work. Salient problems associated with high power ultrasonic transducer-coupling systems for welding machines were considered and solutions to such problems were formulated. Thus, the ultrasonic welding of both mono- and bi-metal combinations in gages up to 0.10 inch is considered feasible and the development of the requisite equipment can be accomplished in a reasonable length of time.	

AD
Aeroprojects Incorporated, West Chester, Pa.
DEVELOPMENT OF ULTRASONIC WELDING EQUIPMENT FOR REFRACTORY METALS, by J. B. Jones et al. December 1961. 180p. incl. illus. tables. (ASD Project 7-888) ASD TR-7-888(II)) (Contract AF33(600)-43026)
Unclassified report

The previously demonstrated feasibility of ultrasonically welding thin sheets of Cb(D-31), Inconel X-750, Mo-0.5Ti, PH15-7Mo, René 41 and tungsten was
(over)

UNCLASSIFIED

1. Materials Processing
2. Welding
3. Metals
I. Jones, J. B.
II. Aeroprojects Incorporated
III. Contract AF33(600)-43026
IV. ASD Project 7-888
V. Fabrication Branch

UNCLASSIFIED

AD
Aeroprojects Incorporated, West Chester, Pa.
DEVELOPMENT OF ULTRASONIC WELDING EQUIPMENT FOR REFRACTORY METALS, by J. B. Jones et al. December 1961. 180p. incl. illus. tables. (ASD Project 7-888) (ASD TR-7-888(II)) (Contract AF33(600)-43026)
Unclassified report

The previously demonstrated feasibility of ultrasonically welding thin sheets of Cb(D-31), Inconel X-750, Mo-0.5Ti, PH15-7Mo, René 41 and tungsten was
(over)

UNCLASSIFIED

1. Materials-Processing
2. Welding
3. Metals
I. Jones, J. B.
II. Aeroprojects Incorporated
III. Contract AF33(600)-43026
IV. ASD Project 7-888
V. Fabrication Branch

UNCLASSIFIED

AD
Aeroprojects Incorporated, West Chester, Pa.
DEVELOPMENT OF ULTRASONIC WELDING EQUIPMENT FOR REFRACTORY METALS, by J. B. Jones et al. December 1961. 180p. incl. illus. tables. (ASD Project 7-888) (ASD TR-7-888(II)) (Contract AF33(600)-43026)
Unclassified report

The previously demonstrated feasibility of ultrasonically welding thin sheets of Cb(D-31), Inconel X-750, Mo-0.5Ti, Ph15-7Mo, René 41 and tungsten was
(over)

UNCLASSIFIED

1. Materials Processing
2. Welding
3. Metals
I. Jones, J. B.
II. Aeroprojects Incorporated
III. Contract AF33(600)-43026
IV. ASD Project 7-888
V. Fabrication Branch

UNCLASSIFIED

AD
Aeroprojects Incorporated, West Chester, Pa.
DEVELOPMENT OF ULTRASONIC WELDING EQUIPMENT FOR REFRACTORY METALS, by J. B. Jones et al. December 1961. 180p. incl. illus. tables. (ASD Project 7-888) (ASD TR-7-888(II)) (Contract AF33(600)-43026)
Unclassified report

The previously demonstrated feasibility of ultrasonically welding thin sheets of Cb(D-31), Inconel X-750, Mo-0.5Ti, PH15-7Mo, René 41 and tungsten was
(over)

UNCLASSIFIED

1. Materials-Processing
2. Welding
3. Metals
I. Jones, J. B.
II. Aeroprojects Incorporated
III. Contract AF33(600)-43026
IV. ASD Project 7-888
V. Fabrication Branch

UNCLASSIFIED

extended to heavier gages of these materials. Measurements of the acoustical energy required to join these materials confirm values previously estimated by an equation devised during the course of earlier fundamental research work. Salient problems associated with high power ultrasonic transducer-coupling systems for welding machines were considered and solutions to such problems were formulated. Thus, the ultrasonic welding of both mono- and bi-metal combinations in gages up to 0.10 inch is considered feasible and the development of the requisite equipment can be accomplished in a reasonable length of time.

extended to heavier gages of these materials. Measurements of the acoustical energy required to join these materials confirm values previously estimated by an equation devised during the course of earlier fundamental research work. Salient problems associated with high power ultrasonic transducer-coupling systems for welding machines were considered and solutions to such problems were formulated. Thus, the ultrasonic welding of both mono- and bi-metal combinations in gages up to 0.10 inch is considered feasible and the development of the requisite equipment can be accomplished in a reasonable length of time.

extended to heavier gages of these materials. Measurements of the acoustical energy required to join these materials confirm values previously estimated by an equation devised during the course of earlier fundamental research work. Salient problems associated with high power ultrasonic transducer-coupling systems for welding machines were considered and solutions to such problems were formulated. Thus, the ultrasonic welding of both mono- and bi-metal combinations in gages up to 0.10 inch is considered feasible and the development of the requisite equipment can be accomplished in a reasonable lenght of time.

extended to heavier gages of these materials. Measurements of the acoustical energy required to join these materials confirm values previously estimated by an equation devised during the course of earlier fundamental research work. Salient problems associated with high power ultrasonic transducer-coupling systems for welding machines were considered and solutions to such problems were formulated. Thus, the ultrasonic welding of both mono- and bi-metal combinations in gages up to 0.10 inch is considered feasible and the development of the requisite equipment can be accomplished in a reasonable length of time.

AD
Aeroprojects Incorporated, West Chester, Pa.
DEVELOPMENT OF ULTRASONIC WELDING EQUIPMENT FOR REFRACTORY METALS, by J. B. Jones et al. December 1961. 180p. incl. illus. tables. (ASD Project 7-888) ASD TR-7-888(II)) (Contract AF33(600)-43026)
Unclassified report

The previously demonstrated feasibility of ultrasonically welding thin sheets of Cb(D-31), Inconel X-750, Mo-0.5Ti, PH15-7Mo, René 41 and tungsten was
(over)

UNCLASSIFIED

1. Materials Processing
2. Welding
3. Metals
I. Jones, J. B.
II. Aeroprojects Incorporated
III. Contract AF33(600)-43026
IV. ASD Project 7-888
V. Fabrication Branch

UNCLASSIFIED

AD
Aeroprojects Incorporated, West Chester, Pa.
DEVELOPMENT OF ULTRASONIC WELDING EQUIPMENT FOR REFRACTORY METALS, by J. B. Jones et al. December 1961. 180p. incl. illus. tables. (ASD Project 7-888) (ASD TR-7-888(II)) (Contract AF33(600)-43026)
Unclassified report

The previously demonstrated feasibility of ultrasonically welding thin sheets of Cb(D-31), Inconel X-750, Mo-0.5Ti, PH15-7Mo, René 41 and tungsten was
(over)

UNCLASSIFIED

1. Materials-Processing
2. Welding
3. Metals
I. Jones, J. B.
II. Aeroprojects Incorporated
III. Contract AF33(600)-43026
IV. ASD Project 7-888
V. Fabrication Branch

UNCLASSIFIED

AD
Aeroprojects Incorporated, West Chester, Pa.
DEVELOPMENT OF ULTRASONIC WELDING EQUIPMENT FOR REFRACTORY METALS, by J. B. Jones et al. December 1961. 180p. incl. illus. tables. (ASD Project 7-888) (ASD TR-7-888(II)) (Contract AF33(600)-43026)
Unclassified report

The previously demonstrated feasibility of ultrasonically welding thin sheets of Cb(D-31), Inconel X-750, Mo-0.5Ti, Ph15-7Mo, René 41 and tungsten was
(over)

UNCLASSIFIED

1. Materials Processing
2. Welding
3. Metals
I. Jones, J. B.
II. Aeroprojects Incorporated
III. Contract AF33(600)-43026
IV. ASD Project 7-888
V. Fabrication Branch

UNCLASSIFIED

AD
Aeroprojects Incorporated, West Chester, Pa.
DEVELOPMENT OF ULTRASONIC WELDING EQUIPMENT FOR REFRACTORY METALS, by J. B. Jones et al. December 1961. 180p. incl. illus. tables. (ASD Project 7-888) (ASD TR-7-888(II)) (Contract AF33(600)-43026)
Unclassified report

The previously demonstrated feasibility of ultrasonically welding thin sheets of Cb(D-31), Inconel X-750, Mo-0.5Ti, PH15-7Mo, René 41 and tungsten was
(over)

UNCLASSIFIED

1. Materials-Processing
2. Welding
3. Metals
I. Jones, J. B.
II. Aeroprojects Incorporated
III. Contract AF33(600)-43026
IV. ASD Project 7-888
V. Fabrication Branch

UNCLASSIFIED

extended to heavier gages of these materials. Measurements of the acoustical energy required to join these materials confirm values previously estimated by an equation devised during the course of earlier fundamental research work. Salient problems associated with high power ultrasonic transducer-coupling systems for welding machines were considered and solutions to such problems were formulated. Thus, the ultrasonic welding of both mono- and bi-metal combinations in gages up to 0.10 inch is considered feasible and the development of the requisite equipment can be accomplished in a reasonable length of time.

extended to heavier gages of these materials. Measurements of the acoustical energy required to join these materials confirm values previously estimated by an equation devised during the course of earlier fundamental research work. Salient problems associated with high power ultrasonic transducer-coupling systems for welding machines were considered and solutions to such problems were formulated. Thus, the ultrasonic welding of both mono- and bi-metal combinations in gages up to 0.10 inch is considered feasible and the development of the requisite equipment can be accomplished in a reasonable length of time.

extended to heavier gages of these materials. Measurements of the acoustical energy required to join these materials confirm values previously estimated by an equation devised during the course of earlier fundamental research work. Salient problems associated with high power ultrasonic transducer-coupling systems for welding machines were considered and solutions to such problems were formulated. Thus, the ultrasonic welding of both mono- and bi-metal combinations in gages up to 0.10 inch is considered feasible and the development of the requisite equipment can be accomplished in a reasonable lenght of time.

extended to heavier gages of these materials. Measurements of the acoustical energy required to join these materials confirm values previously estimated by an equation devised during the course of earlier fundamental research work. Salient problems associated with high power ultrasonic transducer-coupling systems for welding machines were considered and solutions to such problems were formulated. Thus, the ultrasonic welding of both mono- and bi-metal combinations in gages up to 0.10 inch is considered feasible and the development of the requisite equipment can be accomplished in a reasonable length of time.

AD
Aeroprojects Incorporated, West Chester, Pa.
DEVELOPMENT OF ULTRASONIC WELDING EQUIPMENT FOR REFRACTORY METALS, by J. B. Jones et al. December 1961. 180p. incl. illus. tables. (ASD Project 7-888) ASD TR-7-888(II))
(Contract AF33(600)-43026)
Unclassified report

The previously demonstrated feasibility of ultrasonically welding thin sheets of Cb(D-31), Inconel X-750, Mo-0.5Ti, PH15-7Mo, René 41 and tungsten was
(over)

UNCLASSIFIED

1.Materials Processing
2.Welding
3.Metals
I.Jones, J. B.
II.Aeroprojects Incorporated
III.Contract AF33(600)-43026
IV.ASD Project 7-888
V.Fabrication Branch

UNCLASSIFIED

AD
Aeroprojects Incorporated, West Chester, Pa.
DEVELOPMENT OF ULTRASONIC WELDING EQUIPMENT FOR REFRACTORY METALS, by J. B. Jones et al. December 1961. 180p. incl. illus. tables. (ASD Project 7-888) (ASD TR-7-888(II))
(Contract AF33(600)-43026)
Unclassified report

The previously demonstrated feasibility of ultrasonically welding thin sheets of Cb(D-31), Inconel X-750, Mo-0.5Ti, PH15-7Mo, René 41 and tungsten was
(over)

UNCLASSIFIED

1.Materials-Processing
2.Welding
3.Metals
I.Jones, J. B.
II.Aeroprojects Incorporated
III.Contract AF33(600)-43026
IV.ASD Project 7-888
V.Fabrication Branch

UNCLASSIFIED

AD
Aeroprojects Incorporated, West Chester, Pa.
DEVELOPMENT OF ULTRASONIC WELDING EQUIPMENT FOR REFRACTORY METALS, by J. B. Jones et al. December 1961. 180p. incl. illus. tables. (ASD Project 7-888) (ASD TR-7-888(II))
(Contract AF33(600)-43026)
Unclassified report

The previously demonstrated feasibility of ultrasonically welding thin sheets of Cb(D-31), Inconel X-750, Mo-0.5Ti, Ph15-7Mo, René 41 and tungsten was
(over)

UNCLASSIFIED

1.Materials Processing
2.Welding
3.Metals
I. Jones, J. B.
II.Aeroprojects Incorporated
III.Contract AF33(600)-43026
IV.ASD Project 7-888
V.Fabrication Branch

UNCLASSIFIED

AD
Aeroprojects Incorporated, West Chester, Pa.
DEVELOPMENT OF ULTRASONIC WELDING EQUIPMENT FOR REFRACTORY METALS, by J. B. Jones et al. December 1961. 180p. incl. illus. tables. (ASD Project 7-888) (ASD TR-7-888(II))
(Contract AF33(600)-43026)
Unclassified report

The previously demonstrated feasibility of ultrasonically welding thin sheets of Cb(D-31), Inconel X-750, Mo-0.5Ti, PH15-7Mo, René 41 and tungsten was
(over)

UNCLASSIFIED

1.Materials-Processing
2.Welding
3.Metals
I.Jones, J. B.
II.Aeroprojects Incorporated
III.Contract AF33(600)-43026
IV.ASD Project 7-888
V.Fabrication Branch

UNCLASSIFIED

ASD TR 7-888(II)

ASD INTERIM REPORT 7-888(II)
December 1961

Development of ULTRASONIC WELDING EQUIPMENT for REFRACTORY METALS

J. Byron Jones
Nicholas Maropis
Carmine F. DePrisco
John G. Thomas
Janet Devine

AEROPROJECTS INCORPORATED
West Chester, Pennsylvania

Contract: AF 33(600)-43026
ASD Project No. 7-888

Interim Technical Progress Report
1 June 1961 to 15 December 1961

The previously demonstrated feasibility of ultrasonically welding thin sheets of Cb(D-31), Inconel X-750, Mo-0.5Ti, PH15-7Mo, René 41 and tungsten was extended to heavier gages of these materials. Measurements of the acoustical energy required to join these materials confirm values previously estimated by an equation devised during the course of earlier fundamental research. Salient problems associated with high power ultrasonic transducer-coupling systems for welding machines were considered and solutions to such problems were formulated. Thus, the ultrasonic welding of both mono- and bi-metal combinations in gages up to 0.10 inch is considered feasible and the development of the requisite equipment can be accomplished in a reasonable length of time.

FABRICATION BRANCH
MANUFACTURING TECHNOLOGY LABORATORY

AFSC Aeronautical Systems Division
United States Air Force
Wright-Patterson Air Force Base, Ohio

FOREWORD

This Interim Technical Progress Report covers the work performed under Contract AF 33(600)-43026 from 1 June 1961 to 15 December 1961. It is published for technical information only and does not necessarily represent the recommendations, conclusions, or approval of the Air Force.

This contract with Aeroprojects Incorporated of West Chester, Pennsylvania, was initiated under ASD Manufacturing Technology Project 7-888, "Development of Ultrasonic Welding Equipment for Refractory Metals". It was administered under the direction of Fred Miller (ASRCTF) of the Fabrication Branch, Manufacturing Technology Laboratory, AFSC Aeronautical Systems Division, Wright-Patterson Air Force Base, Ohio.

The authors acknowledge with appreciation the interest, cooperation, assistance, and criticism of: Dr. William C. Elmore, Chairman, Department of Physics, Swarthmore College; Dr. George S. Ansell, Research Professor of Metallurgy, Rensselaer Polytechnic Institute, Mr. Don A. Berlincourt, Electronic Research Division, Clevite Corporation, and Mr. R. Buck, International Nickel Company, as well as Mrs. Roberta McCutchen, Senior Technical Writer, Aeroprojects Incorporated.

The methods used to demonstrate a process or technique on a laboratory scale are inadequate for use in production operations. The objective of the Air Force Manufacturing Methods Program is to develop on a timely basis, manufacturing process, techniques and equipment for use in economical production of USAF materials and components. This program encompasses the following technical areas:

Rolled Sheet	Powder Metallurgy
Forgings	Component Fabrication
Extrusions	Joining
Castings	Forming
Fiber	Materials Removal
Fuels and Lubricants	Solid State Devices
Ceramics and Graphites	Passive Devices
Nonmetallic Structural Materials	Thermionic Devices.

Your comments are solicited on the potential utilization of the information contained herein as applied to your present or future production programs. Suggestions concerning additional Manufacturing Methods development required on this or other subjects will be appreciated. Direct any reply concerning the above matter to the attention of Mr. W. W. Dismuke, ASRKRA.

****

PUBLICATION REVIEW

Approved by: J Byron Jones
J. Byron Jones

ABSTRACT-SUMMARY
Interim Technical Progress Report

ASD Interim Report 7-888(II)
December 1961

Development of ULTRASONIC WELDING EQUIPMENT for REFRACTORY METALS

J. Byron Jones
et al
Aeroprojects Incorporated

The previously demonstrated feasibility of ultrasonically welding thin sheets of Cb(D-31), Inconel X-750*, Mo-0.5Ti, PH15-7Mo, René 41 and tungsten was extended to heavier gages of these materials. Measurement of the acoustical energy required to join these materials confirm values previously estimated by an equation devised during the course of earlier fundamental research work. Salient problems associated with high power ultrasonic transducer-coupling systems for welding machines were considered and solutions to such problems were formulated. Thus, the ultrasonic welding of both mono- and bi-metal combinations in gages up to 0.10 inch is considered feasible and the development of the requisite equipment can be accomplished in a reasonable length of time.

Information pertinent to the development of ultrasonic welding equipment for joining such materials as columbium-10Mo-10Ti, Inconel X-750*, molybdenum-0.5Ti, PH15-7Mo steel, René 41, and tungsten is summarized and discussed in this report.

A first approximation of the energy required, based on previous experimental work, was supplemented by new data obtained by ultrasonically welding the above materials in gages up to 0.040-inch with a 6-8 kilowatt laboratory device; thus, confirming the feasibility of joining such materials and of developing the necessary equipment to produce such junctions in thicknesses up to 0.10 inch.

Pertinent information on transducer, coupler, and terminal element materials is presented and the most promising materials were ascertained experimentally. The requisite ultrasonic welding equipment is considered to be practical and amenable to early development.

---

* Formerly designated as Inconel X.

TABLE OF CONTENTS

		Page No.
FOREWORD		5
ABSTRACT-SUMMARY		7
LIST OF FIGURES		13
LIST OF TABLES		15
INTRODUCTION		19
SECTION:		
I.	MATERIAL WELDING FEASIBILITY	23
	Background	23
	Selection of Materials	23
	Material Properties and Other Pertinent Data	23
	Surface Films and Finishes	28
	Cleaning and Surface Preparation	28
	Feasibility Data and Other Pertinent Information	29
	Metallurgical Considerations	32
	Weld-Zone Temperature	32
	Temperature Measurements	36
	Microstructural Features of Weld Interface	38
	Mono-Metal Welds	38
	Bi-Metal Welds	43
II.	WELDING ENERGY REQUIREMENTS	47
	Introduction	47
	Predicting Weldability and Power Requirements	47
	Seam Welding	50
III.	ACOUSTICAL MATERIALS SURVEY	55
	Transducer Materials	55
	Coupler Materials	59
	Tip Materials	64

IV. ACOUSTICAL MATERIAL STUDY 67

Transducers 67
Couplers 71
Impedance Matching 72
Power Handling Capacity 75
Internal Friction 77
Tip Materials 78

V. ENERGY DELIVERY METHODS 83

Systems 83
Mechanical Arrays 86
Continuous Roller Seam Welder -- Limitations 90
Combination of a Spot and Seam Welding Machine 93
Components 93
Transducers and Couplers 93
Tips 93
Spot-Type Welder 93
Roller Seam-Welding Disks 96

VI. EQUIPMENT FEASIBILITY 97

Introduction 97
Basic Requirements 97
Clamping Force 97
Power 97
Welding Machine Design Problems 105
Direct Read-Out Acoustical Watt-Meter 105
Power-Force Programming 106
Tip Amplitude Indicator 106
Sonotrode Work Contacting Tips 107
High Performance Transducer Assemblies 107
Switching Problem 107

VII. DESIGN SPECIFICATIONS 109

Introduction 109
Power Source 109
Clamping Force 110
Transducer-Coupling System 110
Machine Dimensions and Structure 111
Instrumentation 111
Controls 113
Safety 114

VIII. SUMMARY, CONCLUSIONS AND RECOMMENDATIONS 115

APPENDIX 117

I. DETAILS OF 8-KW ULTRASONIC WELDING MACHINE ASSEMBLY . . 117

II. DETAILS OF WELDING STUDIES 123

III. TRANSDUCER MATERIAL STUDIES 129

IV. COUPLER MATERIAL STUDIES 135

V. LIMITATION ON AMPLITUDE SET BY MAXIMUM STRAIN ENERGY IN VIBRATORY SYSTEMS 145

VI. EQUIVALENT CIRCUIT OF A VIBRATING DISK SEAM WELDER . . . 151

VII. TORSIONAL VIBRATION OF A SHAPED DISK 157

REFERENCES 163

LIST OF FIGURES

DESCRIPTION	FIGURE No.	PAGE No.
SKETCHES OF TYPICAL ULTRASONIC WELDING SYSTEMS	1	21
CLAMPING FORCE AS A FUNCTION OF MATERIAL THICKNESS . .	2	31
TYPICAL CURVES OF WELD-ZONE TEMPERATURE AS A FUNCTION OF CLAMPING FORCE AND WELDING TIME	3	35
TEMPERATURE RISE CURVES FOR 0.032-INCH MOLYBDENUM-0.5 TITANIUM AND 0.002-INCH TUNGSTEN AT WELDING POWER . .	4	37
MONO-METAL WELD MICROGRAMS	5	39
DISSIMILAR-METAL WELD MICROGRAMS	6	40
ACOUSTICAL ENERGY CALCULATED FROM ENERGY EQUATION . .	7	49
ELECTRICAL INPUT ENERGY AS A FUNCTION OF MATERIAL THICKNESS	8	51
CERAMIC TRANSDUCER DESIGNS	9	68
PERIPHERAL BOLT DESIGN CERAMIC TRANSDUCER ASSEMBLY WITH HALF-WAVE SLUGS BRAZED TO ONE END-PLATE AND COUPLER TO OTHER END-PLATE	10a	70
SIX STACK NICKEL TRANSDUCER	10b	70
POWER LOSS AND STRAIN CHARACTERISTICS OF CANDIDATE COUPLER MATERIALS	11	79
ASTROLOY TIP-CHARACTERISTIC SURFACE DAMAGE	12a	81
-AFTER FAILURE	12b	81
-REMOVABLE TIP WITH INSERT	12c	81
ROLLER-ROLLER CONFIGURATION	13a	88
TRAVERSING TABLE CONFIGURATION	13b	88
TRAVERSING HEAD CONFIGURATION	13c	88
EXPERIMENTAL 25-KILOWATT WELDER	14	112
EXPERIMENTAL 8-KILOWATT ULTRASONIC SPOT WELDING MACHINE	15	118

(Concluded on next page)

LIST OF FIGURES (Concluded)

DESCRIPTION	FIGURE No.	PAGE No.
BLOCK DIAGRAM OF COMPONENTS IN 8-KILOWATT ULTRASONIC WELDING ARRAY	16	120
TRANSDUCER EVALUATION EQUIPMENT	17	131
TEMPERATURE DISTRIBUTION IN LEAD ABSORBER AFTER 8-MINUTE TEST PERIOD	18	133
POWER LOSS AND STRAIN CHARACTERISTICS OF CANDIDATE COUPLER MATERIALS	19	139
GEOMETRY OF STRAIN DISTRIBUTION ALONG TEST SPECIMEN . .	20	140
POWER LOSS AND STRAIN CHARACTERISTICS OF CANDIDATE COUPLER MATERIALS	21	142
DESIGN CURVES FOR A SHAPED-DISK	22	160

LIST OF TABLES

TITLE	TABLE No.	PAGE No.
WELDMENT MATERIALS: PHASE I MATERIAL-PROCUREMENT SOURCES	1	24
WELDMENT MATERIALS: MECHANICAL PROPERTIES	2	25
WELDMENT MATERIALS: DENSITY AND THERMAL PROPERTIES . .	3	26
WELDMENT MATERIALS: METALLURGICAL PROPERTIES AND ANTICIPATED WELD ZONE TEMPERATURES	4	27
WELDMENT MATERIALS: CLEANING AND SURFACE PREPARATIONS.	5	30
WELDMENT MATERIALS: PREPARATION OF SPECIMEN SURFACES PRIOR TO WELDING	6	29
MONO-METAL WELDS: COMPARISON OF TENSILE SHEAR STRENGTH DATA	7	33
BI-METAL WELDS: SUMMARY OF TENSILE-SHEAR STRENGTH DATA	8	34
WELDMENT MATERIALS: MELTING AND RECRYSTALLIZATION TEMPERATURES	9	36
WELDMENT MATERIALS: ESTIMATED ACOUSTICAL ENERGY AND POWER REQUIREMENTS FOR WELDING 0.10-INCH MATERIAL . . .	10	48
ELECTRICAL INPUT ENERGY REQUIRED TO WELD MATERIALS OF VARIOUS THICKNESSES	11	53
TRANSDUCER MATERIALS: PHYSICAL AND THERMAL PROPERTIES.	12	57
TRANSDUCER MATERIALS: DESIGN CHARACTERISTICS	13	58
COUPLER MATERIALS: THERMAL AND MECHANICAL PROPERTIES .	14	62
COUPLER MATERIALS: ACOUSTICALLY RELEVANT PROPERTIES .	15	63
COUPLER MATERIALS: MACHINING AND JOINING CHARACTERISTICS	16	61
TIP MATERIALS: DENSITY AND THERMAL PROPERTIES	17	65

(Continued on Next Page)

LIST OF TABLES (Continued)

TITLE	TABLE NO.	PAGE NO.
TIP MATERIALS: PHYSICAL AND MECHANICAL PROPERTIES . . .	18	66
TRANSDUCER EFFICIENCY AS DETERMINED FROM CALORIMETRIC STUDIES	19	69
COUPLER AND TRANSDUCER MATERIALS: IMPEDANCE MATCHING .	20	73
CANDIDATE COUPLER MATERIALS: POWER HANDLING CAPACITY AND TRANSMISSION EFFICIENCY	21	75
VIBRATORY MODES: RELATIVE STRAIN DENSITY AND AMPLITUDE.	22	76
COUPLER MATERIALS: DYNAMIC STRESS AND STRAIN IN 2-INCH DIAMETER ROD AT 10-KILOWATT INPUT POWER LEVEL	23	77
APPLICABILITY OF CLASS AND TYPE OF ULTRASONIC SYSTEMS TO SPOT- AND SEAM-TYPE WELDERS	24	83
TERMINAL TIP-COUPLER CHARACTERISTICS FOR CONTINUOUS SEAM ROLLER WELDER	25	91
TERMINAL TIP-REED CHARACTERISTICS FOR SINGLE-SPOT WELDERS	26	94
WELDMENT MATERIALS: ESTIMATED CLAMPING FORCE VALUES FOR 0.10-INCH MATERIAL	27	98
TRANSDUCER-COUPLING SYSTEMS: COMPARISON OF RELATIVE EFFICIENCIES	28	100
ESTIMATED ELECTRICAL POWER REQUIRED TO WELD 0.060-INCH MATERIAL AT VARIOUS WELD INTERVALS	29	101
ESTIMATED ELECTRICAL POWER REQUIRED TO WELD 0.090-INCH MATERIAL AT VARIOUS WELD INTERVALS	30	102
ESTIMATED ELECTRICAL POWER REQUIRED TO WELD 0.10-INCH MATERIAL AT VARIOUS WELD INTERVALS	31	103
8-KW ULTRASONIC SPOT WELDER: PERFORMANCE DATA	32	121

(Concluded on next page)

LIST OF TABLES (Concluded)

TITLE	TABLE No.	PAGE No.
MONO-METAL WELDS: WELDING CONDITIONS AND TENSILE-SHEAR STRENGTH DATA	33	125
BI-METAL WELDS: WELDING CONDITIONS AND TENSILE-SHEAR STRENGTH	34	128
CERAMIC TRANSDUCER ELEMENTS: OPERATING CHARACTERISTICS	35	132
TRANSDUCER ASSEMBLIES: RELATIVE ENERGY CONVERSION EFFICIENCY	36	134
DESIGN DATA FOR TEST SPECIMENS	37	136
COUPLER MATERIAL: POWER DISSIPATION AND PEAK STRAIN LEVELS	38	141
COUPLER MATERIALS: RELATIVE ACOUSTIC TRANSMISSIVITY AT HIGH STRAIN LEVELS	39	144

Development of ULTRASONIC WELDING EQUIPMENT for REFRACTORY METALS

INTRODUCTION

The increasing use of the newer, high-temperature, corrosion-resistant metals and alloys, such as molybdenum-0.5Ti, Inconel X-750, René 41, PH15-7Mo, and others, in missile, space vehicle, and atomic applications has introduced metal joining problems that have not yet been solved by conventional techniques. Producing satisfactory bonds in such materials, in both similar and dissimilar combinations of medium and heavy gages, presents certain difficulties.

Since publication of the first information on ultrasonic welding (1)*, this subject has received increasing attention at metallurgical conferences (2-6), from American Industry (7-15), from the metal fabrication industry (16-23), and from foreign investigators (24-29).

Ultrasonic welding equipment has demonstrated its effectiveness in joining various materials of interest in the aerospace industries. Only in some of the aluminum alloys, however, has welding been possible in the heavier gages (up to about 0.12 inch). With existing equipment, the gage for most other materials is limited to about 0.040 inch and lower. Extension of the process to heavier and harder materials, therefore, requires substantial increases in the net vibratory power delivered to the weld zone. Such power increases can be achieved via two primary avenues:

1. increased power to the transducer-coupling system.

2. development of welding machines with transducer-coupling systems of greater power handling capacity and/or increased efficiency of the transducer-coupling systems.

---

* Numbers in parentheses refer to references listed at end of report.

The objective hereof is to develop ultrasonic welding equipment adequate for joining the harder, higher-strength metals and alloys in thicknesses up to about 0.10 inch. To accomplish this, it is necessary to establish the feasibility of joining metallic materials, as exemplified by columbium-10Mo-10Ti, Inconel X-750, PH15-7Mo, René 41 and tungsten, in mono-metallic and dissimilar material combinations and to outline a systematic approach to the development of techniques and equipment necessary to make reliable, reproducible ultrasonic welds.

Determination of equipment requirements for ultrasonically welding metallic materials in a specific thickness range must begin with a study of the energy requirements for making the welds. This is not a matter of merely defining the line power required to operate welding equipment, nor does it deal solely with the more complex problem of the acoustical energy delivered into the weld zone. Actually, energy transmission through the entire electro-acoustical system must be considered and its efficiency maximized on a practical basis.

Electrical power from a standard power line (60 cycles) is delivered into the "ultrasonic generator", or power source, where it is converted by means of auxiliary electrical equipment, such as electronic oscillators and power amplifiers, into electrical power at the operating frequency of the welding machine. This high-frequency electrical power is delivered to the transducer, which converts it into vibratory power of the same frequency. The power then passes through the coupling system, which may consist of one or more members, including the work-contacting tip, and into the metal members being joined.

Certain elements, common to transducer-coupling systems, require development for effective use in higher-power ultrasonic welding machines. Transducer material may be selected from a variety of candidates, but transducer designs depend in large measure on the material selected. Coupler materials must also be selected with consideration of certain material properties, some of which may not have been quantitatively established. Requirements for welding machine tips present additional difficulties.

The basic elements of these systems include a transducer, a coupling system, welding tips, and an anvil or support for the workpiece, which may or may not deliver vibratory power. After the most promising elements are determined, the potentially best coupling system must be selected from two general classes (the reaction-element, or anvil, and the opposition-drive) and a variety of types (wedge-reed, lateral-drive, and torsional):

> In the wedge-reed system, used in higher-power, spot-type welders, acoustical energy is delivered to a wedge-shaped member (a mechanical transformer) which executes longitudinal

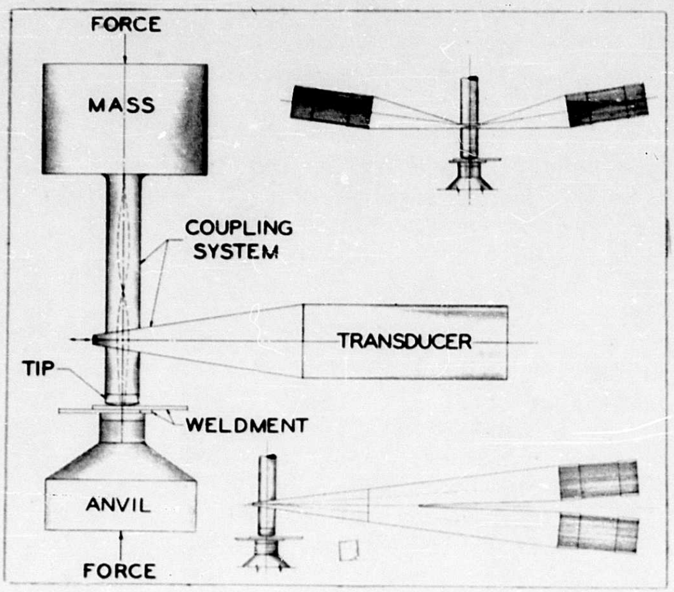

A. WEDGE-REED

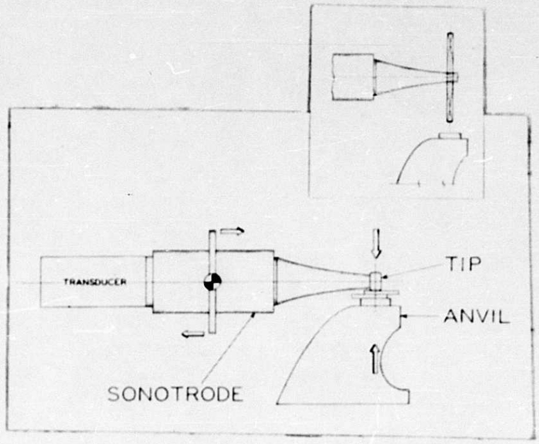

B. LATERAL-DRIVE

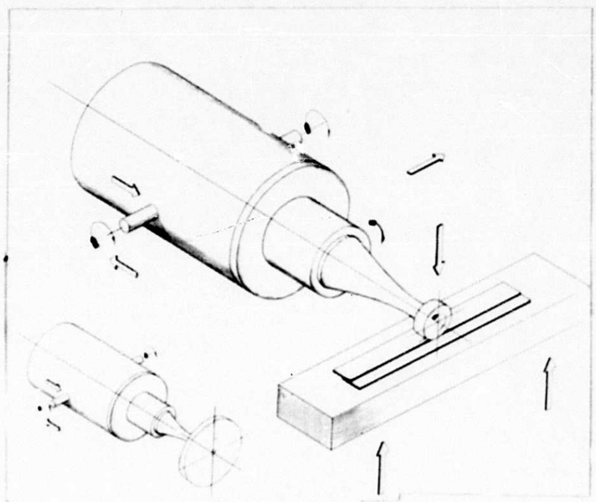

C. CONTINUOUS-SEAM

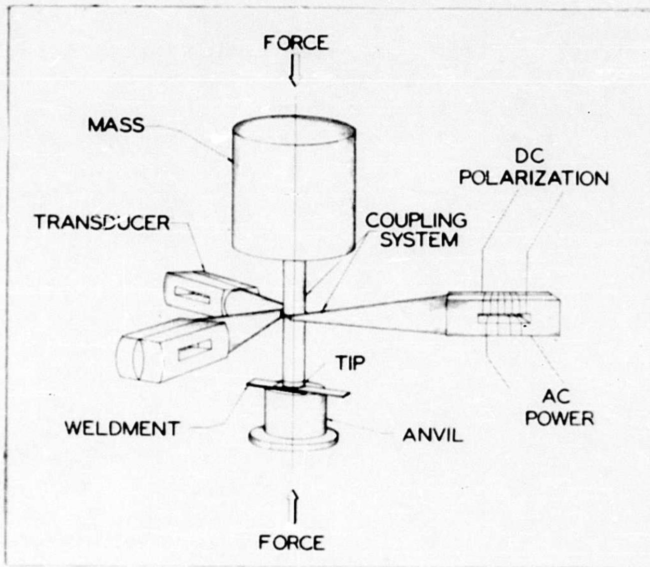

D. RING WELDER

Figure 1: SKETCHES OF TYPICAL ULTRASONIC WELDING SYSTEMS

vibration at a somewhat greater amplitude than is produced by the transducer, thus causing the welding tip to vibrate essentially parallel to the weld interface.

Smaller welders and portable-type welders conveniently incorporate the lateral-drive system of Figure 1. In this case, the tip is attached to a coupler, carried on force insensitive mounts, which vibrates longitudinally to produce tip excursion parallel to the weld interface. Clamping force is applied through bending of the coupler.

A ring-welding machine is essentially a special kind of spot-type welder that produces an uninterrupted annular weld with a single, short power interval. Such a welder utilizes a torsionally driven coupling system. In one type of ring welder arrangement, illustrated in Figure 1, the longitudinally vibrating mechanical-transformers are attached approximately tangent to the torsional reed member; thus, producing torsional displacements of the welding tip. Other arrangements for producing this torsional displacement, or vibration, have also been developed.

A continuous roller-seam welder incorporates a lateral-drive transducer-coupling system, positioned on force-insensitive mounts, and rotating on anti-friction bearings with driving power introduced through slip rings; usually, rotation of the entire transducer-coupling, disk-tip system is provided by a motor drive. A disk tip operates in contact with the work so there is essentially no slippage between the tip and the work.

Data and other information, pertaining to the development of the requisite ultrasonic welding equipment for joining refractory materials, are summarized in sections corresponding to the major contract items for Phase I as listed below:

I. Material Welding Feasibility
II. Welding Energy Considerations
III. Acoustical Materials Survey
IV. Acoustical Materials Study
V. Energy Delivery Methods
VI. Equipment Feasibility
VII. Design Specifications
VIII. Summary and Recommendations.

Theoretical concepts and details of the experimental work are presented in the Appendix.

I. MATERIAL WELDING FEASIBILITY

"ESTABLISH THE FEASIBILITY OF JOINING REFRACTORY METALS IN MONO-METALLIC AND DISSIMILAR MATERIAL COMBINATIONS"

BACKGROUND

This work is concerned with the feasibility of ultrasonically welding such refractory metals and superalloys as tungsten, molybdenum-0.5Ti, tantalum, columbium-10Mo-10Ti, Inconel X-750*, AM-355 (PH15-7Mo) steel and Udimet 700. These materials are relatively new and their properties are not as well defined as those of the more common metals and alloys such as aluminum, copper, nickel, and steel.

SELECTION OF MATERIALS

Manufacturing Technology personnel of the Aeronautical Systems Division, Air Force Systems Command, recommended the six materials listed below for the focus of effort during this feasibility investigation.

1. AM-355 steel (PH15-7Mo)
2. Columbium-10Mo-10Ti alloy (Union Carbide Cb-74 or DuPont D-31)
3. Inconel X-750*
4. Molybdenum-0.5Ti alloy
5. René 41
6. Tungsten

Modest quantities of these materials in sheet gages ranging from 0.005 to 0.040 inch were secured from these manufacturers (see Table 1). Since AM-355 was unavailable from stock and accelerated delivery of this alloy, plus rolling to the required gages, could not be arranged to meet the work schedule hereof; PH15-7Mo, which exhibits essentially the same properties as AM-355, was substituted.

MATERIAL PROPERTIES AND OTHER PERTINENT DATA

With a view to correlating the characteristics of these specific materials with existing ultrasonic welding theory, as well as for reference and to assist in applying such theory to the problems hereof, data on the mechanical properties of these materials are given in Table 2, density and thermal properties are presented in Table 3, while other relevant information is summarized in Table 4.

---

* Formerly designated as Inconel X.

Table 1

WELDMENT MATERIALS: PHASE I MATERIAL-PROCUREMENT SOURCES

Weldment Material[a]	Procurement Source	Material Thickness (inch)
Cb(D-31)	E. I. duPont deNemours & Company	0.010 .015 .025
Inconel X-750*	International Nickel Compa[illegible]	0.010 .020 .031 .043
Mo-0.5Ti	Universal-Cyclops Steel Corporation	0.010 .015 .020 .030
PH15-7Mo	Armco Steel Corp.	0.005 .010 .020 .030
René 41	Cannon-Muskegon Corporation	0.008 .020 .030 .040
Tungsten	Fansteel Metallurgical Corporation	0.010 .015 .020 .030

[a] All material procured in the condition noted in Table 2.

* Formerly designated as Inconel X.

Table 2

WELDMENT MATERIALS: MECHANICAL PROPERTIES (31-58)

Weldment Material				Strength				
Designation	Condition[a]	Temperature (°F)	Elongation (%)	Ultimate Tensile (10^3 psi)	Yield (0.2% offset) (10^3 psi)	Modulus of Elasticity (10^6 psi)	Shear Modulus (10^6 psi)	Poisson's Ratio
Cb(D-31)	SR	70	15	100	90	16.5	6.0	0.380
		1000	5	68	68	12.8	---	---
Inconel X-750	SHT-A	70	49	115	47	31.0	12.0	.290
		1000	25	95	--	25.0	---	---
Mo-0.5Ti	VAC-SR	70	14	130	120	45.5	17.4	.324
		1000	--	110	100	--	---	---
PH15-7Mo	A	70	35	130	55	29.0	10.5	---
		1000	--	---	--	--	---	---
René 41	A	70	20	185	140	31.6	12.1	.310
		1000	13	178	134	27.3	10.2	.325
Tungsten	A	70	0	120	--	50.0	21.8	.284
		1000	--	75	18	55.0	---	---

[a] A: annealed; SR: stress relieved; SHT: solution heat-treated; VAC: vacuum arc-cast.

Table 3

WELDMENT MATERIALS: DENSITY AND THERMAL PROPERTIES (31-58)

Weldment Material		Temperature (°F)	Density (ρ) (lb/in^3)	Linear Coeff. of Thermal Expansion 10^6(in/in-°F)	Thermal Conductivity (K) (BTU-in/Ft^2-hr-F)	Thermal Diffusivity $\alpha = K/\rho c$ (Ft^2/hr)	Specific Heat (c) (BTU/lb-°F)
Designation	Condition[a]						
Cb(D-31)	SR	70	0.292	4.1	---	---	0.074
		1000	---	---	---	---	---
Inconel X-750	SHT-A	70	.298	6.9	83	0.132	.103
		1000	---	8.1	131	.169	.130
Mo-0.5Ti	VAC-SR	70	.368	3.1	936	2.01	.061
		1000	---	3.2	840	1.75	.063
PH15-7Mo	A	70	.282	8.0	---	---	---
		1000	---	9.4	---	---	---
René 41	A	70	.296	6.5	63	0.095	.108
		1000	---	7.5	105	.158	---
Tungsten	A	70	.697	2.6	1150	.249	.032
		1000	---	2.7	900	---	---

[a] A: annealed; SR: stress relieved; SHT: solution heat-treated; VAC: vacuum arc-cast.

Table 4

WELDMENT MATERIALS: METALLURGICAL PROPERTIES AND ANTICIPATED WELD ZONE TEMPERATURES (31-58)

Weldment Material		Crystal Structure	Recrystallization Temperature (°F)	Melting Temperature (°F)	Estimated Weld-Zone Temperature (°F)	
Designation	Condition[a]				Minimum	Maximum
Cb(D-31)	SR	bcc	1800-2100	4100	1135	1820
Inconel X-750	SHT-A	fcc	(b)	2540-2600	590	1040
Mo-0.5Ti	VAC-SR	bcc	2100(c)	4730	1360	2135
PH15-7Mo	A	fcc (10%) bcc (90%)	1300	2500	--	--
René 41	A	fcc	(b)			
Tungsten	SR	bcc	2650	6170	2270	2855

[a] See Table 2.

(b) Alloys normally hardened by precipitation heat treatment.

(c) 50% recrystallization in one hour.

As will be shown later in this report, current theories of ultrasonic welding relate the energy requirements, associated with producing welds, to the hardness and thickness of the weldment material. Pertinent data on the energy requirements for spot welding thin gages of the six weldment materials, as well as the tensile shear strength of such bonds, were assembled from the results of previous experimental work.

SURFACE FILMS AND FINISHES (59-68)

Since fabrication processes for the refractory metals and alloys undergo almost continual revision, the nature of the surface finish and films may vary considerably. With the manufacturing operations in this state of flux, there is a paucity of information concerning the nature of the surface film on the selected weldment materials. Accordingly, information on surface films and their properties, as well as cleaning and surface preparation procedures, was requested directly from the research department of the manufacturer from whom metals were purchased (59-66).

At the present time, a refractory metal sheet-rolling program, initiated by the U. S. Navy Bureau of Naval Weapons, is oriented toward the production of high-quality, refractory-metal sheet: Universal-Cyclops Steel Corporation is investigating fabrication of molybdenum (Contract NOas 59-6142-c), and the Fansteel Metallurgical Corporation is studying tungsten (Contract NOw 60-0621-c). The Air Force is sponsoring "Manufacturing Methods for Columbium Alloy Sheet" at the Crucible Steel Company of America (Contract AF 33(600)-39942). Since this research is not well advanced, much information directly related to sheet quality and surface condition should become available during the forthcoming months.

CLEANING AND SURFACE PREPARATION

Ultrasonic welding data indicate that, although meticulous attention to surface preparation is not necessary, oxide-free and degreased surfaces may respond somewhat more readily to welding. Because knowledge of surface properties is scantly, cleaning procedures vary within the industry. For example, with commercial René 41 sheet, usually supplied in the 2 D mill finish (annealed and pickled), it is common practice to descale the material in a Virgo salt (product of the Hooker Chemical Company) and pickle in a hydrofluoric-nitric acid solution; then, before conventional welding or brazing, the surface is ground locally to remove a surface layer which is usually depleted of both aluminum and titanium during the initial processing to the 2 D mill condition. In other cases, surface preparation procedures may vary from none at all to elaborate methods similar to the one outlined for René 41.

The cleaning and surface preparation procedures listed in Table 5 represent only a few of the several methods described in the literature for the removal of surface films. A more comprehensive list is given in DMIC Memorandum 85, "Pickling and Descaling of High-Strength, High-Temperature, Metals and Alloys" (68). The cleaning and surface preparation procedures used in these experimental studies are given in Table 6 for each of the six weldment materials.

Table 6

WELDMENT MATERIALS: PREPARATION OF SPECIMEN SURFACES PRIOR TO WELDING

Weldment Material	Surface Preparation
Cb(D-31) PH15-7Mo Tungsten	Degreased with A-27 Commercial Degreaser, Pennsalt Chemical Corporation
Mo-0.5Ti	H_2SO_4 -- 95 wt % HNO_3 -- 4.5 wt % HF -- 0.5 wt % CrO_3 -- 18.8 g/l (Solution used at room temperature.)
Inconel X-750 René 41	HNO_3 (57 at %) -- 10 parts/volume HF (40 at %) -- 1.5 parts/volume H_2O -- 10 parts/volume (Solution used at 160°F.)

FEASIBILITY DATA AND OTHER PERTINENT INFORMATION

The feasibility of joining thicker gages of the weldment materials than had been accomplished previously was demonstrated by ultrasonically welding similar and dissimilar combinations of Cb(D-31), Inconel X-750, Mo-0.5Ti, PH15-7Mo, René 41 and tungsten with an experimental 8-kw laboratory welding machine. These welds were made at clamping force levels established for the various gages of each material (see Figure 2) and at weld intervals that were adjusted to ensure delivery of the required energy under maximum power conditions. (For details of this work, see Appendix II).

Table 5

WELDMENT MATERIALS: CLEANING AND SURFACE PREPARATIONS

Weldment Material	Surface Treatment			Comments	Ref. No.
	Etch-Type	Etchant Constituent	Etchant Quantity		
AM-355 and PH15-7Mo	Pickling	HNO_3 HF	15 wt-% 3 wt-%	Used to remove scale after annealing. Time required is 3 minutes at 135 F.	59
	Electrolytic	Oxalic Acid	10%	Used for light etching.	
Cb(D-31)	Electrolytic	HF	5-50%	For cleaning surface before plating with Fe or Ni.	60 66
	Chemical	Lactic Acid HNO_3 HF	50 ml 30 ml 2 ml	Chemical polish also suitable for tungsten.	
Inconel X-750 and René 41	Pickling	HNO_3 HF H_2O	5 parts 1 part 15 parts	Used at 120 - 140 F for removal of light oxide coating.	61 62
Mo-0.5Ti	Chemical	H_2SO_4 HNO_3 HF CrO_2	95 wt-% 4.5 wt-% 0.5 wt-% 18.8 g/l	For removal of surface film.	63 66
	Metallographic	$K_3Fe(CN)_6$ KOH H_2O	30 grams 10 grams 100 ml	Satisfactory for pre-plating treatment.	
Tungsten	Electrolytic	HF	5-50%	Cleaning prior to plating.	66
	Chemical	$K_3Fe(CN)_6$ KOH H_2O	10 grams 10 grams 100 ml	Used for cleaning - also, suitable for molybdenum.	

Figure 2: CLAMPING FORCE AS A FUNCTION OF MATERIAL THICKNESS

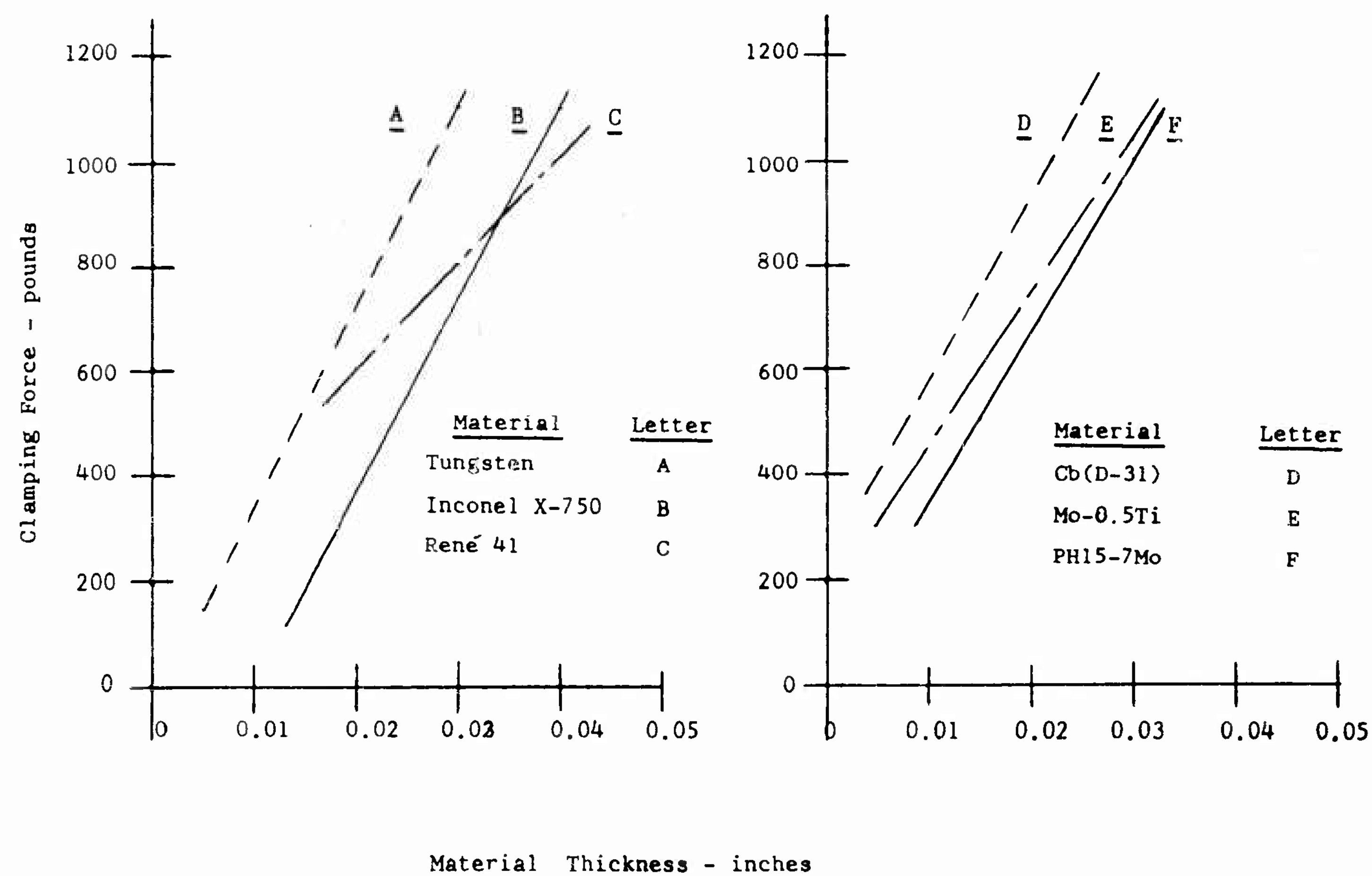

The tensile-shear strength of the mono- and bi-metal bonds was measured as described in Appendix II, and the data for the mono-metal welds are compared with similar results obtained previously, (Table 7). Strength data for the bi-metal welds are presented in Table 8.

The differences in spot strength at the various energy levels is not presently significant because these experiments were concerned only with the feasibility of joining these materials and not with attainment of junctions approaching either high strength or optimum quality.

METALLURGICAL CONSIDERATIONS

WELD-ZONE TEMPERATURE

Recent research shows that the temperature rise in ultrasonic welds reaches about 35-50 percent of the homologous melting temperature. In most cases, this is below the temperature at which grain growth (recrystallization) occurs. Both the thermal properties of the weldment material and the welding conditions (such as clamping force and weld interval), however, contribute to the interfacial temperature rise during the formation of the ultrasonic bond (see Figure 3).

The heat developed locally within the weld zone may be of sufficient magnitude to initiate diffusion and, consequently, solid state reactions. While the influence of ultrasonic vibration on the rate of diffusion has not been extensively investigated, the results of scattered research in this field indicate that ultrasonics accelerate such reactions. The volume of metal within the weld zone, having been subjected to heating and simultaneous high frequency vibration, may exhibit unique characteristics.

Many of these features are described in the literature. Several examples of solid state phenomena, such as transformation, sub-grain formation, precipitation, etc. demonstrate the wide range of weld characteristics that have been obtained with ultrasonics (69-70).

Since the temperature rise in the weldment is determined in part by the welding conditions, a measure of control can be exercised over the microstructure produced. Previous experience with precipitation-hardenable stainless steels (71) indicated that the highest strength welds were produced at welding conditions which resulted in re-solution of the precipitate, but re-solution could be prevented by suitable adjustment of the operating conditions. Similarly, modification of welding conditions has produced satisfactory bonds in materials strengthened by cold work without microstructural evidence of recrystallization.

Table 7

MONO-METAL WELDS: COMPARISON OF TENSILE-SHEAR STRENGTH DATA

(Input Power: 6.3 to 7.5 kilowatts)

Material					Tensile Strength	
Designation	Gage (inch)	Number of Measurements	Clamping Force (pounds)	Weld Energy (kw-sec)	Old Data (pounds/spot)	New Data (pounds/spot)
Cb(D-31)	0.006	-	350	1.20	38	--
	.010	4	600-700	0.90		290
	.015	6	800-1000	3.00		243
		7	800	4.00		196
	.025	3	900-1100	3.50		330
		6	500-1100	7.00		492
		10	700-1100	10.00		577
Inconel X-750*	0.012	-	100	0.5-1.0	207	--
	.020	-	150	1.5	290	--
	.033	4	400-900	3.6		893
		3	900-1100	6.0		1287
	.040	3	1100	5.0		1937
		6	1000-1100	9.0		1268
Mo-0.5Ti	0.008	15	350-550	1.2		148
	.015	-	400	2.0	220	
	.017	-	600	3.0	250	
	.020	15	650-1050	3.6		237
	.032	3	1000-1100	7.5		293
		6	1000-1100	9.0		308
		3	1100	10.5		421
PH15-7Mo	0.008	-	350	1.5	280	
	.020	25	700-1000	1.95		1266
	.030	18	800-1000	3.90		1976
René 41	0.010	-	800	1.00	350-500	
	.020	10	600-800	6.00		380
	.030	3	1000	6.35		330
		6	800-1000	9.52		491
Tungsten	0.005	-	150	0.7	18	
	.010	-	900	2.60	75	
	.015	12	500-900	6.38		128
	.020	3	700-900	7.50		177
		4	700-900	9.00		131
	.030	11	700-1100	11.25		213
		7	900-1000	15.00		237

* Formerly designated as Inconel X.

Table 8

BI-METAL WELDS: SUMMARY OF TENSILE-SHEAR STRENGTH DATA

(Input Power: 6.3-7.5 kilowatts)

Weldment Combinations				Clamping Force (pounds)	Weld Energy (kw-sec)	Tensile Strength (pounds/spot)
Material	Gage (inch)	Material	Gage (inch)			
Cb(D-31)	0.025	Inconel X-750*	0.040	900	6.30	680
				700	9.45	680
		Mo-0.5Ti	.032	700	7.00	200
		PH15-7Mo	.030	800	3.78	1240
				800	5.04	1100
				600-1000	6.3	1110
				800	9.45	960
		René 41	.030	900	7.00	750
				900	10.50	900
		Tungsten	.030	700	6.3	90
Inconel X-750*	0.040	Mo-0.5Ti	0.032	800-1000	9.45	533
		PH15-7Mo	.030	800	3.78	820
				800	4.41	1560
				800	6.30	1118
		René 41	.030	800-1000	5.04	1753
		Tungsten	.030	900	10.50	180
Mo-0.5Ti	0.032	PH15-7Mo	0.030	800	5.60	550
				800	7.00	750
		René 41	.030	600-800	9.45	330
		Tungsten	.030	700	6.30	115
PH15-7Mo	0.030	René 41	0.030	800	4.41	1025
				800	6.30	1527
René 41	0.030	Tungsten	0.030	700	6.30	115

* Formerly designated as Inconel X.

Figure 3: TYPICAL CURVES OF WELD-ZONE TEMPERATURE AS A FUNCTION OF CLAMPING FORCE AND WELDING TIME

(Acoustic Power: 300-watts)

A. CLAMPING FORCE

(Welding Time: 1 second)

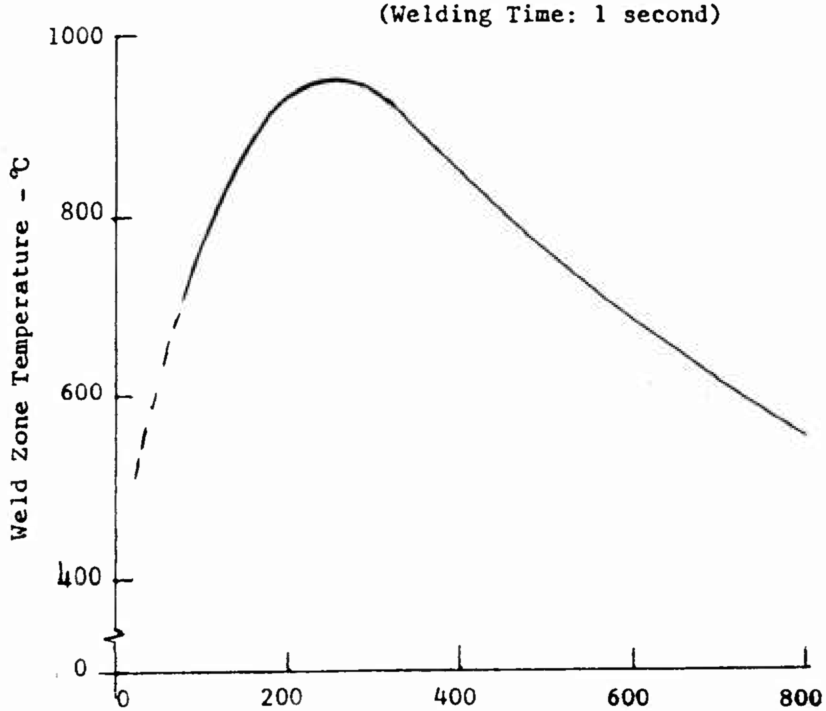

B. WELDING TIME

(Clamping Force: 200 pounds)

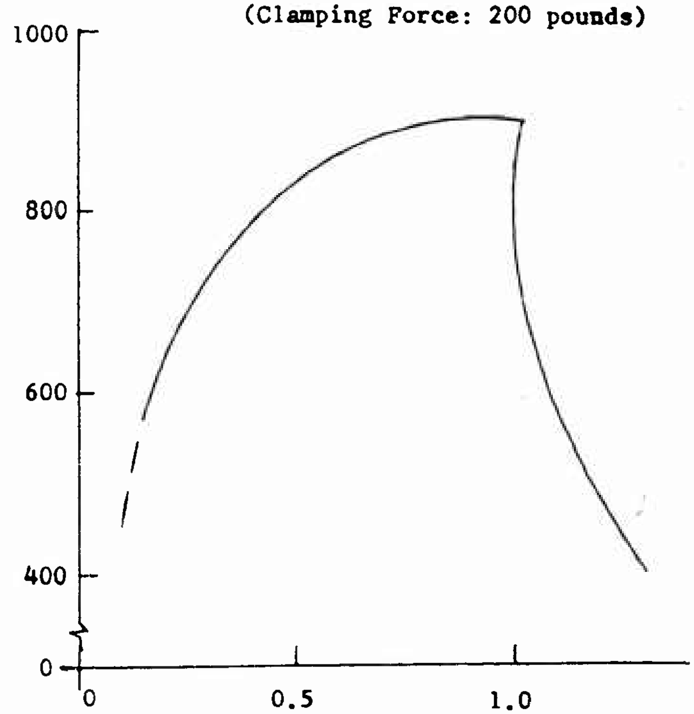

TEMPERATURE MEASUREMENTS

The transient interfacial temperature at a weld locale during ultrasonic welding is difficult to obtain but it has been accomplished with a single, fine-wire thermocouple technique (69-70). Limitation of this feasibility investigation precluded an extensive investigation of the weld-zone temperature but sufficient data were obtained to show that recrystallization need not occur.

Because of the particular interest in tungsten and the molybdenum-titanium alloy, however, effort was made to obtain such data; representative temperature records for these two materials and the temperatures achieved are shown in Figure 4. Additional work would be required to establish the absolute range. It is significant, however, that these temperatures fall below 50% of the absolute melting temperature as well as below the recrystallization temperature for both of these materials.

The recrystallization temperatures given in Table 9 represent a summary of published data and of expected transient weld-zone temperatures associated with ultrasonic welding. Thus, with delineation of suitable welding conditions, the avoidance of recrystallizations is practical.

Table 9

WELDMENT MATERIALS: MELTING AND RECRYSTALLIZATION TEMPERATURES

Weldment Materials	Melting Temperature (MT) °C	Melting Temperature (MT) °K	Recrystallization Temperatures °C	Recrystallization Temperatures °K	Recrystallization Temperatures Relative to MT (percent)[b]
Cb(D-31)	2270	2543	1000	1273	50
Inconel X-750	1393	1666	732	1005	60
Mo-0.5Ti	2625	2898	1100	1373	47
PH15-7Mo	1427	1700	840	1113	50
René 41	--	--	--	--	--
Tantalum	2996	3269	1300	1573	48
Tungsten	3410	3683	1400	1673	47

[b] Relative to absolute melting temperature.

Figure 4: TEMPERATURE RISE CURVES FOR 0.032-INCH Mo-0.5Ti AND 0.020-INCH TUNGSTEN AT WELDING POWER

A. Mo-0.5Ti (0.032-inch)

Input Power: 7.5 kilowatts
Clamping Force: 1100 pounds

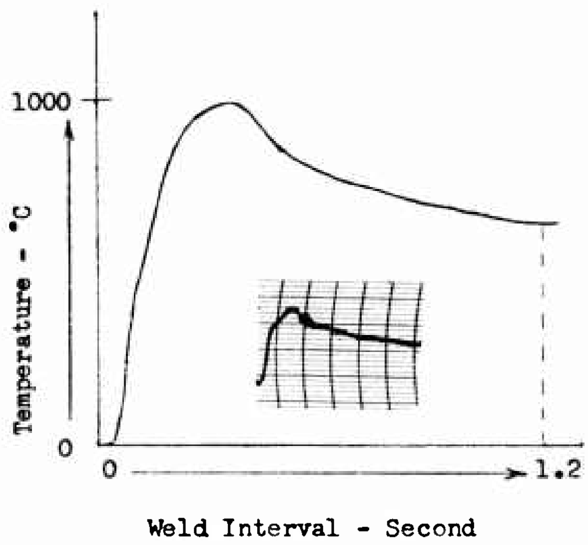

B. Tungsten (0.020-inch)

Input Power: 7.5 kilowatts
Clamping Force: 900 pounds

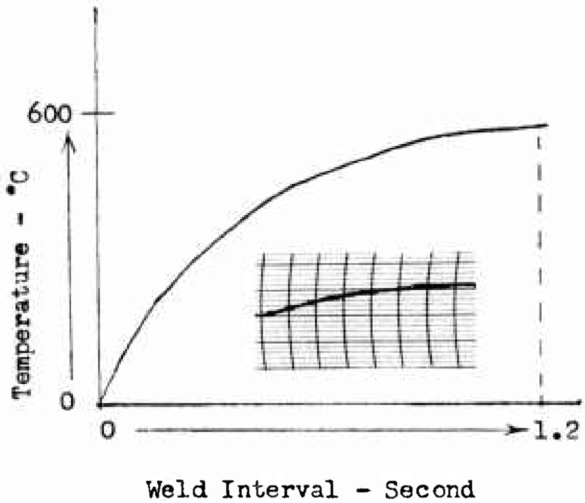

MICROSTRUCTURAL FEATURES OF WELD INTERFACE

The microstructure of the refractory and superalloys is exceedingly complex. AM-355, for example, consists of a three-phase mixture of austenite, martensite and delta ferrite. Within the martensite and ferrite there is a distribution of fine complex carbides and other finely dispersed particles. In order to properly delineate the microstructures of these alloys, an extensive program involving both optical and electron metallography, x-ray and electron diffraction is required. Superimposing the effect of the welding conditions upon the fabrication process undoubtedly affects this microstructure. To completely evaluate the changes associated with ultrasonic welding however, would require an extensive program of study of the structure of both the as-received and welded alloys.

Only a cursory metallographic examination is required, however, to furnish evidence, or the absence thereof, of recovery, grain growth (recrystallization phenomena) or surface effects such as weld interpenetration, oxide dispersion, etc. in the microstructure of the weld area. Accordingly, the microstructure of randomly selected specimens, welded in connection with the feasibility studies described in Appendix II, were studied optically. The specimens were selected to include all of the mono- and bi-metal combinations of the refractory materials. The results of these examinations are described below and are discussed in connection with the strength data reported in Tables 7 and 8, while photomicrographs of the weld area are presented in Figures 5 and 6.

MONO-METAL WELDS

Cb(D-31) Alloy (0.015-inch):

This weld was characterized by only small amounts of interpenetration along the faying surfaces. The grain structure appears uniform throughout the welded sheet. No grain growth or other evidence of recrystallization was observed within the weld zone, indicating a negligible thermal effect on the alloy structure (see Figure 5a). The original interface is visible throughout the length of the bond. Coupling these observations with the weld strength data, indicates that ultrasonic bonding was established without any changes in sheet microstructure.

Inconel X-750 (0.015-, 0.020-, 0.030-inch):

Good metallurgical bonding was achieved in three gages of the Inconel X-750 alloy. The micrograph shown in Figure 5b illustrates the unique microstructural characteristics of welds made in this and similar materials. Within the weld region, the microstructure assumes a block-like appearance

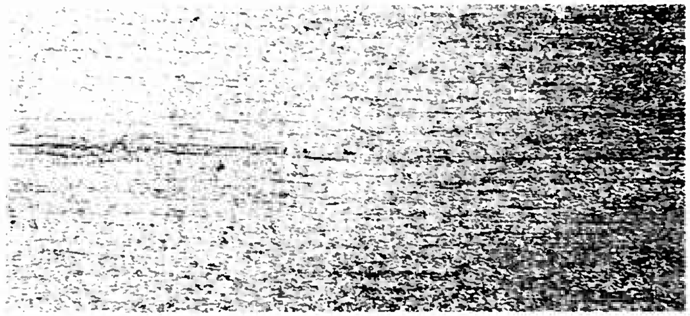

a. Cb(D-31), 0.015/0.015 Inch (40X)

b. Inconel X-750, 0.033/0.033 Inch (30X)

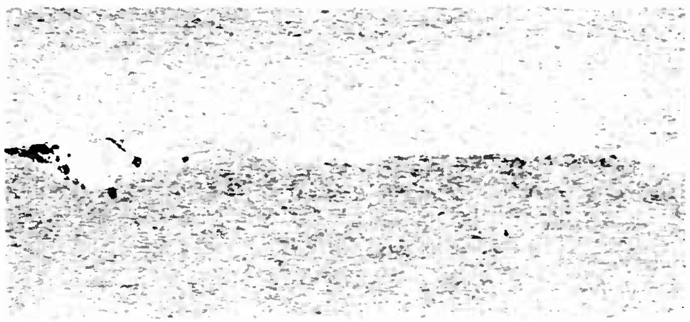

c. Mo-0.5Ti, 0.030/0.030 Inch (40X)

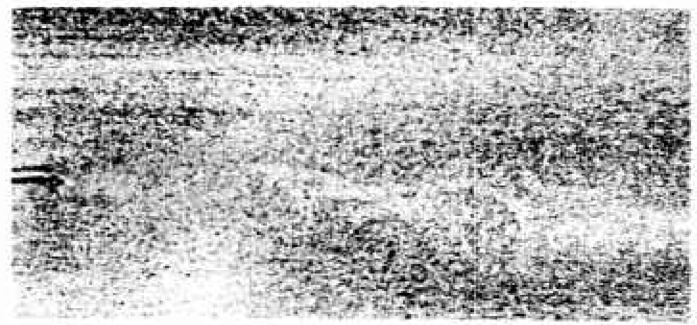

d. PH15-7Mo, 0.030/0.030 Inch (40X)

e. René 41, 0.010/0.010 Inch (40X)

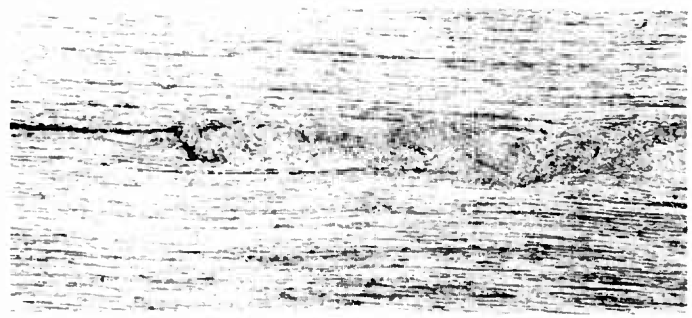

f. Tungsten, 0.015/0.015 Inch (60X)

Figure 5: MONO-METAL WELD MICROGRAMS

Figure 6: DISSIMILAR-METAL WELD MICROGRAMS

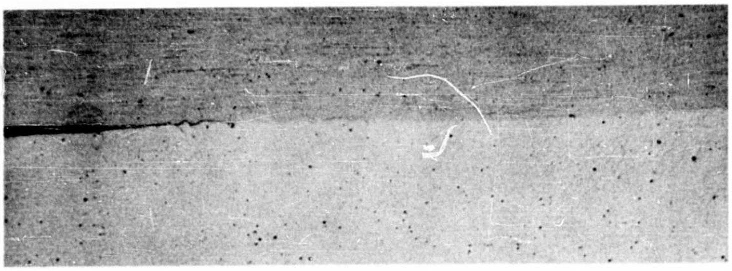

A. Tungsten (0.030-inch)
Inconel X-750 (0.040-inch)
(40X)

B. Tungsten (0.030-inch)
Mo-0.5Ti (0.032-inch)
(40X)

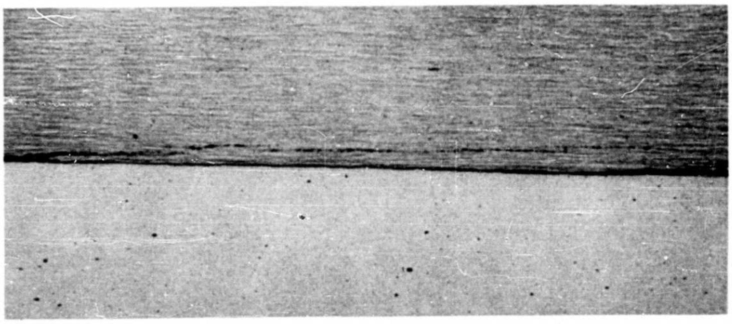

C. Tungsten (0.030-inch)
PH15-7Mo (0.030-inch)
(40X)

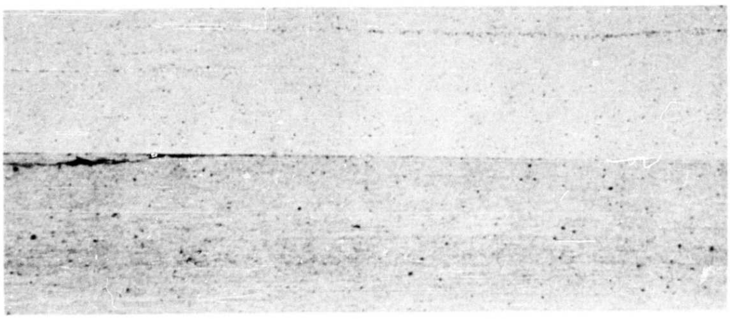

D. René 41 (0.030-inch)
PH15-7Mo (0.030-inch)
(40X)

(Concluded on Next Page)

Figure 6: (Continued from Previous Page)

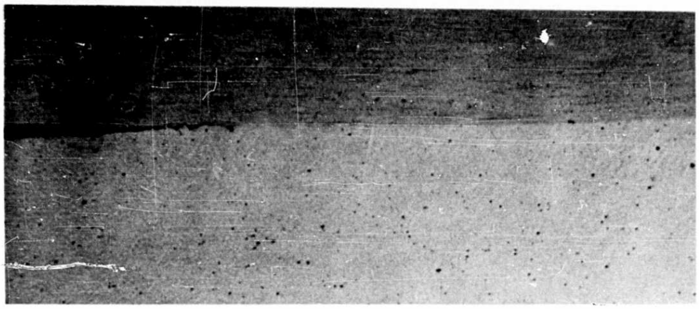

E.
Cb(D-31) (0.025-inch)
PH15-7Mo (0.030-inch)
(40X)

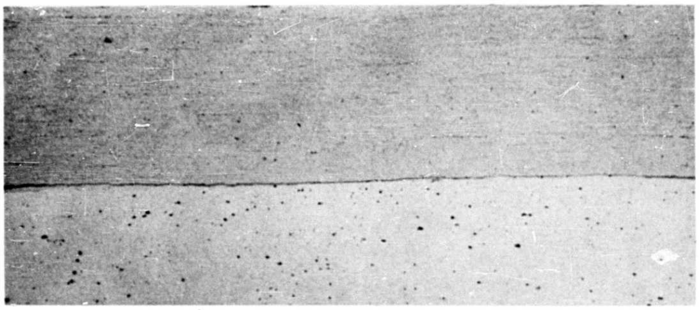

F.
Cb(D-31) (0.025-inch)
Inconel X-750 (0.040-inch)
(40X)

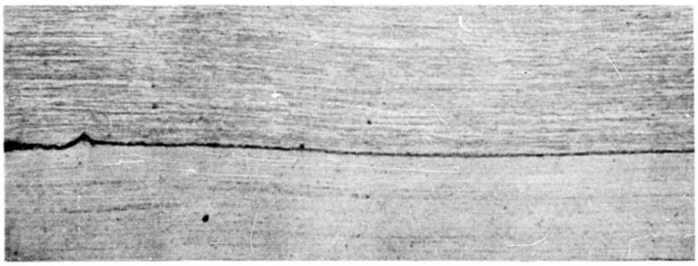

G.
Cb(D-31) (0.025-inch)
Mo-0.5 Ti (0.032-inch)
(40X)

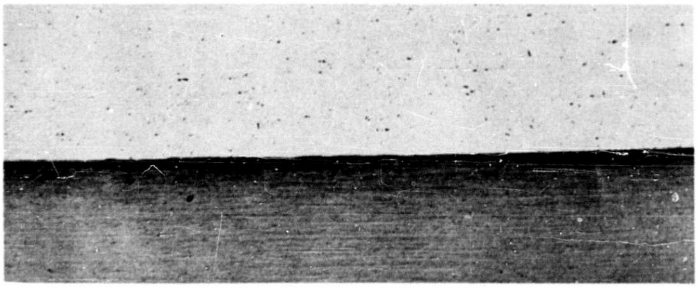

H.
Mo-0.5Ti (0.032-inch)
Inconel X-750 (0.040-inch)
(40X)

possibly resulting from subgrain formation and orientation of the grain boundaries. Orientation effects probably arise from the vibratory stresses to which the material was subjected during welding. Grain refinement occurred adjacent to the weld zone. The high degree of plastic turbulence within the periphery of the weld spot evidenced by the block-like grain structure, also produced some extrusion of plasticized weld material between the sheets. The good weld strengths reflect the bond-achieved without any occurrence of grain growth. The unique characteristics of these weld microstructures deserve further study; however, additional investigation is not within the immediate scope of this program.

Mo-0.5Ti (0.008-, 0.020-, 0.032-inch):

Excellent metallurgical bonding was achieved in all three gages of the molybdenum-0.5 titanium alloy investigated. The bonds were characterized by mutual interpenetration of the faying surfaces and negligible reduction in thickness. Very small interface and edge cracks were observed in some specimens. A region is observed along the interface which is etched lightly as shown in Figure 5c. This probably arises from localized grain refinement along the weld interface. No grain growth was observed in any of the welded specimens. The variability of the weld strength data is probably due to the presence of the fine cracks observed in some of the samples but such cracks and the associated strength variation can be eliminated. The high strength data is indicative of the ability of ultrasonic welding to produce welds of good integrity in this alloy.

PH15-7Mo (0.020-0.030-inch):

Satisfactory welds were achieved in all gages of the PH15-7Mo alloy. A thin sliver of extruded plasticized material was observed at the edge of several of these welds. Some differences were observed in the etching characteristics along the weld interface. It is difficult to establish the cause of this etching behavior. The bond itself was achieved without extensive interpenetration of the faying surfaces (see Figure 5d). The high weld strengths obtained are indicative of the excellent metallurgical bond achieved.

René 41 (0.010-inch):

The lack of interfacial turbulence and the large heat-affected zone, Figure 5e, indicate that this weld was not made at machine settings closely associated with the M.E.C.

The strength of welds between 0.010-inch René 41 sheet was of the proper order, but in heavier gages, the strength of these welds also indicate improper machine settings. It is significant that the bi-metal combination, involving René 41, did not exhibit serious heat effects (see Figure 6D); thus additional work will establish machine settings productive of a quality weld, free of serious heat-affected zones.

Tungsten:

Both in mono-metal and bi-metal combination, tungsten proved to be the most troublesome material to weld. Inasmuch as the estimated power required to join this material was based on a reported 300 VHN instead of 460 (the hardness value measured in our laboratory) considerable effort was expended at inadequate power levels. Differences were noted between the sheet stock acquired for this work and other stock studied previously; "in plane" cracks or delamination, constituted an altogether different type of problem than has been observed with other material. Nevertheless, the micrograph of Figure 5e indicates satisfactory bonding and while the strength values of Table 8 are not impressive, it can be concluded that joining tungsten is feasible. Work with more sophisticated controls, already shown to be effective in ultrasonic welding (Power-Force programming) (72) will permit ultrasonic joining of tungsten on a practical basis.

BI-METAL WELDS

Illustrations of welds between tungsten and Inconel X-750, tungsten and molybdenum-0.5Ti as well as tungsten and PH15-7Mo, are shown in Figure 6A, B, and C, respectively. The dissimilar metal welds involving tungsten had one feature in common, bonding was achieved at the sheet interface, but delamination occurred within the tungsten sheet away from the interface.

The tungsten-Inconel X-750 weld was satisfactorily bonded with mutual interpenetration at the periphery of the weld; the block-type grain structure was observed within the weld region of the Inconel X-750 sheet. Interdiffusion at the weld interface was not observed.

The weld between tungsten and molybdenum-0.5Ti shows exceptional interpenetration of the mating surfaces, accompanied by some delamination failure of the tungsten adjacent to the interface. The etching characteristics of the molybdenum-titanium sheet near the weld interface suggest some microstructural effect, although no evidence of recrystallization was observed.

The tungsten-PH15-7Mo couple exhibited edge extrusion of the PH15-7Mo material between the weld sheets, similar to mono-metal welds in this latter material. The etching characteristics of the material in the region of this extrusion again suggest local re-solution softening. Similar edge extrusion was observed in the weld between PH15-7Mo and Cb(D-31) alloy (Figure 6E).

The bond between the PH15-7Mo and Rene 41, shown in Figure 6D, indicates a well-defined interface without interpenetration. No interdiffusion along the interface was observed optically. Although the quality of these bonds cannot be determined metallographically (evidence of structural continuity is lacking), the weld strength (see Table 8) alone appears sufficient to establish the quality of these joints.

The dissimilar metal welds made with the Cb(D-31) alloy, shown in Figure 6E, F, and G, illustrate the individual structural effects which are obtained in each component of the weld as a result of the heat dissipation and vibratory stress. The bond between the Cb(D-31) and Inconel X-750 displays the local grain refinement effects in the Inconel X-750 near the interface similar to the structure developed in mono-metal Inconel X-750 welds. As in the mono-metal welds of the Cb(D-31) alloy, no significant thermal effects were observed. Microstructural evidence of a constituent along the interface, which is probably an alloy layer resulting from interdiffusion of the weld components, was observed. The weld between the Cb(D-31) and the PH15-7Mo, however, did not exhibit a similar layer at the interface, although edge extrusion of the PH15-7Mo material on one side of the weld was evident. The lack of any degree of interpenetration, and the continuity of the bond line across the weld between the Cb(D-31) alloy and the molybdenum-0.5Ti makes metallographic interpretation of bond quality between the materials unreliable.

The weld between the Mo-0.5Ti and Inconel X-750, shown in Figure 6H, displays characteristics which are essentially similar to mono-metal welds made in each material. The particular grain pattern of each material is developed within the weld zone and a high degree of plastic turbulence is evident in the periphery of the weld.

The bi-metal weld combinations exhibited reasonable weld strengths. These are indicative of the achievement of ultrasonic bonding. The strengths of tungsten combination welds were most variable, probably due to the inherent cracking observed within the sheet but away from the weld zone. The structural characteristics of the bi-metallic joints were essentially the same in each component as those observed for the same components of the mono-metallic welds.

It is apparent from these studies that ultrasonic welding will achieve bond formation in these materials without the accompanying problem of grain growth due to temperature effects and recrystallization associated with fusion welding.

Since this work is a limited feasibility study, virtually no effort could be expended to optimize weld conditions. Use of the proper welding parameters, however, will give better and more representative results. The feasibility of joining all materials except tungsten is quite favorable. Welding of tungsten will require special attention, particularly with regard to delamination, unless the weakness of the parent stock is alleviated by the manufacturer.

II. WELDING ENERGY REQUIREMENTS

"STUDY THE ENERGY REQUIREMENTS FOR WELDING INCONEL X-750, COLUMBIUM-Mo-10Ti, MOLYBDENUM-0.5Ti, PH15-7Mo STEEL, RENÉ 41 AND TUNGSTEN."

INTRODUCTION

The energy requirements for vibratory welding a variety of materials, including some of the refractory metals, have been studied extensively. Appropriate equipment, techniques, and instrumentation were developed for identifying the various critical factors associated with the delivery of ultrasonic welding energy and for measuring the magnitude of such factors (including weld-zone temperature (69-70). Experience and information, accumulated for welding thin gages of refractory metals (such as columbium-10Mo-10Ti, molybdenum-0.5Ti, tantalum and tungsten) and of superalloys (such as PH15-7Mo, AM-355, Inconel X-750, and René 41), were assembled. (See Section I).

PREDICTING WELDABILITY AND POWER REQUIREMENTS

On the basis of earlier fundamental ultrasonic welding research (70), a first approximation criterion for determining the energy required to produce a simple lap-type spotweld between two sheets of metal, in terms of single sheet thickness and material hardness, was postulated and defined by the equation

$$E = K H^{3/2} t^{3/2}$$

where E = energy in joules (watt-seconds)
H = Vickers microindentation hardness number
t = thickness of one sheet of the material -- inches
K = a constant which incorporates other contributing factors.

By proper selection of K the following can be computed:

1. acoustical energy into the weldment or,
2. electrical energy into a specific magnetostrictive transducer or,
3. electrical energy into a specific electrostrictive transducer,
4. etc.

This equation was initially derived from experimental data obtained over a period of time for both common and exotic materials, but its use can also be justified on the basis of fundamental ultrasonic theory (70). As will

be evident later, weld energy requirements estimated by means of this equation apparently are reliable for various types of materials in specific gages and of different hardnesses. This equation is based upon the simplest type of welding situation in which two sheets of equal thickness are joined by means of a single spot-type ultrasonic weld.

Such techniques as the use of foil interleaf (73) power-force programming, etc., are not considered in estimating energy values by this equation.

Using this equation, the acoustical energy required to weld 0.10-inch material was computed for several metals -- these values are shown in column 3 of Table 10. The acoustical power demanded of the welding equipment to produce such welds, at different weld intervals, is shown in columns 4-5-6 of Table 10. The estimated acoustical energy values are also shown in Figure 7 for gages 0.10-inch or less of the six weldment materials.

Table 10

WELDMENT MATERIALS: ESTIMATED ACOUSTICAL ENERGY AND POWER REQUIREMENTS FOR WELDING 0.10-INCH MATERIAL

Weldment Materials		Estimated	Weld Interval (sec)		
Designation	Hardness VHN[a]	Acoustical Energy (kw-sec)	0.1	0.5	1.0
			Power Required - kilowatts		
Cb(D-31)	195	5.4	54	11	5
Inconel X-750	165	4.2	42	8	4
Mo-0.5Ti	265	9.2	92	18	9
PH15-7Mo	180	4.8	48	10	5
René 41	380	14.8	148	30	15
Tungsten	490	22.4	224	45	22

[a] Vickers Hardness Number as measured for the materials in the received and used condition - see Tables 1-3 for material condition.

Figure 7: ACOUSTICAL ENERGY CALCULATED FROM ENERGY EQUATION *

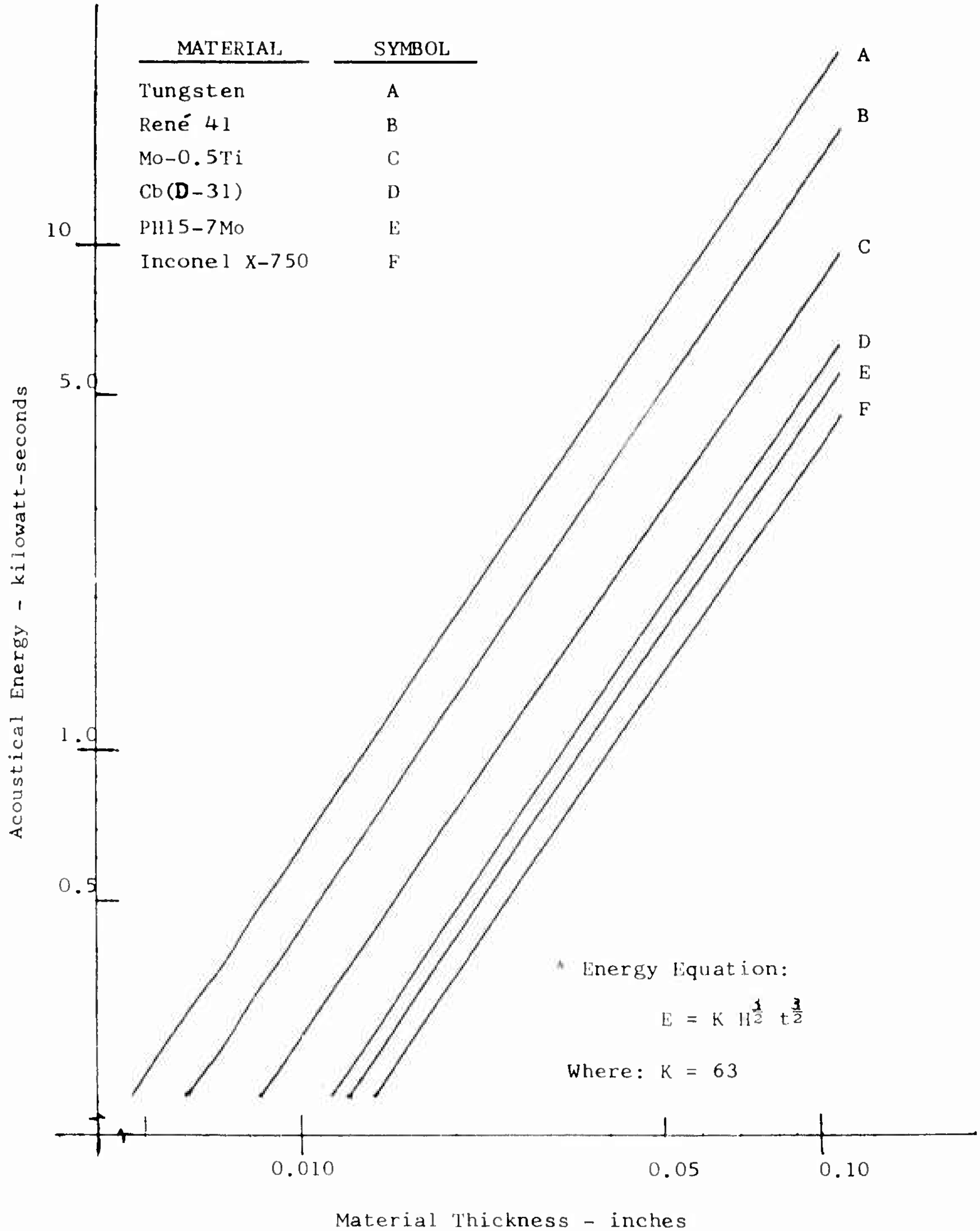

In Figure 8, the electrical power that must be delivered into a nickel transducer to join 0.10-inch or lighter gages of all the material is indicated for each metal. (Values of "K" used in these calculations are noted on both Figures 7 and 8.) Points corresponding to the electrical power actually delivered into nickel transducers, when these materials were welded, are also shown in Figure 8. These points were based either on old data or that obtained with the 6-8 kw laboratory welding array in the experimental work described in Appendix II. A different symbol is used for each material. While specimens were welded at various energy levels (see Appendix II), the experimental data shown in Figure 8 and tabulated in Table 11, represent welding experience at energy levels comparable to those derived from the energy equation and approximating minimum energy conditions (MEC).

In the foregoing paragraphs, the electrical input power and the corresponding acoustical power required at various weld intervals, to join the stipulated gages of the specified weldment materials have been delineated. Data accumulated from earlier investigations and results of the work done in the course of this program confirm the reliability of the energy equation and its applicability to the specified weldment materials; this work also shows that the electrical energy delivered into a magnetostrictive nickel transducer is about five times the acoustical energy requirements. The validity of the "K" values, 63 and 315, for acoustical and electrical energy, respectively, as well as an overall transducer efficiency of 20 percent, was also confirmed by this work. Transducer efficiency will be discussed more fully in Section IV.

The following factors will operate to reduce the disparity between electrical and acoustical power requirements:

1. Power Force Programming
2. Foil Interleaf
3. Altered Tip Radius
4. More Efficient Transducers and Coupling Systems.

SEAM WELDING

As established in previous investigations*, the actual energy requirements for continuous roller seam welding are in close agreement with those predicted for various materials by the energy equation. Because of low welding speed (about six inches per minute), however, the power requirements associated with seam welding correspond roughly to the acoustical power level in column 6 of Table 10. Energy considerations and the limitations imposed by the terminal element (disk) design (see Appendix V) of the transducer-coupling system, therefore, preclude the immediate development of a roller seam welding machine for joining the materials of interest in this program. This will be discussed in greater detail in Section V.

* Unpublished work.

Figure 8: ELECTRICAL INPUT ENERGY AS A FUNCTION OF MATERIAL THICKNESS

CALCULATED AND EXPERIMENTALLY DETERMINED VALUES

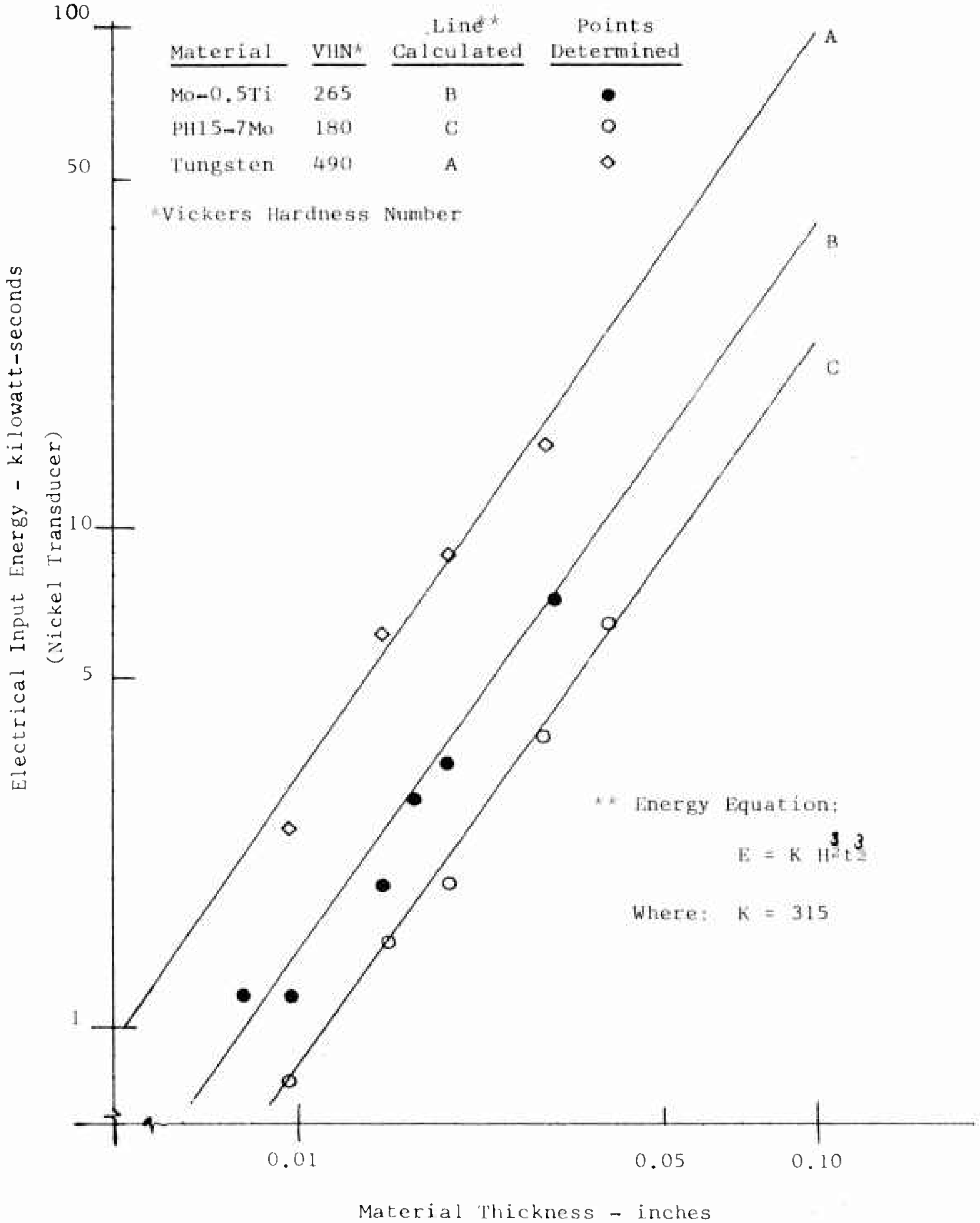

(Concluded on next page)

Figure 8: (Continued from previous page)

CALCULATED AND EXPERIMENTALLY DETERMINED VALUES

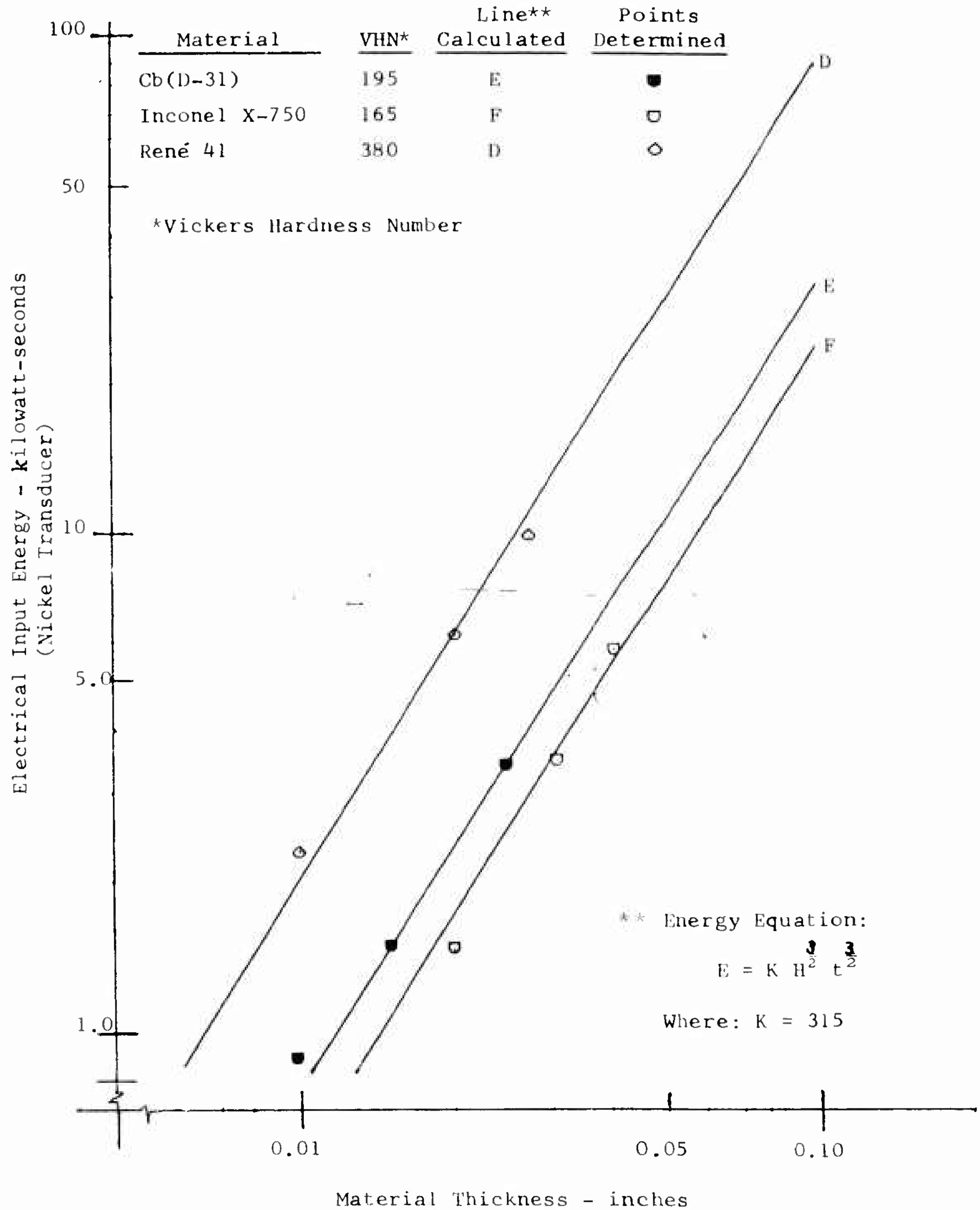

Table 11

ELECTRICAL INPUT ENERGY REQUIRED
TO WELD MATERIALS OF VARIOUS THICKNESSES

Weldment Material	Tensile Shear Strength* Old Data (pounds/spot)	Tensile Shear Strength* New Data (pounds/spot)	Specimens Tested (number)	Material Thickness (inch)	Electrical* Energy (kw-sec)
Cb(D-31)	38	--	--	0.006	1.20
	--	220	11	.010	1.00
	--	205	9	.015	2.25
	--	330	3	.025	3.50
Inconel X-750	207	--	--	0.012	0.5-1.0
	290	--	--	.020	1.5
	--	725	6	.033	4.0
	--	1100	11	.040	6.8
Mo-0.5Ti	--	145	27	0.008	1.2
	220	--	--	.015	2.0
	250	--	--	.017	3.0
	--	235	15	.020	3.6
	--	300	9	.032	8.2
PH15-7Mo	280	--	--	0.008	1.5
	--	1265	25	.020	2.0
	--	1975	18	.030	3.9
René 41	350-500	--	--	0.010	1.5
	--	380	10	.020	6.0
	--	491	3	.030	6.4
Tungsten	18	--	--	0.005	0.7
	75	--	--	.010	2.6
	--	130	12	.015	6.7
	--	150	7	.020	8.3
	--	450	18	.030	13.2

* Average values.

In connection with other work, a different approach to the problem of the seam-welding, tip is under development. This new equipment, which is suitable for welding hard, high temperature materials, could not be performance tested in time to meet the work schedule for PHASE I hereof. Preliminary data for this new system, however, indicates a major breakthrough in ultrasonic welding. Probably this equipment can be evaluated with the stipulated weldment materials in the course of PHASE II of this program.

III. ACOUSTICAL MATERIALS SURVEY

"SURVEY OF CURRENT AND PROJECTED STATE-OF-ART MATERIALS FOR THEIR APPLICATION AS TRANSDUCERS AND ASSOCIATED EQUIPMENT WITH THE OBJECTIVE OF DELIVERING SUFFICIENT POWER TO JOIN THE SELECTED MATERIALS IN THICKNESSES UP TO 0.10 INCH."

("TRANSDUCERS AND ASSOCIATED EQUIPMENT" embrace the entire electro-acoustical system -- from the wired connections for electrical energy input to the point of vibratory energy output in the locale where the transducer-coupling tip contacts the weld area.)

TRANSDUCER MATERIALS

Ideally, a superior transducer material for ultrasonic welding equipment should:

1. Convert alternating-current, electrical energy into mechanical vibratory energy with high efficiency.

2. Have a capacity to convert high levels of electrical power into high levels of vibratory power.

3. Resist high stresses, both electrical and mechanical, without fatigue or failure.

4. Provide an acoustic impedance (ρc) that is readily matched into the material and into the cross-section of the coupling material into which the vibratory power is radiated.

5. Exhibit a high coefficient of thermal conductivity.

6. Possess a high Curie temperature.

7. Be available in appropriate sizes and be convenient to fabricate and join.

The transducer materials, in general, fall into two categories: 1) magnetostrictive metallic and 2) electrostrictive ceramic.

During recent years, a wide variety of magnetostrictive metallic materials have been evaluated in experimental- and production-type ultrasonic welding arrays. These materials have a lower efficiency than some of the electrostrictive ceramics but, with metallurgical methods such as brazing, rugged and durable systems that are relatively insensitive to overloading can be built. Furthermore, such magnetostrictive systems can be operated without permanent damage at temperatures much higher than could be tolerated by any ceramic available until recently. Nickel has been the most effective and widely used of the magnetostrictive materials. Most ultrasonic welding equipment incorporates laminated stacks of thin, annealed "A" nickel sheets which are satisfactory for heavy-duty, continuous operation.

The electrostrictive, barium titanate ceramic, currently used in certain types of ultrasonic equipment, dates back to about 1950 when the material was investigated extensively and used in ultrasonic arrays for solid-state metal treatment. Since that time, barium titanate has been used in ultrasonic arrays for various purposes. While its electromechanical conversion efficiency is higher than that of magnetostrictive materials, barium titanate has not been used extensively in production-type ultrasonic welding equipment because ceramic transducers of this type are fragile and somewhat difficult to install on a practical basis in coupling systems. Furthermore, its low Curie point (120°C) introduces an almost insurmountable cooling problem -- overheating must be avoided to prevent depolarization.

Recently, effort has been directed toward the development of new ceramic materials which will withstand high temperatures. These newer ceramics include such family groups as titanates, niobates, tantalates, and zirconates. One of the most promising of the new materials is lead zirconate titanate, which has a reported Curie temperature of about 340°C and a high electromechanical coupling coefficient. Large-size transducers have been fabricated from this material (designated as Brush Type PZT-4) and evaluated.

In order to bring the transducer material problems into focus, available data (31, 74-86) on magnetostrictive and electrostrictive types were compiled, or calculated, and summarized in Tables 12 and 13. In a final effort to ascertain if the materials listed in Tables 12 and 13 are indeed representative of the current and projected state of technology for transducers, personnel in organizations (87-95) that are clearly in a position to provide meaningful and valid opinions were consulted.

These men generally agreed that current developments are being directed to the improvement of analytical techniques for establishing the composition of transducer materials and to the refinement of manufacturing processes and thus optimizing the performance of the materials listed in Tables 12 and 13. It was therefore concluded that standard "A" nickel

Table 12

TRANSDUCER MATERIALS: PHYSICAL AND THERMAL PROPERTIES (31, 74-86)

Transducer Materials	Curie Temperature (°C)	Density (ρ) 10^3 (kg/m^3)	Velocity of Sound (c) (m/sec)	Linear Coeff. of Thermal Expan. 10^{-6} (m/cm-C)	Thermal Conductivity (K) $10^{-3} \frac{(\text{Kcal-m})}{(\text{m}^2\text{-sec-C})}$	Thermal Diffusivity $\alpha = K/\rho c$ 10^{-6} (m^2/sec)	Specific Heat (c) (Kcal/kg-°C)
ELECTROSTRICTIVE:							
Lead Titanate Zirconate							
PZT-4	340	7.5	3960	2.2-4.0[c]	0.30	0.40	0.10
PZT-5	340	7.5	3590	2.2	.30	.40	.10
Barium Titanate[a]	120	5.5	5680	6.8[d]	.60	.91	.12
Lead Metaniobate[b]	500	5.9	3125	---	--	--	--
MAGNETOSTRICTIVE:							
Nickel - "A"	360	8.9	4780	13.3	14.5	12.5	0.13
- 204	410	8.9	4790	13.3	12.1	10.5	.13
2V Permendur	525	8.2	5260	9.5	--	--	--
Alfenol	500	6.7	4500	--	--	--	--

a Brush Ceramic (B)
b General Electric (LM-391)
c 25°-300°C
d 25°-75°C.

Table 13

TRANSDUCER MATERIALS: DESIGN CHARACTERISTICS (31, 74-86)

Transducer Materials	Electro-Mech. Coupling Coeff. (K_{33})	Power Handling Capacity[a] 10^4(watts/m^2)	Piezoelectric Strain 10^{-12}(m/volt)	Magnetostrictive Stress (λ) 10^6(Newtons/weber)	Characteristic Specific Impedance (Z_1) 10^7(kg/m^2-sec)	Driving Impedance
ELECTROSTRICTIVE:[b]						
Lead Titanate Zirconate-PZT-4	0.64[d]	15[f]	256		3.1	Intermediate (500-1000 volts per millimeter thickness)
PZT-5	.67	--	320		2.7	
Barium Titanate	.50[e]	12	150		3.1	
Lead Metaniobate	.40	--	90		1.8	
MAGNETOSTRICTIVE:[c]						
Nickel - "A"	0.30-.35	8		16.7-20	4.3	Adjusted by controlling number of coil turns.
- 204	.50-.60	9		32	4.3	
2V Permendur	.23-.30	12		21	4.3	
Alfenol	.27-.29	--		6.7	3.0	

[a] Reported for continuous operation with only moderate cooling.

[b] Practical Joining Methods: adhesives or mechanical.

[c] Practical Joining Methods: Usually by brazing.

[d] At 100°C

[e] At 75°C

[f] For thin wafer-type units the above is correct, although direct communication with Clevite Research Center, Cleveland, Ohio, indicates that 6 watts/cm^3/kc is a more realistic way of reporting this value

and lead zirconate titanate are representative of the current and projected state of the art for magnetostrictive and electrostrictive transducers, respectively, and are suitable for high power transducer coupling systems.

COUPLER MATERIALS

Parallel with consideration of transducer materials, candidate coupler metals were surveyed and the problems involved in selecting coupler materials for specific application were identified.

Couplers for ultrasonic welding systems are not ordinarily exposed to high temperature environments so, from that point of view, the requirements are straightforward. The engineering strength factors, however, have not been adequately explored under cyclic loading in the frequency range of interest (between approximately 5,000 and 40,000 cycles per second). For this and other reasons, which will become evident later, coupler material selection is not yet altogether determinate. Essentially, material for a coupling element or system in an ultrasonic welding machine must:

1. Permit a reasonable impedance match with adjacent system-components such as transducers.

2. Transmit high-cyclic stress without fatigue.

3. Exhibit low vibratory energy losses at levels of cyclic stress attendant to transmission of the requisite levels of vibratory power.

4. Have engineering practicability, i.e., it must be

    a. Available in suitable sizes

    b. Practical to fabricate

    c. Capable of carrying the non-vibratory loads imposed

    d. Metallurgically joinable (welding or brazing).

The background, which serves as the basis of this survey, included studies, sometimes cursory and sometimes in depth, of such materials as titanium, aluminum, R Monel, K Monel, and, recently, aluminum bronze. So far as is known aside from the above requirements, there are no other theoretical justifications for selecting a candidate coupler material. Some information concerning coupler materials has appeared in the patent literature, some in research investigations on tangent subjects by various investigators, and some have evolved from previous experience

in our own laboratory. Observations based on the practical application of the aforementioned materials are interesting: for example, the replacement of a steel coupler with one made of K Monel in one type of seam-welding equipment, permitted an increase of up to two gages in the thickness of the material that could be effectively welded at a constant energy input -- thus, acoustical attenuation of K Monel was substantially lower than that of steel

As a result of 15 inquiries sent to likely sources of information on potential coupler materials (96-110), replies from Dr. Robert E. Maringer, Lazan, Head of the Department of Aeronautical and Engineering Mechanics, University of Minnesota; Dr. Russell W. Mebs, Physicist, National Bureau of Standards; and, Dr. Julius J. Harwood, Engineering and Research Staff Ford Motor Company, provided information that brought the current work into sharper focus.

In particular, their information reaffirmed the inapplicability of data from low-frequency torsional pendulums, or from ultrasonic attenuation in the megacycle range, to our problem. Little data are available at relatively high strain amplitudes in the frequency range of 5,000 to 50,000 cycles per second, and values which are available for low strain amplitude are unlikely to reflect, to any appreciable degree, the damping figures at higher amplitudes.

As a general rule, some relationship between fatigue limit and damping probably exists at high strain levels. Fatigue in a metal occurs when stresses are high enough to induce movement of internal defect structures, usually dislocations (111), and this movement produces damping; thus, for a given stress level, higher damping would be expected for materials with lower endurance limits. Caution is suggested in using this hypothesis because other mechanisms also contribute to damping, and the above generalization may not always be applicable.

A study was conducted by Professor Lazan (112) wherein two types of damping were investigated. The first involved internal damping of the materials -- this is associated with stress-strain hysteresis. The second type, referred to as joint or external damping, is associated with the relative motion at a joint interface. Our concern is with the problem of minimizing internal energy dissipation in materials, whereas maximizing damping and suppressing vibrations forms the basis of Lazan's work. Almost without exception, the latter type of damping comprises the basis of previous research in this field. Unfortunately, most of the materials examined by Lazan were selected for their relatively high damping properties -- consequently, materials which would be of interest for use in ultrasonic welding systems were not included.

Accordingly, for want of a better theoretical understanding of the mechanism of internal friction and its relationship to the frequency range of importance in vibratory welding, we can only rely on those materials, which have been found by various means either to exhibit good performance characteristics, or to show promise of satisfactory performance. The beryllium-copper alloy, for example, was selected for evaluation on the basis of its similarity to aluminum bronze and because of its known performance as a spring material.

Inasmuch as all the materials of Tables 14 and 15 can be obtained in suitable sizes, and since they can carry the non-vibratory load imposed satisfactorily, it was deemed advisable to consider their machineability and joining characteristics. This information is summarized in Table 16. The engineering practicability of all these materials is indicated as being potentially satisfactory.

Table 16

COUPLER MATERIALS: MACHINING AND JOINING CHARACTERISTICS

Coupler Material	Machining	Welding**	Brazing	References
Al-Bronze	1	1	1	117
Be-Copper	1	1	1	31
Inconel X-750*	1	1	1	121, 122
K Monel	2	1	2	124
Stainless Steel (300 Series)	1	1	1	31, 125
Steel (Carpenter 883)	1	1	1	31, 125
Titanium (6Al-4V)	2	2		31, 127

1: Not difficult, satisfactory.
2: Somewhat difficult.

* Formerly designated Inconel X
**Data concerning the performance of welded joints are not available.

Table 14

COUPLER MATERIALS: THERMAL AND MECHANICAL PROPERTIES (31, 114-127)

Coupler Materials	Linear Coefficient Thermal Expansion 10^{-6}(m/m-C)	Thermal Conductivity(K) $10^{3}\ \frac{\text{Kcal-m}}{\text{m}^2\text{-sec-°C}}$	Thermal Diffusivity (α) 10^{-6}(m^2/sec)	Ultimate Tensile Strength 10^{8}(Newtons/m^2)	Yield Strength (0.2% offset) 10^{8}(Newtons/m^2)
Al-Bronze	16.2	9.1	11.3	7.6	3.6
Be-Copper	16.7	13.7	16.6	5.8-8.9	5.1-7.2
Inconel X-750	13.7	3.0	3.2	11.5	6.2
K Monel	14.4	4.2	3.9	11.3	8.1
Stainless Steel[a]	17.3	3.8	4.0	6.2	2.4
Tool Steel[b]	11.0	6.7	7.7	7.2	4.7
Titanium (6Al-4V)	9.5	1.7	2.9	10.0	9.3

[a] Series 300

[b] Carpenter 883

Table 15

COUPLER MATERIALS: ACOUSTICALLY RELEVANT PROPERTIES (31, 41, 114-127)

Coupler Materials	Density (ρ) (Kg/m^3)	Young's Modulus (E) 10^{10}(Newtons/m^2)	Shear Modulus (μ) 10^{10}(Newtons/m^2)	Poisson's Ratio (σ)	Velocity: Shear $c_s = \sqrt{\mu/\rho}$ (m^2/second)	Velocity: Rod $c_1 = \sqrt{E/\rho}$ (m^2/second)	Shear Impedance $Z_s = \sqrt{\mu\rho}$	Characteristic Specific Impedance $Z_1 = \sqrt{E\rho}$ 10^7(Kg/sec-m^2)
Al-Bronze	7.58	12.5	4.6	0.350	2470	4060	1.87	3.08
Be-Copper	8.23	11.7	4.3	.350	2310	3800	1.90	3.12
Inconel X-750	8.51	21.4	8.3	.290	3110	5000	2.65	4.25
K Monel	8.46	17.3	6.6	.320	2760	4480	2.33	3.79
Stainless Steel[a]	7.90	19.3	7.4	.285	3140	5030	2.48	3.97
Tool Steel[b]	7.84	20.4	7.8	.300	3160	5100	2.47	3.98
Titanium (6Al-4V)	4.43	11.4	4.3	.340	3100	5076	1.37	2.25

[a] Series 300

[b] Carpenter 883

TIP MATERIALS

Delivery of vibratory energy to the weldment exposes the terminal tip of the sonotrode to high dynamic stresses and elevated temperatures for short time periods -- these conditions can quickly damage a tip. The relationship of tip performance to the dynamic stress distribution, associated with the tip-weldment interface (69-70), and to the physical characteristics of various tip materials has been considered previously.

Ordinary tool steels provide satisfactory performance and tip-life in welding aluminum and copper alloys, while Inconel X-750 tips are satisfactory for welding mild steels, titanium, zirconium and similar alloys. In welding high-strength, high-temperature, hard, and brittle metals and alloys, the life of tool steel tips has been short, but, Inconel X-750, in the heat-treated and aged condition, provided a substantial improvement. Type 301 stainless steel can be welded with a wide range of tip materials but the selection of a terminal element material for welding AM-355 steel is more critical. Only Inconel X-750 exhibited a reasonable tip-life in welding this type of steel.

The relatively new nickel alloy, Astroloy*, with superior high-temperature properties, exhibited extended life and good performance in joining several high-strength, high-temperature alloys.

Several kinds of spot-type welding tips have been investigated (see Section V). Examples are a full tip, silver-brazed to the coupler, and a tapered insert tip, which is used for certain materials that are either obtainable only in rod stock or cannot be readily brazed, or are too brittle for unsupported use. Previous evaluation studies included full tips of tool steel, tungsten carbide, K Monel, and austenitic manganese steel. Some of these materials were found to crack under high loads, some spalled readily and required frequent re-dressing, and some exhibited excessive sticking to the weldment.

Information relevant to welder-tip designs is summarized in Tables 25 and 26 of Section V. The material must be tough and resistant to wear so the tip does not deform, spall, erode, or crack when high vibratory power is applied; also, satisfactory physical properties must be retained at the elevated temperatures required by the materials being welded. Tip materials with good thermal conductivity are desirable because liquid cooling of spot-type welding machine tips has already become a standard machine feature.

In the final analysis, however, tip materials must be tested under actual welding conditions before a proper evaluation can be made. Accordingly, additional performance data for the more promising tip materials will be obtained as this program proceeds. Information concerning the physical and mechanical properties of promising materials for fabrication of terminal elements is summarized in Tables 17 and 18.

---

* Product of the General Electric Company (113)

Table 17

TIP MATERIALS: DENSITY AND THERMAL PROPERTIES
(31, 41, 42, 44, 46, 47, 122, 124, 125)

Tip Material	Density (ρ) (lb/in.^{3})	Linear Coefficient Thermal Expansion 10^{-6} (in./in.-°F)	Thermal Conductivity (K) (BTU-in./ft^2-hr-°F)	Thermal Diffusivity α =K/ρc (ft^2/hr)	Specific Heat (c) (BTU/lb-°F)
Astroloy	0.287				
Inconel X-750	.298	7.6	85	0.131	.105
K Monel	.304	8.0	122	.152	.127
Molybdenum	.369	2.7	936	1.94	.063
Mo-0.5Ti	.368	3.1	936	2.01	.061
René 41	.296	6.5	63	.095	.108
Steel:					
M-2	0.293	--			--
T-2	.312	--			.115
4340	.280	6.2			

Table 18

TIP MATERIAL: PHYSICAL AND MECHANICAL PROPERTIES
(31, 41-42, 44, 46-47, 122, 124-125)

Tip Material	Density (ρ) (lb/in^3)	Modulus 10^6 (lb/in^2)	Poisson's Ratio	Tensile Shear Strength 10^3 (lbs/in^2)	Yield Strength (0.2% offset) 10^3 (lbs/in^2)	Rockwell C Hardness Range
Astroloy	0.287			194	142	
Inconel X-750	.298	31.0	0.290	167	110	20-28
K Monel	.304	25.1	.320	140	100	21-28
Molybdenum	.369	46.0	.310	102	78.8	
Mo-0.5Ti	.368	46.0	.310	132	99.5	
René 41	.296	31.6	.310	160	120	
Steels:						
M-2	.293			--	--	62-66
T-2	.312			--	--	62-66
4340	.280			191	180	41

IV. ACOUSTICAL MATERIALS STUDY

"DETERMINE THE MOST EFFICIENT MATERIAL OR COMBINATION OF MATERIALS FOR THE TRANSDUCER AND ASSOCIATED EQUIPMENT TO PRODUCE A DISTORTION-FREE, SOLID-STATE BOND"

TRANSDUCERS

The important considerations in evaluating transducer materials for ultrasonic welding equipment are summarized in Section III; pertinent information for the candidate magnetostrictive and electrostrictive materials is tabulated in Tables 12 and 13 thereof.

As a result of its extended utilization over the years, there exists established and applicable engineering data on magnetostrictive materials (74, 75, 77-79, 82, 86) and much needed information has been acquired with nickel (a magnetostrictive metal) transducers in ultrasonic welding systems (69-70). No such extensive and applicable technical background exists for candidate electrostrictive ceramic materials. Moreover, application of theoretical data, as found in Tables 12 and 13, to practical assemblies is not straightforward as will be shown henceforth. Accordingly, this study was concentrated on the most promising electrostrictive material, lead zirconate titanate.

Electrostrictive ceramic elements do not in themselves constitute useful transducers for welding machines; just as nickel sheet requires punching to certain dimensions, oxidizing to provide eddy current insulation, assembly of many pieces into stacks, brazing to a coupler member and winding of an RF excitation and polarizing coil, similarly ceramic elements must be fabricated into transducer assemblies. Unlike nickel stacks, however, practical designs for ceramic transducer assemblies, to ensure axial radiation into metal coupling members and predictable performance, have not been evolved. Tubular ceramic elements held in place with an axial tie-bolt and possibly an adhesive, are in limited use but such designs seem to have numerous disadvantages for high power applications requiring continuing performance, and do not appear to warrant consideration at this time.

In order to obtain some practical indication of the reported theoretical performance of such ceramic materials in large transducers for extended operation, certain designs for such transducers were partially evaluated (Figure 9). In these assemblies, lead zirconate titanate washers or disks (Clevite PZT-4) are incorporated into preloaded mechanical assemblies which preclude the need of adhesives, permit satisfactory cooling, and especially, avoid cyclic tension-loading of the ceramic elements.

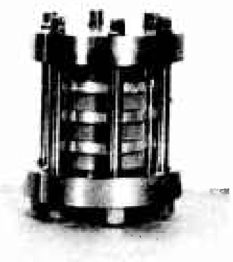

A. Peripheral Tension Bolts

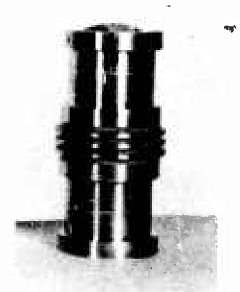

B. Center Tension Bolt

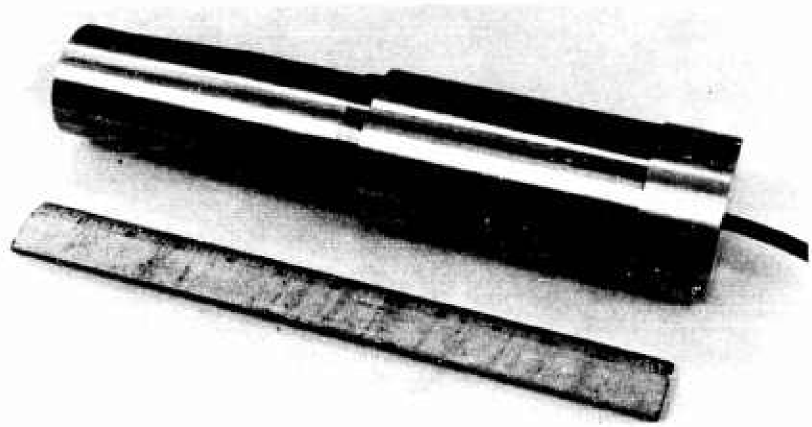

C. Assembled Tension Shell

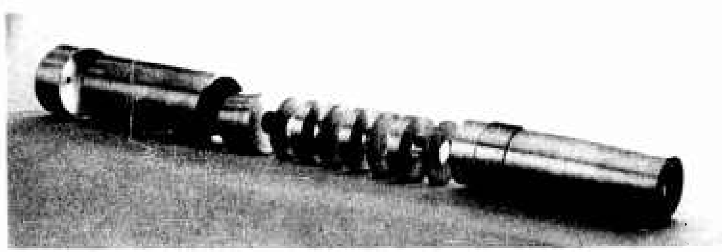

D. Tension Shell Disassembled

Figure 9: CERAMIC TRANSDUCER DESIGNS

Preloading to maintain the ceramic elements in a permanent state of compression is applied in various ways: In Figure 9A, peripherally located tie-bolts apply the necessary loading via end-plates. As shown in Figure 9B, a center tie-bolt serves the same purpose, while in Figure 9C and 9D (assembled and exploded), the containing tube provides the tension reaction.

Results of the calorimetric measurements described in Appendix III for the lead zirconate titanate transducer assemblies are summarized in Table 19. Similar tests with a magnetostrictive transducer showed an overall efficiency of about 21 percent (Table 19) -- the best efficiency that can reasonably be expected from available magnetostrictive material probably will not exceed 30 percent.

Table 19

TRANSDUCER EFFICIENCY AS DETERMINED FROM CALORIMETRIC STUDIES

Transducer Type	Energy Input (kilowatt-seconds)	Energy Output (kilowatt-seconds)	Efficiency (percent)
Nickel	540	119	21
Ceramic:			
Peripheral tension-bolt	540	140	26
Center tension-bolt	288	95	33

The design of Figure 9A initially exhibited spurious plate-type resonance but this unsatisfactory condition was partially eliminated by brazing a 1/2-wave slug to one end-plate with the opposite plate brazed to the coupler (see Figure 10). The first measurements (see Table 19) were made with this unit. The design of Figure 9C, which could not be revised and evaluated to meet the schedule of this Phase I, exhibited complex modes of vibration in the tension shell. After symmetry was achieved with the center bolt-type, the data in Table 19 were obtained.

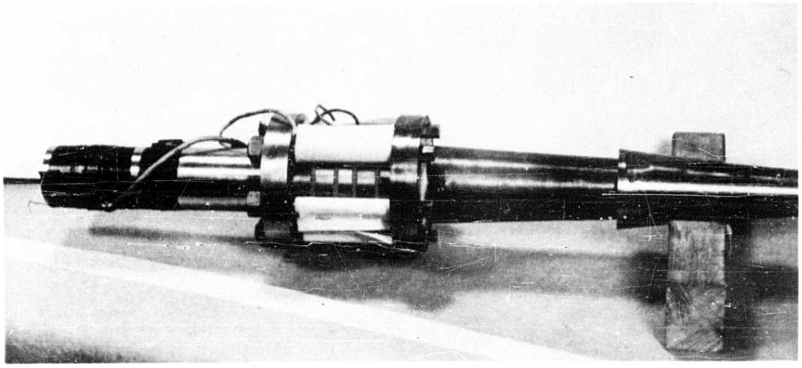

Figure 10a: PERIPHERAL BOLT DESIGN CERAMIC TRANSDUCER ASSEMBLY WITH HALF-WAVE SLUGS BRAZED TO ONE END-PLATE AND COUPLER TO OTHER END-PLATE

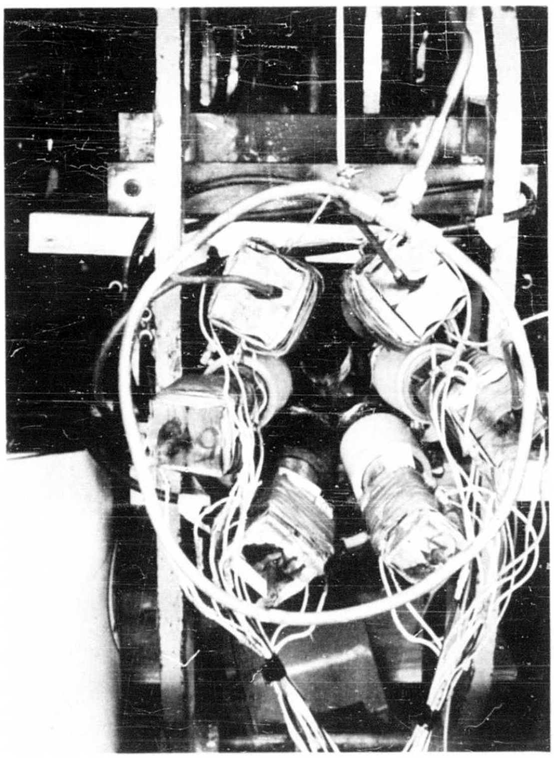

Figure 10b: SIX STACK NICKEL TRANSDUCER

While these measurements must be considered as preliminary, the practicability of multiple washer designs and the utility of ceramic transducer assemblies as well as the fact that the efficiency is substantially greater than can be achieved with presently available magnetostrictive materials was confirmed.

Evaluation of the transducer assembly designs (see Appendix III), and information from scientific personnel at Brush Development Company (95) leave essentially no doubt that the overall efficiency of properly designed ceramic transducer assemblies for ultrasonic welding equipment will be in the range of 70 to 80 percent.

The power handling capacity of PZT-4 in thin disk geometry, as noted in Table 13 of Section III, is 6 watts/cubic centimeter/kilocycle. Thus, a disk with a diameter of 4 inches, 0.16-inch thick and with a center hole equal to 50 percent of its area has a power handling capacity of about 1400 watts when operating at a frequency of 15 kilocycles. A four-disk assembly can handle about 5600 watts and a three-assembly cluster (similar to that shown in Figure 10) about three times that, or approximately 16 kilowatts of electrical input power. The immediate necessity of more than 2 or 3 assembly clusters appears unlikely at this time.

The number of ceramic washers can be increased beyond 4 but development effort will be required. Cooling of these elements can be designed-in at least for high repetition rate spot-welding equipment. Both Al-bronze and Be-copper coupler materials have good thermal diffusivity and will dissipate excess heat from the ceramic elements. Compressed air, with adiabatic expansion, introduced through edge orifices in the transducer assembly space plates, will probably dissipate the heat from the inner washers.

Thus, it is concluded that a multiple transducer assembly cluster can be designed to deliver approximately 12-15 kilowatts of acoustical power into a single coupling member. By means of the Opposition-Drive class of welding system (described later in Section V) this power output can be doubled to provide a welder system capable of delivering up to 25 kilowatts of acoustical power into a weldment.

COUPLERS

Acoustical power is delivered from the transducer through the intermediate coupling members to the terminal element or welding tip and ultimately to the weld interface. The problem areas relative to the coupling members of this system, as outlined in Section III, indicate that power transmission is not straightforward, and careful attention to material properties and acoustical design detail is necessary throughout the entire transmission system.

IMPEDANCE MATCHING

Maximum power transmission can occur only when the impedances of the component elements are properly matched at their junctions. Under idealized conditions, no standing waves exist in the coupling system so that all parts of the system are subject to the same cyclic strain. Ideally, the impedance at the junctions between the various components of the transducer-coupling system should match, but in practice this cannot always be accomplished.

Table 20 shows the percentage of energy transmitted across the interface between the indicated transducer and coupler materials. This is determined for the case of equal areas from the equation (128):

$$T = \left[1 - \left(\frac{\rho_1 c_1 - \rho_2 c_2}{\rho_1 c_1 + \rho_2 c_2}\right)^2\right] \times 100,$$

where T = the percentage of incident energy transmitted across the interface

$\rho_1 c_1$ = the specific acoustic impedance of one material (ρ = density, c = thin rod sound velocity)

$\rho_2 c_2$ = the specific acoustic impedance of the second material.

As is evident from this equation, not more than 2 to 5 percent reflection losses need be expected at an ordinary planar interface between the transducer and coupler materials and a modest correction in the abutting areas will largely eliminate such losses.

When the junction is more complex, as for example at the connection between the wedge and the reed (see Figure 1, page 21) where axial vibration is converted to flexural vibration, the reflection losses can amount to a substantial percentage of the total vibratory energy, and the correction necessary to compensate for this loss is not a simple matter.

Table 20

COUPLER AND TRANSDUCER MATERIALS: IMPEDANCE MATCHING

	Transducer Materials				
	Barium	Lead Titanate Zirconate		Nickel	
Coupler Materials	Titanate	PZT-4	PZT-5	"A"	204
	TRANSMISSION ACROSS INTERFACE[a]-(percent)				
Al-Bronze	99.8	99.7	99.8	97.0	97.3
Be-Copper	99.7	99.4	99.8	97.3	97.5
Inconel X-750	95.8	96.8	96.0	100.0	100.0
K Monel	97.7	98.5	97.9	99.5	99.6
Stainless Steel[b]	97.0	97.9	97.2	99.8	99.8
Tool Steel[c]	97.0	97.7	97.2	99.8	99.8
Titanium (6Al-4V)	98.8	98.1	98.7	89.8	90.4

[a] Interface between indicated coupler and transducer materials.

[b] Series 300.

[c] Carpenter 883.

The input impedance, Z*, at any point on a flexurally driven reed is reactive with a positive reaction (mass-like) equal to the resistive component. This is shown by the equation:

$$Z = 2Z_f (1 + j)$$

where

$$Z_f = A\rho C_\ell \ (\omega k/C_\ell)^{1/2}$$

and

A = sectional area, square centimeters (cm^2)
ρ = density, grams/cubic centimeters (g/cm^3)
C_ℓ = thin-rod velocity, meters/second (m/sec)
ω = radial frequency, $2\pi f$
k = radius of gyration for the reed, centimeters (cm)

the subscripts denote flexural vibration.

The characteristic impedance for the longitudinal mode is given by,

$$Z_1 = A\rho C_\ell$$

thus, the dimensionless factor

$$(\omega k/C_\ell)^{1/2}$$

serves to convert longitudinal to flexural impedance.

An impedance match into the weldment itself, (70) is associated with tip contact area and clamping force, both of which are essentially "machine setting" variables under the equipment user's control. In previous research, instrumentation capable of ascertaining the degree of mismatch, and of indicating the proper machine settings required to eliminate this problem was developed.

Both reflection and impedance matching are important factors that affect the power handling capacity of couplers. With a standing-wave ratio of unity (no reflection or mismatch) a metallic coupler is about as good a conductor for vibratory energy as a copper wire is for electrical energy. When the standing-wave ratio is high, however, the power handling capacity can decrease to the point that only 1 or 2 percent of the maximum amount of vibratory energy is transmitted. For this reason, both reflection losses and impedance mismatch must be minimized in any transducer-coupling system to achieve optimum transmission of vibratory energy.

* Unpublished work by W. C. Elmore.

POWER HANDLING CAPACITY

Recent theoretical considerations (70) indicate that the power transmitted by any elastic system can be defined by the equation:

$$P_m = \frac{1}{2} A \frac{\sigma_m^2}{\sqrt{E\rho}}$$

where P_m = the maximum power

A = the cross-sectional area of the coupler or wave guide

σ_m = the maximum allowable stress

E = the elastic (Young's) modulus for the material of which the coupling member is made

ρ = the density of this material.

The maximum power that can be delivered by a transducer-coupling system for welding appears to be independent of frequency per se, but it does depend upon the mechanical and physical properties of the materials of which the system is made. Here σ_m represents the maximum allowable stress and $E\rho$ represents the characteristic specific impedance for the material. Thus, it appears that the ratio $\sigma_m^2/\sqrt{E\rho}$ is one figure-of-merit for evaluating the potential coupler material for use as an acoustic transmitter in high powered applications.

In the following table, power handling efficiencies of the various coupler materials are compared at a given fixed strain level of 0.0008 inch/inch; the efficiency is determined on the basis of the measured dissipation for 1/2 wavelength per square centimeter of cross section.

Table 21

CANDIDATE COUPLER MATERIALS: POWER HANDLING CAPACITY AND TRANSMISSION EFFICIENCY

(Strain Level = 0.0008 inch/inch)

Material	Power Handling Capacity (watts/cm^2)	Transmission Efficiency (percent)
Be-Copper	20,600	100
Al-Bronze	20,600	99.8
K Monel	16,850	99.7
Ti (6Al-4V)	27,400	99.5
Steel (303 SS)	16,400	99.8

The higher capacity indicated for titanium does not, of course, reflect the problem of energy dissipation associated with the mismatch that results when titanium is coupled to other materials.

Further theoretical considerations (Appendix V) carried out in part during a previous study (129) compared the strain-energy associated with the various vibratory modes as shown in Table 22. These data indicate that the ratio of the maximum strain energy to material density, $\mathcal{E}_m/\rho$, is another way of expressing a figure-of-merit for elastic materials.

Table 22

VIBRATORY MODES: RELATIVE STRAIN ENERGY DENSITY AND AMPLITUDE

Mode of Vibration	Constant Amplitude, (Relative Strain Energy Density)	Constant Strain Energy Density (Relative Amplitude)
Longitudinal	1.0	1.0
Lateral:		
Round	2.4	0.65
Rectangular	1.8	0.75
Torsional	1.0	1.0
Flexural (disk)	5.1	0.45

Application of Hooke's law and simple algebraic manipulation show that the earlier figure-of-merit is equivalent to $\mathcal{E}_m/\rho$ multiplied by the characteristic impedance of the material. Thus, it is clear that either ratio

$$\frac{\sigma_m^2}{\sqrt{E\rho}} \quad \text{or} \quad \mathcal{E}_m/\rho$$

can serve as a useful guide in any preliminary screening of candidate coupler materials.

Without quantitative information on σ_m, (the maximum allowable stress in the frequency range noted above) or on $\mathcal{E}_m$, the strain-energy density, application of these factors is not helpful.

With E and ρ known, however, assumed values for power and coupler cross section can be substituted into the equation,

$$P_m = 1/2\, A \frac{\sigma_m^2}{\sqrt{E\rho}}$$

the equation solved for stress, and σ_m, values can be obtained for comparison with the mechanical properties in Table 14. To establish tentative equipment requirements, relevant to the objectives of this program, we can assume P_m = 10,000 acoustical watts, and A (2-inch diameter rod) = 20.1 square centimeters. The values in Table 23 were computed from the above equation for three coupler materials.

Table 23

COUPLER MATERIALS: DYNAMIC STRESS AND STRAIN IN 2-INCH DIAMETER ROD AT 10-KILOWATT INPUT POWER LEVEL

Coupler Material	Stress (psi)	Strain 10^{-3}(in./in.)
Be-Copper	2545	0.150
Al-Bronze	2530	.140
K Monel	2800	.112

INTERNAL FRICTION

The mechanism by which energy is dissipated in the metal coupling members is usually termed internal friction (130). For our application, it is desirable that the coupler material offer minimum internal friction to the transmission of vibratory energy in the frequency range of interest. Such losses are affected by both power level and frequency with greater losses occurring at high-power levels and frequencies. For small deformations (low power) the loss per cycle is low because essentially good elastic behavior prevails; at stress levels associated with high power delivery the problem of internal friction, and fatigue failure can be serious if the design is not sound.

To our knowledge there is at present no satisfactory theory for internal friction in solids that embraces a broad vibratory frequency spectrum, although such losses can be measured by several experimental methods. For example, at low stress levels (on the assumption of simple harmonic motion) the natural logarithm of the ratio between successive oscillations (log decrement), as determined with a torsional pendulum, may be used to estimate the internal friction losses.

Many investigators (131-133) have worked at frequencies up to about 200 cps, and some studies (114, 134) have been made at higher frequencies. Except for the recent work of Mason et al and Neppiras (134), little information is available on the energy losses and fatigue properties of various metallic materials at frequencies in the range of 5 to 50 kilocycles per second.

In the light of the foregoing, it is evident that there is not enough information available to permit selection of a reasonably optimum low-loss, high-endurance, material for handling substantial levels of vibratory energy in the frequency range of interest. Accordingly, a system, based on the work of Neppiras (134), was designed, constructed and utilized to determine the power dissipation in a coupler as a function of peak strain and thereby establish a tentative criterion for the selection and evaluation of potential coupler materials (see Appendix IV).

Resonant specimens of representative materials from Table 14 were fabricated from 300 stainless steel, titanium, Be-copper, Al-bronze, and K Monel in the form of dumbell-like stubs with an axial hole. These specimens were similar to those used by Neppiras. The axial flow of water through the specimen was monitored during the test and the temperature difference between the in-flow and out-flow was measured by means of thermocouples. The energy dissipation in the specimen was thus determined at various strain levels, from these data, the energy dissipation-strain curves of Figure 11 were obtained. The large difference in attenuation of the candidate materials is clearly apparent and the superiority of Al-bronze and Be-copper at high strain levels is obvious. It is also evident that the losses at ordinary strain levels is not insignificant. These data were compared with those reported by Neppiras, and found to be in close agreement. On the basis of this work, both Al-bronze and Be-copper are considered as satisfactory coupler materials.

TIP MATERIAL

In Section III, the performance and other characteristics of tool steel, Inconel X-750 and other tip material were discussed on the basis of previous experience with these terminal elements. While the superior high temperature properties and other desirable characteristics of Astroloy

Figure 11: POWER LOSS AND STRAIN CHARACTERISTICS OF CANDIDATE COUPLER MATERIALS

(Frequency - 15 kilocycles)

Material	Letter
Be-Copper	A
Al-Bronze	B
K Monel	C
Ti(6Al-4V)	D
Steel, (303 SS)	E

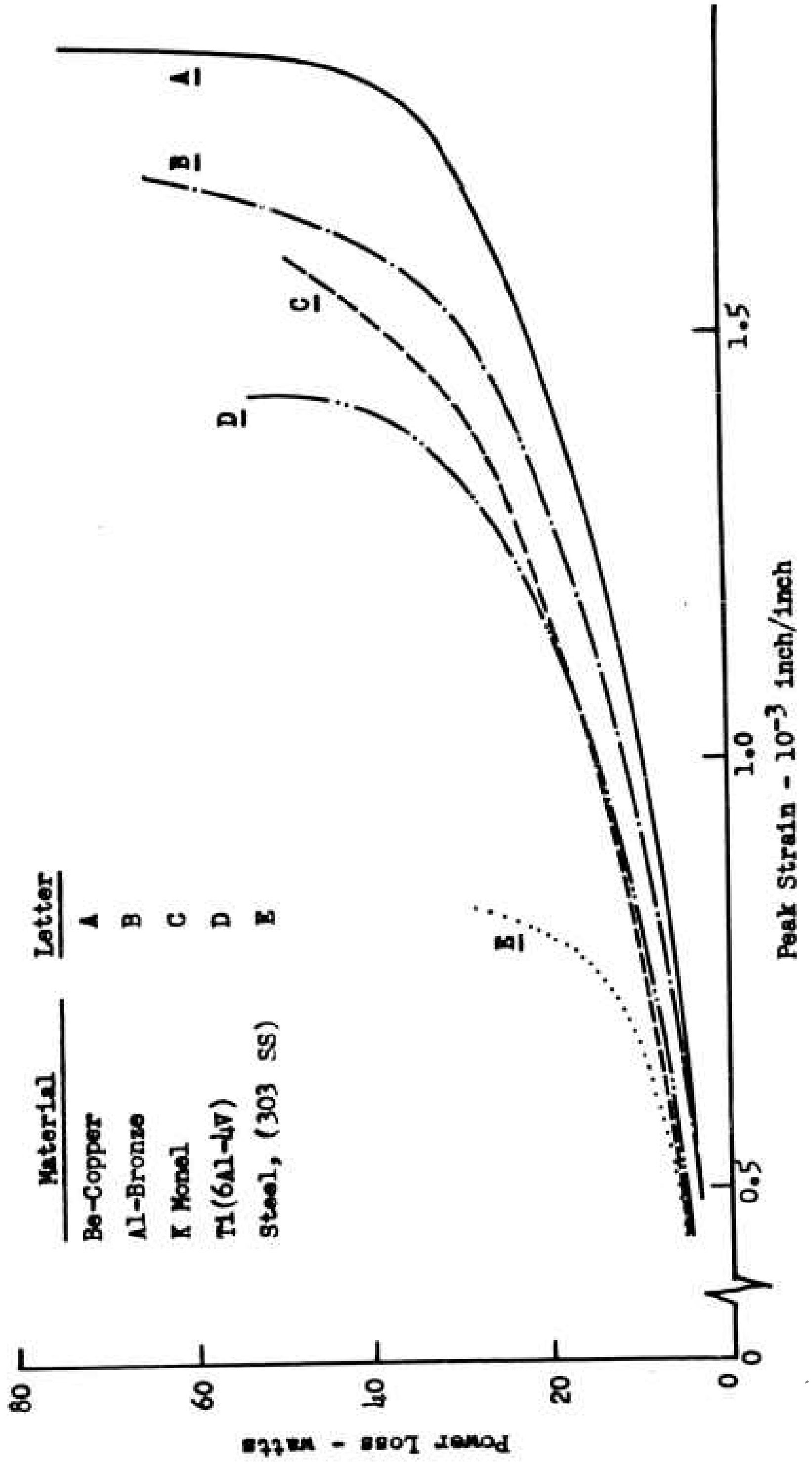

were recognized and included in Tables 17 and 18, there was little experience to report. During the course of the present work, however, Astroloy tips of various designs were studied. The results of this experience are described below.

Astroloy tips have been fabricated from three types of commercial stock, wrought-bar, wrought-plate, and cast-bar. Of these, the performance of the wrought-bar tip was the more satisfactory. Tip wear was somewhat excessive initially but this decreased with use. The initial surface damage, as shown in Figure 12A, has the appearance of fretting.

Preliminary study of a damaged wrought-bar tip (cracked during welding operations) revealed certain metallurgical characteristics (see Figure 12B): lack of homogeneity in the matrix, coarse grain structure, uneven distribution of particle size and some tendency to crack along the grain boundaries. All but the latter characteristic was tentatively attributed to the complex nature of the Astroloy alloy, which is a nickel-base (approximately 55%) alloy with 15 Cr, 15 Co, 5 Mo, 4.5 Al, 3.5 Ti, and less than 1.0 percent of B, C, Si, and Mn combined.

Astroloy exhibits a tendency, in some cases, to precipitate a second-phase along grain boundaries. Consequently, the grain periphery may be depleted and thus weaker than the grain cores; also the sensitivity to intergranular cracking may be greater. The quality of Astroloy tips can probably be improved by cold and/or hot reduction or homogenization and other heat-treatments, but further study is necessary to establish the value of such treatments.

A removable tip with an Astroloy insert shaped like a frustrum of a cone, is shown in Figure 12C. This tip was designed to permit the use of a relatively thin plate material for the insert. An Astroloy insert was "pressed-in" a holder made of Carpenter 883 steel. Because of machining problems involved in matching the insert and holder surfaces however, this design was considered somewhat impractical.

While Astroloy is the best tip material investigated to date, tips for ultrasonic welding machines still present a problem requiring further study. The performance of Astroloy tips are reasonably satisfactory for welding the refractory weldment materials of this project but such tips can be improved. Materials similar to Astroloy will be investigated as they become available.

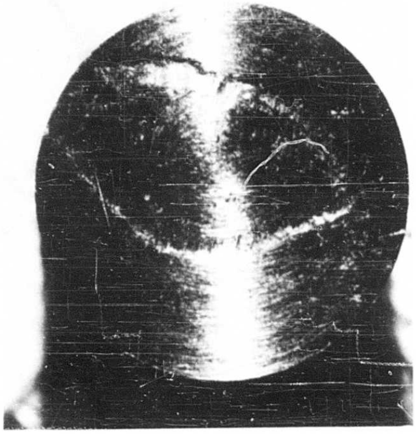

Figure 12A: CHARACTERISTIC SURFACE DAMAGE OF ASTROLOY TIP

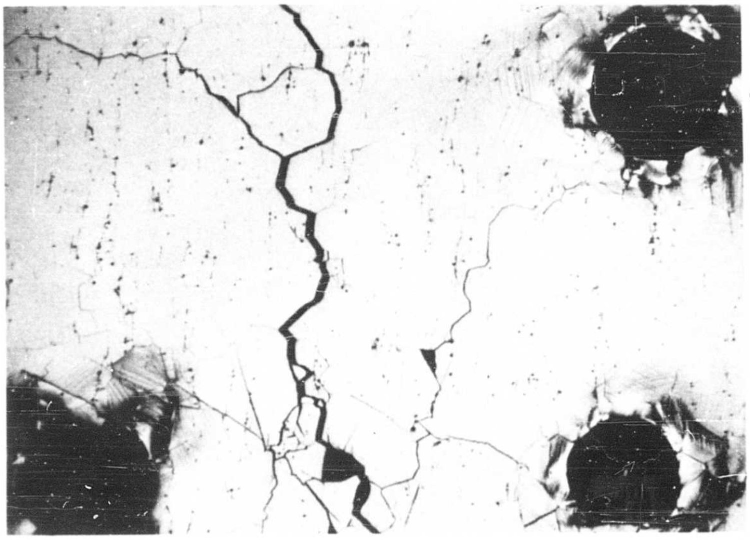

Figure 12B: SECTION OF ASTROLOY TIP AFTER FAILURE
(HF-HNO_3 Etch; 30X)
(Dark Spots are Rockwell Brole Indentations)

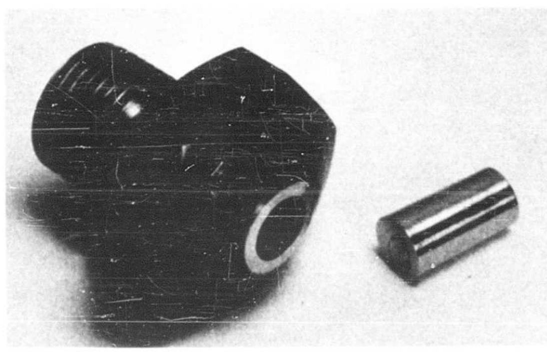

Figure 12C: REMOVABLE TIP WITH ASTROLOY INSERT

V. ENERGY DELIVERY METHODS

"DETERMINE THE MOST EFFICIENT METHODS OF SUPPLYING VIBRATORY ENERGY TO THE WELD INTERFACE"

SYSTEMS

Several ultrasonic welding systems, of different geometry, have been developed for spot-type, roller-seam, and ring-welding, but the efficiencies, specific advantages and disadvantages of each remain to be defined.

In general, there are two broad classes of systems which are independent of the weld geometry. The first embraces all those types in which a "Reaction Anvil", supports the work pieces and statically resists compliance thereof with the vibratory forces exerted by the powered sonotrode. The second or "Opposition-Drive" class comprises systems wherein vibratory energy is delivered to both sides or members of the weldment -- no reactive element such as an anvil is involved.

As indicated in Table 24, either class, (The Reaction-Anvil or the Opposition-Drive,) can incorporate any of the three types of transducer coupling systems.

Table 24

APPLICABILITY OF CLASS AND TYPE OF ULTRASONIC SYSTEMS TO SPOT- AND SEAM-TYPE WELDERS

Ultrasonic System		Welders**	
Class	TC* Type	Spot	Seam
Reaction-Anvil	Lateral Drive	X	X
	Wedge Reed	X	
	Torsional	X	X
Opposition-Drive	Lateral Drive	X	X
	Wedge Reed	X	
	Torsional	X	X

* Transducer-coupler.
** An "X" indicates applicability to that particular type of welder.

Examples of most of these have been constructed and operated. On the basis of extended experience, the Opposition-Drive welding machine is virtually implicit in meeting the objectives of this project if both practical and theoretical considerations are to be fulfilled. Briefly, the Reaction-Anvil type when attached to a complex structural system, such as the framework of a welder, usually requires considerable debugging to eliminate extraneous resonance that reduces machine performance. Moreover, some compliance always exists in machines of the Reaction-Anvil class; this variable sometimes interacts with power and force settings so that machine performance is imperfectly controlled. Whereas, with the Opposition-Drive system, the problems associated with the Reaction-Anvil type are less significant; furthermore, acoustic stresses throughout the transducer coupling system are considerably less because the vibratory energy is delivered through two, rather than a single conductor.

Opposition-Drive eliminates the necessity for a massive, noncompliant anvil and the problems so entailed. However, unless the design of an Opposition-Drive system incorporates solutions to problems peculiar thereto, it is possible that actual welding performance will be inferior to that experienced with the Reaction-Anvil type. For example, a slight shifting of phase in the tip excursion of either sonotrode (from the 180° out-of-phase condition that must prevail) will abruptly decrease the amount of energy delivered. As a matter of fact, under certain circumstances, one transducer-coupling system may act as an alternator with the opposing system serving as a motor so that almost no work will be done at the weld locale.

There are at least three avenues to satisfactory Opposition-Drive operation which have previously been investigated and developed:

1. Mechanical intercoupling, in which all the transducers drive a common coupler and the energy output of the coupler is divided by means of a locked mechanical out-of-phase system, to provide 180° out-of-phase displacement to the sonotrode tips.

2. Electrical intercoupling, which involves standing-wave ratio or other monitoring equipment on each coupler or tip, for detecting and automatically maintaining the proper phase relationship by a servotechnique.

3. Electromechanical intercoupling which utilizes a combination of these techniques.

The electrical intercoupling system shown in Appendix I operates reproducibly.

The Reaction-Anvil class of welders includes the wedge-reed design in which the reed may be excited by a single coupler element (wedge-type) or by two diametrically opposed couplers driven 180° out-of-phase (Figure 1A), thus effectively increasing the power capacity. This Reaction-Anvil class can also include the lateral-drive coupler system (Figure 1B), the roller system (Figure 1C), and the torsional system (Figure 1D).

The relative efficiencies of the wedge-reed, the lateral-drive, and the ring-welding systems have not been established precisely, although considerable data has been obtained with all three types. In general, the wedge-reed system has been used with higher power equipment and the lateral-drive with lower power arrays. This trend resulted from early observations that the lateral-drive system, which applies the clamping force via bending of the coupler, was almost inherently "soft" in bending. Previously, acoustical considerations appeared to require a more rigid structural design because an elastically soft clamping-force member usually exhibits tip "bounce" and reduces the clamping force at the instant when it is most essential. The wedge-reed system, however, applies clamping force via a short column which remains unyielding over a satisfactory range of acoustical design variables. Possibly, a "stiff" (in bending) acoustical coupler can be evolved but this may require development work not envisioned under this contract.

To evaluate the potential efficiency of these systems, a theoretical analysis relating the strain energy density to amplitude for the longitudinal and flexural cases, previously carried out, was extended to include the torsional concept (see Appendix V). This more complete analysis indicates that the torsional and longitudinal modes are comparable in power handling capacity (Table 22), whereas the lateral (flexural) or bending mode, involves greater stresses at comparable amplitudes.

Thus, on the basis of theoretical considerations alone, the longitudinal and the torsional modes of vibration offer maximum amplitude at minimum strain energy density. The mode of vibration in the wedge-reed system involves a reed that operates laterally; this is a less favorable mode, that can be somewhat improved with a reed of rectangular cross section, (see Table 22).

The torsional mode of vibration offers a system, free of tip bounce problems, and with the same stress amplitude advantages as the lateral-drive system. Not many of these systems have been built and the largest system in production use today operates at about 2 kilowatts. Moreover, the present torsional systems are affected by a microkinematic problem between the tips of the longitudinal excursioning mechanical transformers and the sockets of the peripherally oscillating torsional element. During recent years, sufficient experience has been obtained

with this system to argue strongly against any attempt, at this time, to develop large, high-power torsional type welders with the flexibility required for the range of weldment geometries that is implicit in this program. Actually, the time scale of this program virtually precludes development of a high power torsional system to accommodate a range of weldment geometries. Such systems are currently being developed in connection with other projects for specific end-item geometries and no doubt, with additional experience and theoretical study, large torsional systems capable of joining a variety of end-item geometries will become available in the future.

From the foregoing, it can be concluded:

1. The Opposition-Drive system is virtually mandatory to meet the objectives of this program because the oscillatory strain levels in each transducer-coupler system are only about one-half that found in the Reaction-Anvil system. As shown in Figure 11, with less strain there is less energy loss.

2. The longitudinal and the torsional mode of coupler vibration are productive of the least strain-energy density and therefore the least hysteresis losses. Since the torsional design can be eliminated, for microkinematic as well as practical reasons, a system operating in the longitudinal mode might be selected.

3. The conclusion of (2) above is predicated on the premise that practical consideration of work clearance can be met and that a sufficiently "stiff" system can be built to preclude tip bounce. As can be deduced from Figure 1B, however, the possibility of developing a satisfactory system of this type is exceedingly doubtful. Since clamping forces, amounting to several thousand pounds, may be required to join the materials in the gages specified in this program, an Opposition-Drive, Wedge-Reed design (See Section VI) is the only system with the capability of operating effectively at these clamping forces, offering reasonable work clearance and providing satisfactory coupler efficiency (only the efficiency of the terminal element of the transducer-coupling system is less than optimum).

MECHANICAL ARRAYS

Three types of mechanical arrays for translating the work beneath the ultrasonic continuous seam welding tip have been developed and operated. Each type of array--the roller-roller, the traversing-table,

and the traversing-head configuration is oriented toward the application of ultrasonic welding to different types of assemblies. All three types of mechanical systems incorporate the means of controlling the ultrasonic welding power, clamping force, linear welding rate, and of synchronizing the welding tip peripheral speed with the surface translation rate of the weldment member. Generally speaking, the transducer-coupling system, force insensitive mounting and the associated mounting hardware are interchangeable between machines.

The roller-roller configuration of ultrasonic welding machine, shown in Figure 13, provides wide flexibility. With this equipment, the materials to be welded pass between the counter-rotating welding tip and the cylindrical anvil. Both the tip and rotating anvil are power driven to propel the weldment at the predetermined welding rate. A minimum of tooling and holding fixtures are required with this welder. Due to its ease of operation, with simple assemblies, the roller-roller machine is desirable for development-type applications in which the ultrasonic weldability of new materials and/or new material combinations is studied.

In production applications, the roller-roller continuous ultrasonic seam welder is used primarily for welding the edges of flat panels or flanged containers to provide a high-strength sealed package. Sealing of electronic units or control system component packages is also practical with this equipment. Flanged fuel or propellant tanks and other containers requiring welds of high strength (to withstand high pressure and to provide leak free closures) are also amenable to production on the roller-roller configuration equipment.

The roller-roller welder is especially well suited for high speed joining of extended light-weight assemblies. Since little or no fixturing is required with this array, the inertia of the parts can be maintained at a minimum, thereby increasing the feasibility of rapid transport, reversal of directional motion as well as rapid starting and stopping of the weldment.

Splicing of concentric tubes or joining of tubes to flanged-end fittings can be accomplished readily on the roller-roller configuration, provided the tube diameter is large enough to allow entrance of the welding head or anvil roller. This type of equipment has also been used in the welding of aluminum splice sleeves to stainless steel LOX lines, and in joining flanged fittings to thin wall stainless steel tubing.

The traversing table machine, wherein the anvil or weldment mounting surface is traversed under the fixed-position, rotating, welding-tip, as in milling machine operation, offers a second geometry for ultrasonic continuous-seam welding. This equipment is particularly adaptable to the continuous welding of smaller assemblies or for the precision placement of welds. As shown in Figure 13B, the traversing table provides

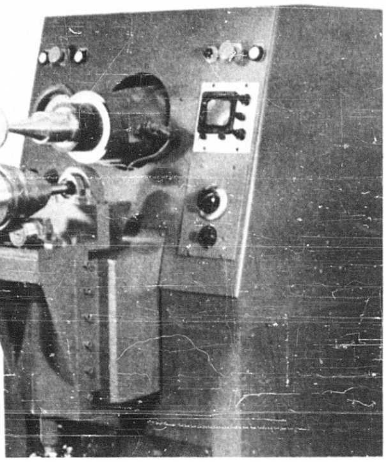

Figure 13A: ROLLER-ROLLER CONFIGURATION

Figure 13B: TRAVERSING TABLE CONFIGURATION

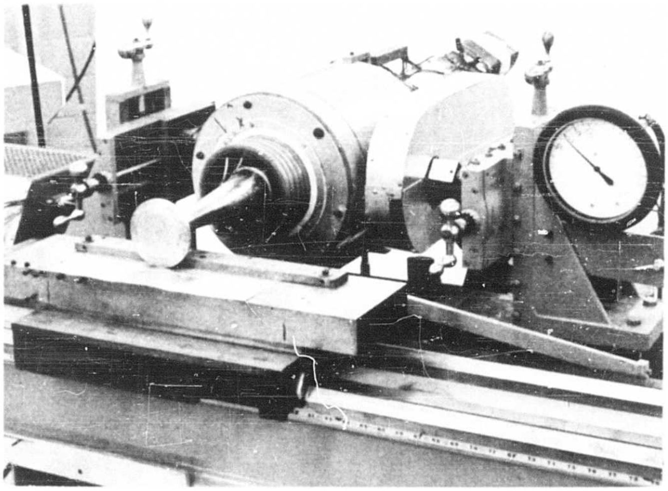

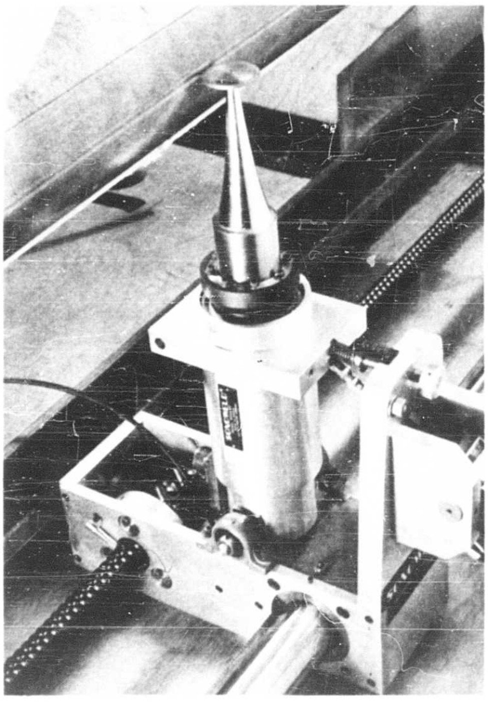

Figure 13C: TRAVERSING HEAD CONFIGURATION

a base for mounting the locating and holding fixtures. The location of these fixtures on the table provides a means of precisely aligning the seam weld in the repetitive assembly of parts. The size of such assemblies is limited by the maximum travel distance of the table on a specific machine and by the mass of the part and fixtures which must be transported.

Parallel seam welds can be produced by means of indexing fixture, or way-slide, on the welder head-mounting. Seam welders have also been used to fabricate corrugated heat-exchanger panels, wherein each corrugation is welded in a continuous seam to a flat sheet. The nodal welding of honeycomb core materials can be readily processed and experimental leading edge panels, employing integral cooling systems, have also been welded with this type of equipment.

To overcome the problems of moving large masses and large size parts on the work bed of the traversing table machine, a third mechanical configuration of ultrasonic seam welding equipment was developed. In this "traversing-head" configuration, the weldment members are held stationary and the transducer-coupling system, constituting a "welding head", is moved over the length of the seam weld. The translation speed of the welding system and the peripheral speed of the welding tip are again synchronized to prevent slippage between the welding tip and the weldment member. With this arrangement, the part fixturing and anvil support can be somewhat flexible in design, provided sufficient rigidity is supplied to withstand the welding clamping forces and to prevent compliance with the welding vibratory frequencies.

The traversing-head, roller seam welder is currently used for splicing essentially continuous rolls of aluminum foil. In this application, the foil bulk and mass makes movement of the aluminum rolls practically impossible. With the traversing head welder, the foil ends can be welded directly in the coiling machine using one of the foil guide rollers as the back-up anvil. Figure 13C is a photograph of a typical foil splicing installation.

A larger version of the same type of equipment is currently in operation on the full scale production of aluminum heating ducts which vary in diameter from approximately 3 inches to as large as 16 inches. The aluminum foil covering, which is usually less than 0.010-inch thick, could not otherwise be metallurgically joined. This same concept should be applicable to the longitudinal seaming of items such as large diameter LOX lines or other types of duct work. In these cases, relatively thin sections of sheet or foil can be fabricated into leak-tight dependable conduits. The welding of raceways or electrical conduit channels or the bonding of longitudinal stiffeners to missile body structures exemplify weldment geometries readily effected by means of a traversing head ultrasonic welder. For example, a missile body might be located in a cradle or fixture under the welding head which could be traversed the full

length of the missile. With a similar approach, skin panels could be assembled. The traversing-head type ultrasonic seam welder is applicable to many phases of the large component assemblies.

CONTINUOUS ROLLER SEAM WELDER -- LIMITATIONS

As shown in Appendix V, any flexural resonant disk, whether sculptured or not, involves high stress levels (note equation 19 of Appendix V). This is confirmed by various experiences with such terminal disk elements in our laboratory. Moreover, the analysis of Appendix VI shows that if surface stresses are decreased by reducing the disk thickness, an altogether different type of vibration occurs which is characterized by flexural wobbling about a horizontal axis. Under these circumstances, the energy delivered to the weldment will not be sufficient to produce a weld.

Thus, at the present time, we are forced to the conclusion that the resonant flexural disk tip on the roller seam welder imposes a ceiling on the performance of such equipment that is too low to permit its consideration in the frame of reference of this project. Furthermore, because of microkinematic problems associated with the toroid tip, this design is also unsatisfactory at high powers.

Because of the small rolling or contact radius, the nonresonant tip, No. 1 of Table 25, may plow or gouge the weldment, but with disks of larger radius this phenomena is practically non-existent. Tip design No. 1 is also unsatisfactory from the standpoint of welding speed and induced rotation of the coupling system; any reasonable welding speed, requires that the coupling system rotate at an unsatisfactory rate (revolutions/minute).

In summary, it must be concluded that a breakthrough in terminal element design is requisite to the use of continuous ultrasonic roller seam welding for joining the material and thicknesses that are the objective of this program.

Two approaches to greatly improved systems appear possible. First, the use of torsional roller systems with a torsionally oscillating disk tip as is developed in Appendix VII. The theoretical analysis of such a system is encouraging because a torsional roller will provide the work clearances associated with flexurally resonant tips and at the same time provide the power handling capacity necessary to join the requisite thicknesses of the materials specified in this program. However, other limitations, already pointed out in connection with torsional system; as well as the work schedule for this project precluded the expenditure of effort in this direction. A second approach, involves an inverted exponential system, with a hoop-like tip, similar to that used to drive the

Table 25

TERMINAL TIP-COUPLER CHARACTERISTICS FOR CONTINUOUS SEAM ROLLER WELDER

Design Details				Characteristics	
Type	Geometry	Terminal Element	Joint	Fabrication	Welding Performance
A. EXPONENTIAL COUPLERS:					
1	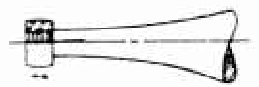	Non-Resonant Tip	Threaded	Relatively easy to fabricate - tip easily replaced.	Good, but not consistent over length of seam
2	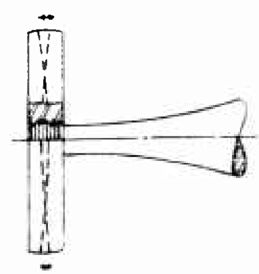	Resonant Flat Disk	Threaded	Relatively easy to fabricate - tip easily replaced. High stresses at junction may cause failure.	Satisfactory weld quality - consistent over length of seam.
3	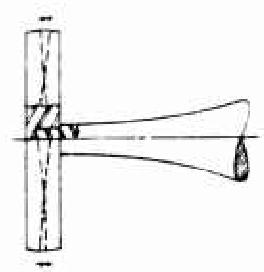	Resonant Flat Disk	Brazed	Relatively easy to fabricate - stresses at brazed joints high. Joint has longer life than threaded component.	Satisfactory weld quality - consistent over length of seam.

(Concluded on next page)

Table 25 (continued from previous page)

Type	Geometry	Terminal Element	Joint	Fabrication	Welding Performance
	Design Details			Characteristics	
A. EXPONENTIAL COUPLERS: (continued)					
4	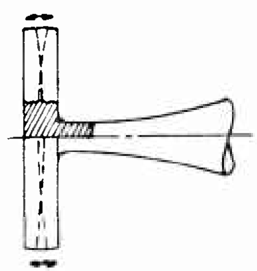	Resonant Flat Disk	Single piece	Difficult and/or expensive to fabricate. High stresses at neck. Piece is slightly longer than types 2 and 3	Satisfactory weld quality-consistent over length of seam.
5	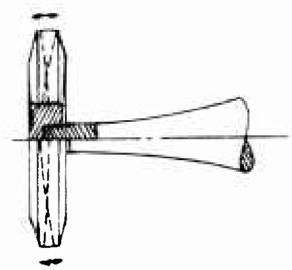	Resonant Sculptured Disk	Brazed	Difficult and/or expensive to fabricate. Sculpturing increases disk life.	Satisfactory weld quality - consistent over length of weld.
B. INVERTED EXPONENTIAL COUPLER:					
6	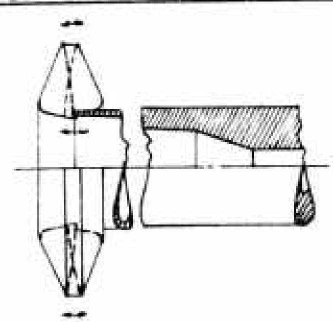	Resonant Toroid	Brazed	Difficult and/or expensive to fabricate. Highly stressed disk area eliminated. Serious microkinematic problems at junction cause failure.	Toroid serves as mechanical transformer. Edge displacement exceeds that at drive point. Satisfactory weld quality - consistent over length of seam. Power delivery superior to that of disks up to 2000 watts.

resonant toroid of Table 25. This equipment was devised and is being evaluated in connection with other projects in our laboratory, but performance tests are not sufficiently advanced to conclude that this approach will fulfill the requirements of this program.

Until additional information becomes available, it must be concluded that ultrasonic continuous roller seam welding of 0.10-inch thick refractory and superalloy metals cannot be achieved to meet the schedule for this project.

COMBINATION OF A SPOT AND SEAM WELDING MACHINE

In view of the foregoing discussion and conclusion, relative to ultrasonic roller seam welding of the 0.10-inch refractory and superalloy materials, it is evident that consideration of a combination spot and continuous roller seam welding machine is not feasible at this time.

Seam welds can be produced successfully, however, by means of overlapping spots with the type of spot welding machine herein projected to meet the requirements and objective of this project.

COMPONENTS

TRANSDUCERS AND COUPLERS

See Section III and Section IV

TIPS

Spot-Type Welder

The problem of attaching welding tips to the sonotrode and/or anvil cannot be ignored; mechanical attachment, while feasible at modest powers, has not been reliable at higher powers; brazing attachment of tips, however, is practical at high power levels. Thus, at least for the present, tip materials, if possible, should be brazable.

Information regarding the various designs of spot-type-welder tips is summarized in Table 26. Mechanically attached tips are highly desirable if not absolutely mandatory. Examples of mechanically attached tips are Types 3 and 7 of 26. For a variety of reasons, Type 7 is the more desirable; also it can be fabricated easily from small pieces of material (often necessary when a new or special alloy is involved). Type 3, however, is difficult to manufacture and, consequently, is more expensive because a modest quantity of tip material in a variety of shapes is frequently difficult and costly to obtain.

Table 26

TERMINAL TIP-REED CHARACTERISTICS FOR SINGLE-SPOT WELDERS

Type No.	Design Details: Geometry	Design Details: Description	Attachment Mechanism	Characteristics: Fabrication	Characteristics: Welding Performance
1	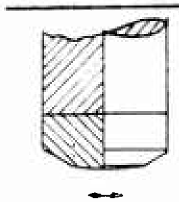	Spherical or sculptured work surface	Brazed	Relatively easy to fabricate Joint strength reduced and troublesome at high temperatures. Quality of joint is difficult to ensure.	Satisfactory at low power levels
2	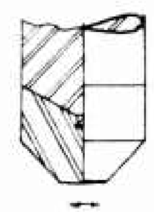	Contoured for greater mating surface	Brazed	Somewhat difficult to fabricate. Brazing requires skill. Brazed joint is not highly loaded in shear.	Satisfactory at all power levels but not at high repetition rates.
3	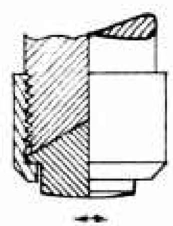	Mechanically attached tip	Threaded	Expensive to fabricate.	Satisfactory.

(Concluded on next page)

Table 26 (continued from previous page)

Design Details				Characteristics	
Type No.	Geometry	Description	Attachment Mechanism	Fabrication	Welding Performance
4	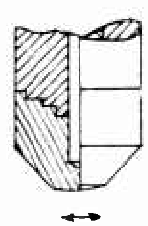	Multistep tip	Brazed	Difficult to fabricate. Successful in reducing shear load on joint for high-power application.	Satisfactory.
5	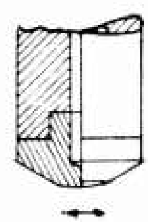	Single-step tip	Brazed	Relatively easy to fabricate. Tip easily located for brazing. Shear load on joint is low. <u>Most</u> <u>satisfactory</u> <u>design</u>.	Satisfactory.
6	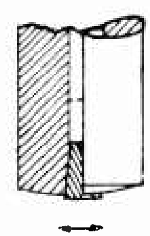	Insert tip	Press-fitted	Difficult to fabricate. Insert may be of difficult-to-machine metal. Press-fit or high power may deform thin end of reed.	Satisfactory.
7	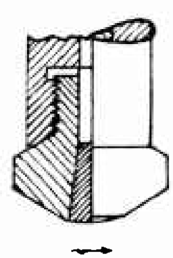	Mechanically attached and insert tip	Threaded and press-fitted	Relatively easy to fabricate. Insert can be of difficult-to-machine metal.	Preliminary indications promising.

Roller Seam-Welding Disks

While spot-type welding tips constitute such a small part of the welding system that their acoustic properties can be neglected, disk tips for roller-seam welders are a critical factor in resonant systems since they must transmit vibratory energy from the center to a point on the periphery. Disks for roller-seam welding machines are sophisticated, and their design has been the subject of various theoretical treatments and experimental measurements. Since such disks continually place fresh cool areas in contact with the workpiece, the metallurgical and physical demands may not be as rigorous as those for spot-type welder tips. These designs have definite boundary acoustic conditions which, because of stress buildup in the center of the disk, cannot be indefinitely extrapolated to higher powers. Inasmuch as hysteresis can cause energy to be absorbed within the disk, unstable operation and an unusual type of metallurgical failure may result.

Information concerning various roller seam-welding tips is summarized in Table 25. The Type 1 tip is an operable nonresonant mass, but any reasonably high welding rate involves an unsatisfactorily high angular velocity of the transducer-coupling system. Types 2, 3, and 4 are characteristic resonant disks, showing several disk-to-coupler attachment methods. Type 6 is a resonant toroid that has received considerable attention but it also involves unsatisfactory microkinematics that prevent its use at the amplitudes associated with the high power levels required to join the materials in the necessary thicknesses. The resonant sculptured disk, No. 5 in Table 25, is an improvement over the resonant toroid in that it provides greater peripheral to center amplitude.

VI. EQUIPMENT FEASIBILITY

"BASED ON THESE PHASE I STUDIES, THE CONTRACTOR SHALL SHOW AND SUPPORT BY ARGUMENT THE FEASIBILITY OF PRODUCING ULTRASONIC WELDING EQUIPMENT CAPABLE OF JOINING MOLYBDENUM, TUNGSTEN, COLUMBIUM, TANTALUM AND OTHER HIGH-TEMPERATURE DESIGN MATERIALS; DEFINE THE PROBLEMS ANTICIPATED IN THE PRODUCTION OF THE EQUIPMENT; AND, SHOW A SYSTEMATIC APPROACH TO THEIR SOLUTION."

INTRODUCTION

The feasibility of ultrasonically welding the stipulated mono- and bi-metal sheet combinations was demonstrated by the data presented in Appendix II and discussed in Section I. Thus, the basic requirements for an ultrasonic welding machine must now be considered not only for joining these materials in gages up to 0.10 inch but for producing quality welds on a reproducible basis in these thicknesses. These matters as well as related problems and a systematic approach to their solution are considered in this section.

BASIC REQUIREMENTS

CLAMPING FORCE

As shown previously (69, 70), clamping force plays a role in making an ultrasonic weld which in no way resembles its effect in conventional pressure welding. In the latter process, pressure causes the metal to extrude away from the die locale resulting in a greatly thinned interfacial film condition which presumably achieves nascent metal contact and thus metallurgical bonding. With ultrasonic welding, however, the static clamping force is not of sufficient magnitude to produce any significant thickness deformation or extrusion radially from the contacting sonotrode tips; instead, the clamping force holds the pieces in intimate contact and produces a radial interfacial shear stress on which is superimposed the oscillating interfacial shear stresses which cause local slip within islands of elastic strain. Gross sliding is avoided as proven by the fact that overlapping spots, and spots between spots, can be made. Surface films are ground up and dispersed -- not extruded to ultra-thin, smooth layers as in pressure welding.

Clamping force, as shown in Section IV, also operates to provide an impedance match between the tip of the transducer-coupling system and the weldment. An optimum clamping force is essential to the production of satisfactory bonds under minimum energy conditions (MEC). Thus, control of the clamping force is essential to welding at minimum power. Extrapolating from Figure 2 of Section I, the maximum clamping force requisite to joining each of the specified materials at thicknesses of 0.10 inches is as shown in the following table.

Table 27

WELDMENT MATERIALS: ESTIMATED CLAMPING FORCE VALUES FOR 0.10-INCH MATERIAL

Weldment Material	Clamping Force* (pounds)
Cb(D-31)	3760
Inconel X-750	3440
Mo-0.5Ti	3120
PH15-7Mo	3280
René 41	2240
Tungsten	3840

* Values obtained by extrapolation from Figure 2, Section I.

Since the maximum clamping force required of the ultrasonic welding equipment hereunder consideration appears to be about 4000 pounds, the clamping force system will be designed to exert at least 4800 pounds, or a 20 percent excess. The precision with which the clamping force should be controlled is related to the width of the threshold curves (70), or of the thermal curves (see Figure 3, Section I). In either of these cases, a clamping-force tolerance of about ± 3% will probably be satisfactory to maintain operation within the MEC envelope. Welding should not be attempted precisely on the horizontal tangent line to the threshold curve, however. Instead, allowance should be made for modest variations in power as well as clamping force so that the welding operation will be easily contained inside of the welding threshold radius. The requisite clamping force and its proper control is straightforward.

POWER

Perusal of the information previously summarized on this subject (Section II and V) discloses two distinct frames of reference for power; first, as electrical power delivered to the transducer and second, as acoustical power delivered to the weldment.

The former embraces the inefficiencies of practical magnetostrictive transducer-coupling systems as will be evident on inspection of the left cluster of columns of Table 28. In such magnetostrictive systems, the efficiency is in the range of 20-25%.

The acoustic power values, across the bottom row of Table 28, do not include those losses characterized as transmission into weldment, coupler efficiency, transmission across system interfaces or the energy conversion efficiency. Inspection of the bottom line (delivered acoustical power) of the right hand, cluster of columns in Table 28 under the caption "Electrostrictive, Lead Zirconate Titanate", shows that the level of acoustical power delivered is more than twice that indicated across the bottom row of the magnetostrictive columns. This is particularly significant considering that both systems have the same energy input, and that, with the lowest assumed energy conversion efficiency (60 percent), the overall systems efficiency may be nearly 50%. With a more optimistic energy conversion efficiency of 80 percent, the delivered acoustic power, as shown in the last row of Table 28, will be in the range up to 60-65 percent.

Since the information provided in Table 28 is on the conservative side, it is reasonable to assume an overall systems efficiency of 50 percent. As will be discussed later in this section, other avenues for improving welding capability, such as power- and force-programming, variation in welding tip radius, use of foil interleaf, etc., are available to increase welding capability in the event the assumed system efficiency of 50 percent proves to be over-optimistic. These techniques, if necessary, will be used to ensure the performance of the equipment at the power levels outlined herein.

Accordingly, the electrical power required to weld the stipulated materials with an overall systems efficiency of 50 percent is summarized in Tables 29-31. First, consider Table 29 -- it is apparent that a welding machine capable of delivering 25 electrical-kilowatts into the transducers will join all materials, except tungsten, in gages of 0.10 inch at weld intervals of 1.5 seconds and less. To join tungsten at 1.5 seconds (the maximum reasonable weld interval that is likely to be productive of sound joints), however, a substantially larger welding machine would be required.

Table 28

TRANSDUCER-COUPLING SYSTEMS: COMPARISON OF RELATIVE EFFICIENCIES

TRANSDUCER Material	Input Power Units	Energy Conversion Efficiency (%)	Coupler Materials	Transmission Across T-C Interface (%)	Coupler Efficiency (%)* (Strain Level-0.0008-in./in.)	Transmission into Weldment (%)	Delivered Acoustic Power Units
MAGNETOSTRICTIVE Nickel-204	100	20	303 Steel	99	93	50	9
						85	16
			Al Bronze	97	97	50	9
						85	16
		35	303 Steel	99	93	50	16
						85	27
			Al Bronze	97	97	50	16
						85	28
ELECTROSTRICTIVE Lead Titanate Zirconate-PZT-4	100	60	303 Steel	98	93	50	27
						85	46
			Al Bronze	99	97	50	29
						85	49
		80	303 Steel	98	93	50	36
						85	62
			Al Bronze	99	97	50	38
						85	65

* Assumes system six half-waves long.

Table 29

ESTIMATED ELECTRICAL POWER REQUIRED TO WELD 0.060-INCH MATERIAL

AT VARIOUS WELD INTERVALS

(Systems Efficiency - 50 per cent)

WELDMENT MATERIAL	WELD INTERVAL - seconds												
	0.3	0.4	0.5	0.6	0.7	0.8	0.9	1.0	1.1	1.2	1.3	1.4	1.5
	ESTIMATED ELECTRICAL POWER - kilowatts												
Inconel X-750	13	10	7.6	6.3	5.4	4.7	4.2	3.8	3.4	3.1	2.9	2.7	2.5
PH15-7Mo	14	11	8.6	7.2	6.2	5.4	4.8	4.3	3.9	3.6	3.3	3.1	2.9
Cb(D-31)	16	12	10	8.1	7.0	6.1	5.4	4.9	4.4	4.1	3.8	3.5	3.3
Mo-0.5Ti		20	16	13	11	10	8.9	8.0	7.3	6.7	6.2	5.7	5.3
René 41				23	20	17	15	14	13	12	11	10	9.2
Tungsten							22	20	18	16	15	14	13

Table 30

ESTIMATED ELECTRICAL POWER REQUIRED TO WELD 0.090-INCH MATERIAL
AT VARIOUS WELD INTERVALS

(System Efficiency - 50 percent)

WELDMENT MATERIAL	WELD INTERVAL - seconds												
	0.3	0.4	0.5	0.6	0.7	0.8	0.9	1.0	1.1	1.2	1.3	1.4	1.5
	ESTIMATED ELECTRICAL POWER - kilowatts												
Inconel X-750	24	18	14	12	10	8.8	7.8	7.0	6.4	5.8	5.4	5.0	4.7
PH15-7Mo		20	16	13	11	10	8.9	8.0	7.3	6.6	6.2	5.7	5.3
Cb(D-31)		23	18	15	13	11	10	9.0	8.2	7.5	7.0	6.4	6.0
Mo-0.5Ti				24	21	18	16	15	13	12	11	10	10
René 41									23	21	19	18	17
Tungsten													24

Table 31

ESTIMATED ELECTRICAL POWER REQUIRED TO WELD 0.10-INCH MATERIAL
AT VARIOUS WELD INTERVALS

(System Efficiency - 50 percent)

WELDMENT MATERIAL	WELD INTERVAL - seconds												
	0.3	0.4	0.5	0.6	0.7	0.8	0.9	1.0	1.1	1.2	1.3	1.4	1.5
	ESTIMATED ELECTRICAL POWER - kilowatts												
Inconel X-750		21	17	14	12	11	9.4	8.4	7.6	7.0	6.4	6.0	5.6
PH15-7Mo			21	17	15	13	12	10	10	8.7	8.0	7.4	6.9
Cb(D-31)			22	18	15	14	12	11	10	9.0	8.3	7.7	7.2
Mo-0.5Ti						22	19	17	16	14	13	12	12
René 41											23	21	20
Tungsten													

An electrical power source of about 25-30 kilowatts constitutes a logical welding machine size, but this does not meet the power requirements for joining tungsten at the stipulated thickness of 0.10 inch. As shown in Tables 30 and 31, however, tungsten can be joined in somewaht reduced thicknesses with a 25-kilowatt machine. As indicated in Tables 30 and 31, 25 electrical-kilowatts are required to join 0.090-inch tungsten at 1.5 seconds, and the same 25-kilowatt machine can be expected to join 0.060-inch tungsten at shorter weld intervals of 1.0 seconds and less.

Subject to the acquisition of more specific information on the probable machine power sizes that can be expected from motor alternators, and solid state devices, it is proposed that Phase II of this program be initiated on the basis of an assumed 25-kilowatt machine which will join all of the materials stipulated, except tungsten, in gages up to 0.10 inches at reasonable weld intervals. This machine should, however, be capable of joining tungsten in all standard gages below 0.10 inches.

THE FOREGOING DISCUSSION ASSUMES WELDING UNDER CONDITIONS OF UTMOST SIMPLICITY; I.E., A "SQUARE" POWER PULSE TO THE TRANSDUCERS, NO FOIL INTERLEAF, NO TIP RADII MODIFICATION, NO AUXILIARY PREHEAT, NO POWER-FORCE PROGRAMMING, ETC.

As has been shown previously, the machine capability can be extended by,

<ins>Foil Interleaf</ins>: The use of foil interleaf of the same material of the weldment or of a different but compatible refractory metal, will extend the capability of any specific welding machine by one or two standard gages.

<ins>Power-Force Programming</ins>: Power programming alone has been shown to permit welding of materials normally unweldable with a specific machine, because programming does, in effect, preheat the weldment, reducing its hardness to promote increased ductility.

<ins>Tip Radii</ins>: Depending on the hardness of the weldment materials, etc., tip radii modifications (may make smaller welds under proper conditions of clamping force, etc.) may also reduce the power required to weld a material of specific thickness and hardness.

Since all of these augmentation factors are effective in extending the range of a welding machine, there is essentially no doubt that a 25-kilowatt machine will be capable of joining even 0.10-inch tungsten sheet at weld intervals of 1.5 seconds and less as well as all of the other materials in Table 29.

For the purpose of Phase II, it is therefore proposed that we undertake the design of an ultrasonic spot-type welding machine, projected on the basis of 25 kilowatts of electrical power, since it has already been established that this power level can be delivered by either an alternator at a frequency of 15,000-20,000 cycles per second, or by solid state devices which have already reached an impressive state of development. Of course, electronic equipment can also be provided. When the specific details of the power source (whether it is a motor alternator, a solid state device, or electronic) are brought into sharper focus, a machine providing up to 28 or 30 kilowatts may be feasible. The next power step above a 25-kilowatt machine that appears to be reasonable, however, is 40 or 50 kilowatts. At this time, consideration of such an increase for the sole purpose of welding 0.10-inch tungsten sheet without benefit of any of the known augmentation factors appears to be unjustified.

WELDING MACHINE DESIGN PROBLEMS

The larger problems, pertinent to the production of a 25-kilowatt ultrasonic spot-type welding machine and requiring further development effort, are as follows:

1. Direct read-out acoustical watt meter.
2. Power-Force programming.
3. Tip amplitude indicator with welding control via amplitude variation.
4. Sonotrode work contacting tips -

   Materials
   Geometry

5. High performance transducer assemblies.
6. Switching of Motor Alternator, (if used).

Additional ultrasonic welding experience with the materials of interest is also necessary to provide information for the use of differing radii tips, power-force programming, tip material performance, and tip geometry (especially mechanically removable tips). Welding investigations with the materials of interest will therefore be continued throughout Phase II so as to make such data available as well as to obtain machine settings, productive of welding below recrystallization temperature.

DIRECT READ-OUT ACOUSTICAL WATT-METER

As established previously (69, 70), the standing-wave ratio existing in an ultrasonic coupler can be utilized in adjusting the system to resonance, to determine the acoustical power being delivered to the weldment, and to compute the total acoustical energy delivered to the

weldment. To date, this equipment has consisted of sensing elements attached to the coupling system which are appropriately connected to the plates of an oscilloscope. While useful in the laboratory, oscilloscope indication is inconvenient for production use. This problem has been treated theoretically and circuitry has been devised to eliminate the oscilloscope and to provide a direct read-out device which will indicate acoustical power just as a VAW meter indicates electrical power. A SWR indicating system will be developed to include a direct read-out instrument. The oscilloscope is also desirable to assist in training operators and explaining the operation of the SWR system. Thus, such a unit will be assembled and its accuracy determined in connection with the standard physics laboratory evaluations of transducer assemblies. If time and funds permit, the unit will be refined for incorporation into ultrasonic welding equipment.

POWER-FORCE PROGRAMMING

Power Programming, which is a system for varying the power delivered during an ultrasonic weld pulse, offers a promising method for controlling the weld quality and reducing the total power necessary to generate an ultrasonic weld. Circuitry has been designed to provide both power-and force (clamping)-programing. Appropriate control instrumentation has been devised, and sources of the various component elements have been located.

Both power and force is controlled through pinboards on which the power-force variations desired during the pre-set weld interval and at suitable increments thereof is programmed. Appropriate application of electronic time-variable, constant-amplitude, ramp generators and pre-set triggering circuits, permits the decremental division of the weld interval for both power and applied force.

This device will be assembled and its performance evaluated in connection with refractory metal welding investigations.

TIP AMPLITUDE INDICATOR

A tip-amplitude indicator unit of the type presently in use at G.E. Hanford will be fabricated and evaluated, during the course of future welding studies in order to determine the significance of the induction and decay intervals that have been observed.

Suitable revisions in the device will be made to extend its usefulness in welding the materials specified in this program.

SONOTRODE WORK CONTACTING TIPS

Astroloy and Inconel X-750, the best tip materials available to date, will be studied further to ascertain the effect of standard metallurgical techniques on tip performance. Investigations of other promising tip material will also continue.

Further effort will be expended to evolve a mechanically removable tip designs that will be practical for high-power use. Present designs that have been satisfactory at contemporary power levels will be used as points of departure.

HIGH PERFORMANCE TRANSDUCER ASSEMBLIES

Utilizing the transducer assemblies of the types described and evaluated in this report, and taking into account the advice of specialists in the field of ceramic transducer materials, designs will be improved, fabricated and calorimetrically evaluated. Both conversion efficiency and power handling capacity will be determined. On the basis of these data and such theoretical treatments as may be indicated, the number of candidate assemblies will be reduced to not over 2, and these will be extended to a single refined transducer assembly design.

SWITCHING PROBLEM (Not present with electronic or solid state power sources)

Switching high-power levels in the electrical industry is routinely done with large vacuum type remotely controlled magnetic contactors. Response characteristics are not as critical in those applications, however, as those encountered in switching 25 kilowatts at the envisioned welding repetition rate, and with an expected accurate control varying from 0.10 to 1.0 second. On the basis of preliminary work, the performance of parallel banks of high current magnetic contactors equipped with arc suppression coils was satisfactory but the service life of these units is unclear for our purposes. As a back-up for these magnetic units, work is under way to evaluate high current solid state switches. Such devices promise trouble free performance without the attendant concern of arc-over and time-lag associated with the opening and closing times of contactor-type controls.

This work will be extended later taking into account the advice and cooperation of at least one group of outside specialists that are keenly interested in this problem.

VII. DESIGN SPECIFICATIONS

"THE CONTRACTOR SHALL OUTLINE, ON THE BASIS OF THE FEASIBILITY STUDIES, THE DESIGN PARAMETERS FOR THE REQUISITE HIGH POWER ULTRASONIC WELDING EQUIPMENT."

INTRODUCTION

In the following pages are provided the overall welding machine design parameters and various preliminary design specifications for ultrasonic welding equipment to join 0.10-inch thicknesses of the stipulated refractory metals and superalloys.

This information is presented under the following headings:

Power Source
Clamping Force
Transducer-Coupling System
Machine Dimensions and Structures
Instrumentation
Controls
Safety

POWER SOURCE

CAPACITY: 25,000 watts (25 kilowatts); adjustable stepwise or continuously from about 2 to approximately 25 kilowatts. (If stepwise, the increments will be of about 250 watts from 2000 watts to 5000 watts and approximately 500 watts from 5000 watts to 25,000 watts.)

FREQUENCY: Nominal 15,000 cycles/second (cps); continuously variable from 14,700 to 15,300 cps; stability at any setting $\pm$ 25 cps for over one hour.

TYPE: Motor-alternator, solid-state, or electronic.

IMPEDANCE: To match transducers.

INSTRUMENTS: See page 111.

CONTROLS: See page 112.

LOCATION: Within about 100 feet of welding machine.

CLAMPING FORCE

RANGE: 350 to 5500 pounds; reproducibility about ± 3 percent of full scale, after warmup.

TYPE: Hydraulic.

STROKE: One-inch hydraulic plus three-inches pneumatic or mechanical; total of four inches.

CYCLE TIME: Three seconds for a one-second weld interval. (20 welds per minute.)

HYDRAULIC SYSTEM:

Pump - Adequate pressure and volume to achieve above cycle time.

Filters - Standard - 100 μ.

Reservoir - Approximately 4 gallons.

Instruments - See page 111.

Controls - See page 112.

TRANSDUCER-COUPLING SYSTEM

CLASS: Opposition-Drive (both sonotrodes powered).

TYPE: Wedge-reed, top and bottom.

TRANSDUCER ASSEMBLIES

Material - Lead zirconate titanate.

Preloaded - 3 or 4 per sonotrode; 6-8 total.

Power input capacity (15 kc nominal) - one sonotrode only, approximately 12 - 13 kilowatts. Both sonotrodes approximately 25 kilowatts.

Preloading method - Tension shell, peripheral tie-bolts or center tie-bolt.

Cooling - Fluid, filtered compressed air or other.

Instruments - See page 111.

Controls - See page 112.

COUPLERS

Materials - Al-Bronze or Be-Copper.

Elements -

Longitudinal - Transformer ratio between 6 and 8; provisions for amplitude and SWR sensing; cooling fluid as required.

Reed - Adequate to carry the static force and to deliver the dynamic shear forces required for welding; provision for amplitude sensing; cooling fluid passage on central axis.

Joining Method - Brazing -- precision laboratory controlled.

TIPS

Materials - Astroloy or better, as indicated.

Joining Method - Mechanically attachment preferred; brazing.

MACHINE DIMENSIONS AND STRUCTURE

THROAT DEPTH: 36 inches or greater.

BEAM DEFLECTION: At clamping force of 4000 pounds; insufficient to permit uncontrollable skidding of weldment.

CONSTRUCTION: Welded; Channels, I beams, etc.

BASE PLATE: Dimensioned to prevent upset under reasonable forces for castoring; castors - lockable or separate jack screws.

PACKAGING: National Electrical Manufacturers Association - Standard.

HEAD MOVEMENT: Four-inch total, or more, on heavy-duty way-slides.

GENERAL LAYOUT: See Figure 14.

INSTRUMENTATION

ELECTRICAL:

Motor Alternator - Field Voltage.

V.A.W. - J. Fluke or equivalent.

Standard Frequency Counter - Hewlett Packard Company or equivalent.

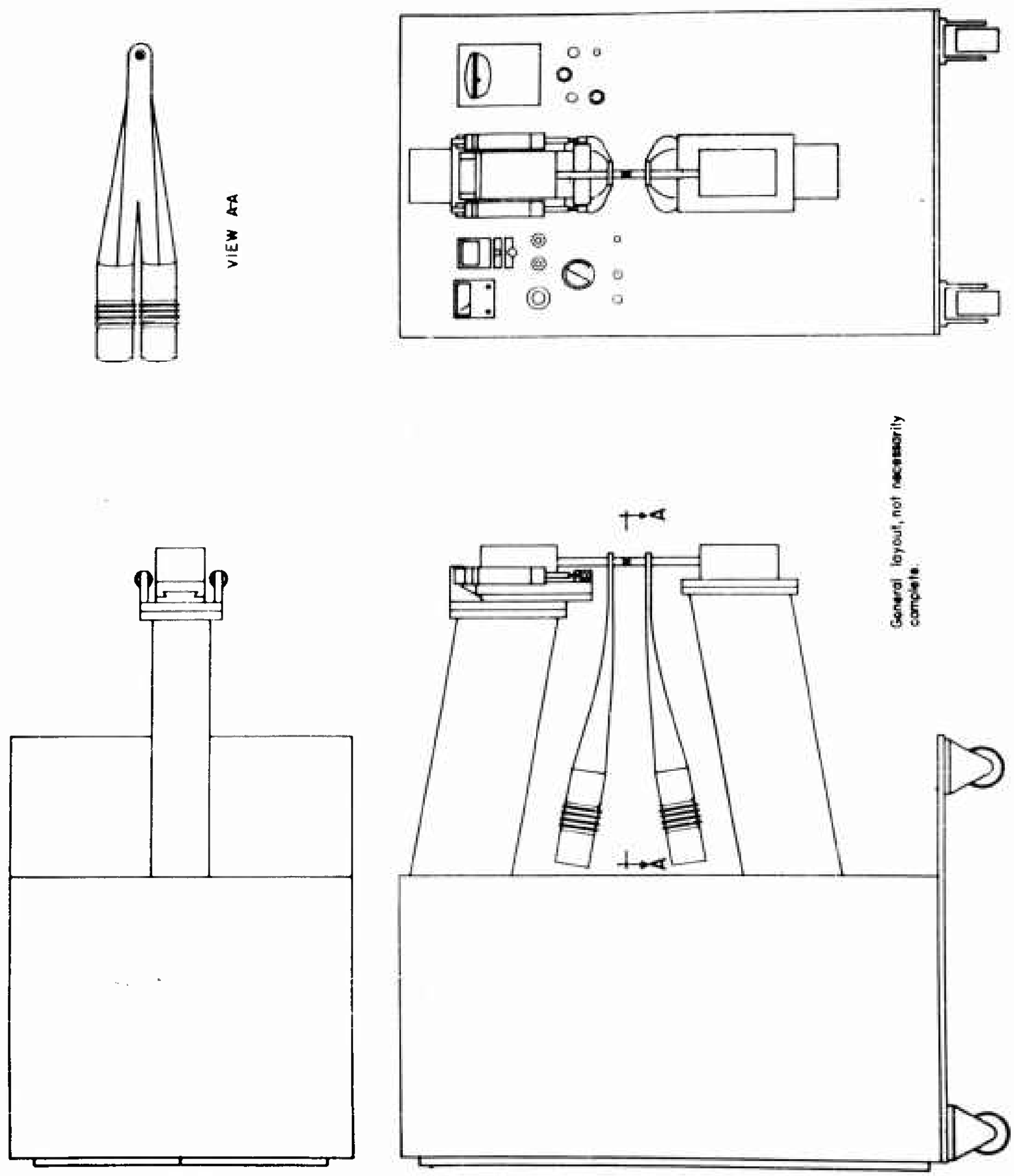

Figure 14: EXPERIMENTAL 25-KILOWATT WELDER

CLAMPING FORCE SYSTEM: Bourdon Gage Type for setting force, pilot-light -- indicating "force reached" for operation.

ACOUSTICAL:

Amplitude Indicator -

Integrating, direct read-out of acoustical watts.

Oscilloscope.

CONTROLS

POWER:

Master Switch -

Power Source -

Welding Machine -

Weld Sequence Control -

Cycle Timer - For weld-pulse length control 0.01 second to 2.0 seconds; electronic.

Foot Switch - To trigger weld-sequence control and weld-interval timer.

Scram Buttons - Energy cut-off, all circuits.

Automatic - Manual sequence - For automatic follow through of complete cycle after footswitch triggering, or permits manual triggering of ultrasonic power.

Power Programming (10 x 10 matrix control) - Any one of 10 power levels at any one of 10 percent increment of any preset weld-power interval of 0.10 seconds and above.

CLAMPING FORCE:

Force Set Valve -

Primary 4-Way Electrical Solenoid Valve -

Pressure Switch (s) - Adjustable, over range 350 - 5500 pounds force to trigger electrical circuits including weld-power pulse and pilot light.

Force Indicator - (Bourdon Gage) Cut-off valve (s).

Force Programming - Preset any one force level at any one of 10 percent increment of weld cycle. Total number of force levels, 3 to 5; integrated with Power Programming.

SAFETY

MASTER CONTROL: Actuates - deactuates all circuits.

POWER AND FORCE: Interlock - No weld power without force.

FAIL SAFE INTERLOCKS:

Minimum Clearance - No weld power without weldment in position.

Cabinet Door - Opens power off.

OVER-PRESSURE RELIEF:

Maximum Gage Scale Fixed - Two, if 2 force-gage ranges are used.

ULTRASONIC READY SWITCH: Prevents accidental triggering of ultrasonic power before clamping force is applied.

VIII. SUMMARY, CONCLUSIONS AND RECOMMENDATIONS

The feasibility of producing ultrasonic welds in both mono-metal and bi-metal combinations of the stipulated stainless, superalloy and refractory metals was demonstrated.

Extending the sheet-thickness, welding capability of a 4-kw ultrasonic welding machine to include the performance of an 8-kw laboratory machine, and utilizing a previously developed first approximation criteria for the energy required to join materials of various hardness and thickness, shows that the joining of these materials in gages of 0.10 inch is also feasible.

Confirmation of the validity of the energy equation at higher material hardnesses and thicknesses than heretofore investigated, permitted delineation of the power required from an ultrasonic machine to join these materials in thicknesses up to 0.10 inch; 25-kw into the transducers is necessary.

"State of the technology" of both transducer materials and coupler materials was ascertained by means of a survey which included known authorities. On the basis thereof as well as from confirming laboratory investigations, it was concluded that the transducer-coupling system for high-power ultrasonic welding equipment should utilize lead-zirconate-titanate ceramic transducer material with aluminum-bronze or beryllium-copper coupling members.

Power should be delivered to the weld area by a machine incorporating the opposition-drive, transducer-coupling geometry. General Electric's Astroloy will provide a suitable sonotrode tip material for the immediate requirements of the equipment.

The required 25-kw of electrical power can be provided now by either a motor-alternator or an electronic power source. Solid state generators are promising candidate power sources in the near future.

Investigation of concepts for ultrasonic spot, seam, and ring welding machines was carried out, and the immediately promising spot-welding machine was studied in considerable detail. Both theoretical and experimental information was derived in sufficient detail to provide preliminary design specifications for equipment to join the stipulated 0.1 inch thickness of the hard, high-strength material.

The design fabrication and demonstration of a 25-kw spot-type welding machine should be completed prior to initiating the development of a roller-seam welding machine. Technical problems implicit in high power seam welding equipment are being solved for commercial purposes.

Phase II of this project as originally called for in the Request for Proposals, remains in order and the work spelled out, namely:

1. The object of Phase II is to develop the necessary methods, techniques and equipment to ultrasonically weld the selected materials,

2. The contractor shall design and construct ultrasonic joining unit(s) in accordance with the approach outlined in Phase I,

3. The contractor shall develop methods and techniques to demonstrate the capability of the equipment developed under Phase II to join the selected materials,

will properly and expeditiously provide ultrasonic welding equipment for the intended purposes.

It is recommended that Phase II be initiated at once.

APPENDIX I

DETAILS OF THE 8-KW ULTRASONIC WELDING MACHINE ASSEMBLY (OPPOSITION-DRIVE SYSTEM)

BACKGROUND

Delivery of high levels of vibratory energy into one side of a weldment subjects the reaction anvil and supporting structure to oscillating stresses and resulting energy losses. Although experience to date has led to several means for maintaining noncompliant characteristics in reaction anvils with concomitant minimum energy loss, these problems become more acute as the power capacity of the machine is increased. The opposition-drive system (see Section V), with energy supplied via both upper and lower sonotrodes, alleviates these difficulties, and permits welding without significant energy loss to the structures.

Opposition-drive systems involve other problems which evolve from any lack of precision in matching, the resonant frequency of the two transducer-coupling systems. Under unstable conditions, one transducer-coupling system may drive the other (as a motor drives a generator) and little energy is delivered into the weldment.

Precise phasing in the initial mechanical coupling between the upper and lower units, as determined by dynamic microphone elements located at stress antinodes along the wedge components, can be achieved by an adjustment in the electrical circuits. This approach was used in connection with the 8-kw equipment described herein.

COMPONENTS AND ASSEMBLY

Previous work demonstrated the feasibility of using essentially identical 4-kw, wedge-reed type transducer-coupling systems, operating in mirror opposition as shown in Figure 15, and excursioning in an out-of-phase relationship, to provide a crude 8-kw ultrasonic welding array. To accomplish this, the standard reactance anvil was replaced by a 4-kw, wedge-reed system. The reed length of this alternate system was adjusted within a clamping-type mass so that its operating frequency matched, precisely, that of the original unit on the machine.

Out-of-phase operation was achieved by adjusting the electrical current through the transducers and the relative phase of the applied

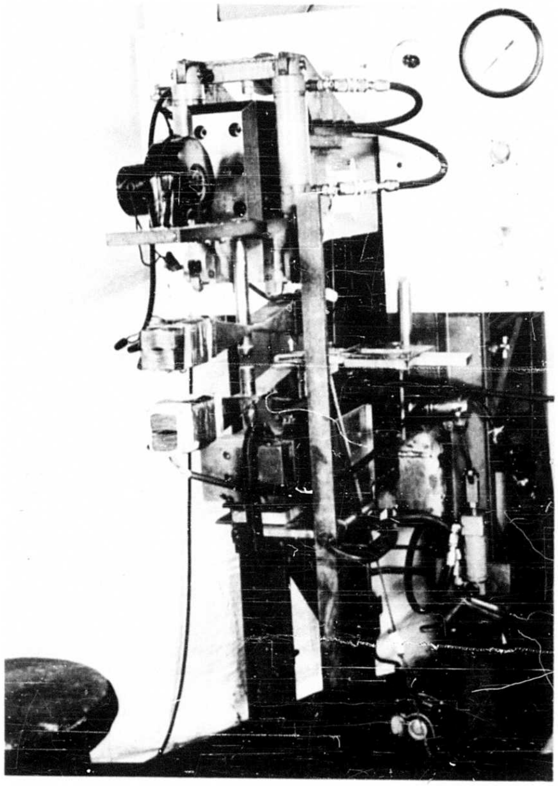

Figure 15: EXPERIMENTAL 8-KILOWATT ULTRASONIC SPOT WELDING MACHINE

signal (to the ultrasonic power generators) to obtain a precise 180° mechanical-phase relationship. The basic elements associated with the electronic and mechanical components of this system are shown in the block diagram of Figure 16.

The tips, terminating the sonotrodes for all of the work done with the 8-kw unit, were made of vacuum-cast Astroloy which was obtained in rod form. The upper sonotrode was terminated by a 3-inch spherical tip while the lower consisted of a flat tip. Both tips were dressed periodically, and two tips changes were made during the investigation.

AUXILIARY EQUIPMENT

Ultrasonic welding machines are equipped with: self-contained, hydraulic pumps and control circuits for application of the clamping forces associated with ultrasonic welding; timer circuits and controls for both sequence and weld-time interval; as well as, both electric and ultrasonic power- and force-control. A laboratory model 4-kw welding machine equipped with such devices was used in this experimental 8-kw unit.

PERFORMANCE DATA

A number of preliminary welds were made in aluminum alloys to determine the relative performance level of the 8-kw system with respect to a standard 4-kw laboratory model machine. These data are summarized in Table 32. The welding performance of the 8-kw unit was generally better than the 4-kw at equivalent power levels; this was expected because the anvil losses are generally eliminated. Refractory metals were welded with this equipment.

At the conclusion of the refractory mono-metal joining studies, a number of 0.063-inch, 2024-T3 bare aluminum specimens were welded to confirm that machine performance had not been substantially altered during the refractory metal work.

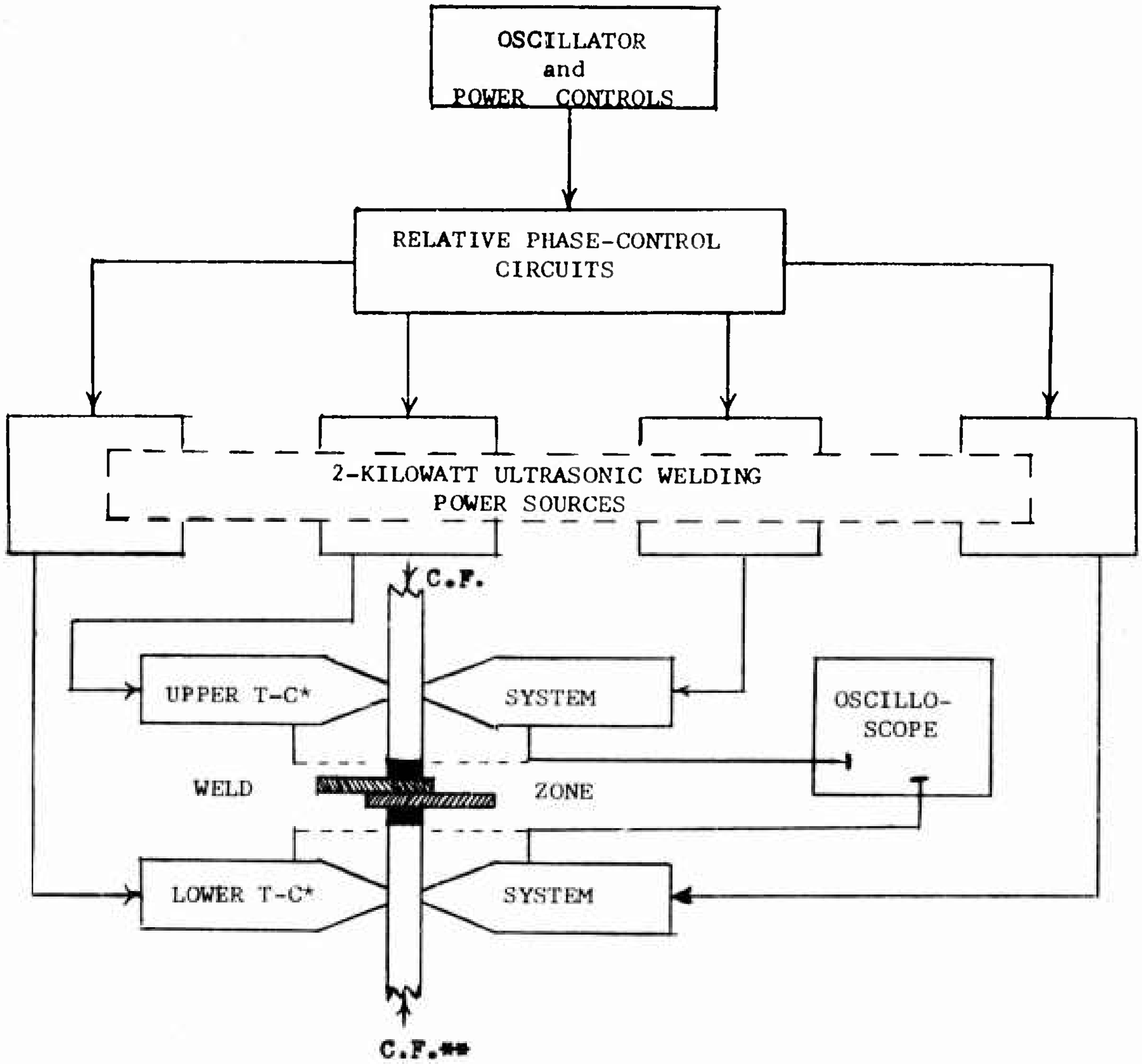

Figure 16: BLOCK DIAGRAM OF COMPONENTS IN 8-KILOWATT ULTRASONIC WELDING ARRAY

* T-C = Transducer-Coupling.
** C.F. = Clamping Force.

Table 32

8-KILOWATT ULTRASONIC SPOT WELDER: PERFORMANCE DATA

Weldment: Aluminum Alloy	Weldment: Gage (inch)	Welding Machine[a] (kw)	Welding Conditions: Input Power (watts)	Welding Conditions: Clamping Force (pounds)	Welding Conditions: Weld Interval (seconds)	Typical Shear Strength (pounds/spot)
2024-T3 Bare	0.050	4	3000	1000	1.5	900-1200
		8	2500	1000	1.5	960-1390
2024-T3 Bare	.063	4	4000	1000	1.5	400-1000
		4	4000	1000	1.5	900-1500 (W.I.)[b]
		8	3500	1000	1.5	920-1690
2014-T6	.080	4	No Weld			
		8	6500	1000	1.5	800-1800
1100 Plate	.125	4	No Weld			
		8	7500	1000	1.0	1400-1600
		8	7500	1000	1.5	1400-1600
2024-T3 Bare	.063	8	3500	1000	1.5	900-1300[c]

[a] 4-kw Laboratory Model
8-kw Experimental Opposition-Drive System

[b] W.I. = With Interleaf (0.001-inch, 1100-0 aluminum).

[c] Welded after refractory mono-metal bond studies were completed.

APPENDIX II

DETAILS OF WELDING STUDIES

WELDING CONDITIONS

Research has established that the minimum energy required to produce a good weld is associated with the clamping force which, within certain limits, permits the best impedance match into the weldment (70). Energy requirements for welding the refractory materials are discussed in detail in the body of this report (Section II). The clamping force range, within which satisfactory welds were obtained for the refractory materials, was approximated by one of the three methods described below but due to the broad scope of this feasibility study, accurate minimum energy conditions were not ascertained nor were optimum welding conditions established.

THRESHOLD CURVE OR NUGGET PULL-OUT METHOD

Clamping force requirements for reasonably malleable materials are established on weld evaluation by a peel test. Welds are made at a single clamping force and a single weld-time interval but with decreasing power until the weld fails in peel instead of by nugget pull-out. This procedure is repeated at various clamping forces to establish power vs clamping-force curves wherein the point of transition from nugget pull-out to peel is considered a threshold of satisfactory welds. The minimum of the curve corresponds to the clamping force that provides the best impedance match between the system and the weldment.

THERMAL RESPONSE METHOD

For brittle materials, the nugget pull-out test is not feasible and the thermal response (temperature in the weld zone itself) is used to establish clamping-force requirements. For a fixed power-setting, the temperature in the weld zone, irrespective of weld quality, is approximately maximum at the clamping force associated with the minimum of the power-clamping-force curve. Thus, for brittle materials, a convex upward curve of temperature as a function of clamping force is obtained. With this thermal response method, it is necessary to ascertain the power settings required to produce a weld at each clamping force, whereas with the nugget pull-out method, the power value is obtained at the same time as the clamping-force level.

STANDING-WAVE RATIO METHOD

The power delivered by any ultrasonic transducer-coupling system can be monitored by observing the elastic standing-wave ratio existent on the coupler; a standing-wave-ratio method is used to establish clamping-force values at a fixed power setting. Microphone-type elements are used to detect the standing-wave pattern along the transmitting system and to measure the ratio of maximum to minimum particle displacement along the acoustic coupler (the associated standing-wave ratio). This is accomplished by applying the electrical signals derived from the microphone elements to the vertical and horizontal plates of an oscilloscope; the result is a varying elliptical pattern, the area of which is proportional to the mechanical power passing through the instrumented portion of the coupler at any instant.

Furthermore, the thickness of a material and the clamping force necessary to produce an ultrasonic weld at minimum power level are definitely related. When the clamping force approximates the optimum for a specific thickness of a given material, the best impedance match between the sonotrode tip and the weldment is automatically obtained; thus, delivery of energy into the weld area is maximized.

Since the requisite clamping force is dependent on both the weldment material and its thickness, and since a clamping-force value established previously for thinner gages of these materials was available, the force range for only one of the heavier gages was determined; the clamping force for other gages was then estimated by interpolation or extrapolation.

The clamping-force values utilized during this work and in previous studies for mono-metal welds are shown in Figure 2 of Section I. As mentioned above, these values of clamping force are approximate and neither minimum energy conditions nor good quality welds are ensured. From the results of the welding studies, however, the clamping force values established for the various gages of each material apparently were of the proper order of magnitude.

EXPERIMENTAL RESULTS

The welding conditions (machine settings) used to make mono-metal welds in each material with the 8-kw laboratory welding array are shown in Table 33. The average tensile-shear strength of the welds is also included in these tables. No significance is attached to the differences in spot strength at the various energy levels because little effort was expended to refine the machine settings or to establish that the materials used were altogether the same -- welding feasibility was the primary objective.

Table 33

MONO-METAL WELDS: WELDING CONDITIONS AND TENSILE-SHEAR STRENGTH DATA

WELDMENT MATERIAL Designation	Gage (inch)	Power (kw)	Weld Interval (second)	Weld Energy (kw-sec)	Clamping Force (pounds)	Number of Measurements	Tensile Strength (lb/spot)
Cb(D-31)	0.010	1.8	0.5	0.9	600-700	4	290
		7.5	.1	0.75	600	2	295
		2.0	.5	1.0	600	2	150
		1.5	.7	1.1	700	1	130
		2.5	.5	1.3	700	2	220
	.015	7.5	0.2	1.5	750	1	110
		5.0	.4	2.0	900	1	230
		6.3	.4	2.5	900	1	230
		6.0	.5	3.0	800-1000	6	245
		6.0	.7	4.2	800	7	195
		4.5	1.5	6.8	800	1	320
	.025	7.0	0.5	3.5	900-1100	3	330
		7.0	.8	5.6	900	2	270
		7.0	1.0	7.0	500-1100	6	490
		6.7	1.5	10.0	700-1100	10	575
		6.5	2.0	13.0	1100	1	530
Inconel X-750	0.033	6.0	0.6	3.6	400-900	4	895
		6.0	0.8	4.8	900	2	550
		6.0	1.0	6.0	900-1100	3	1285
		6.3	0.5	3.2	900	1	1780
	.040	6.3	0.8	5.0	1100	3	1935
		6.0	1.0	6.0	900-1100	1	1060
		6.0	1.2	7.2	1000	1	1030
		6.0	1.5	9.0	1000-1100	6	1270
		6.3	2.0	12.6	1000	1	1250
		6.3	1.3	8.2	1100	1	1010
		6.3	1.5	9.4	1100	3	1445

(Concluded on next page)

Table 33 (Continued)

WELDMENT MATERIAL							
Designation	Gage (inch)	Power (kw)	Weld Interval (second)	Weld Energy (kw-sec)	Clamping Force (pounds)	Number of Measure-ments	Tensile Strength (lb/spot)
Mo-0.5Ti	0.008	3.0	0.4	1.2	350-550	15	150
		6.0	.2	1.2	350-550	12	140
	.020	6.0	.6	3.6	650-1050	15	237
	.032	7.5	1.0	7.5	1000-1100	3	295
		7.5	1.2	9.0	1000-1100	6	310
		7.5	1.4	10.5	1100	3	420
		7.5	1.5	11.2	1100	1	450
PH15-7Mo	0.020	6.5	0.3	2.0	700-1000	26	1265
		6.5	0.2	1.3	800	2	850
		6.5	.4	2.6	800	2	1355
	.030	6.5	0.2	1.3	900	1	1500
		6.5	.3	2.0	900	1	1450
		6.5	.4	2.6	900	2	1905
		6.5	.5	3.3	900	1	1910
		6.5	.6	3.9	800-1000	18	1975
René 41	0.020	6.0	1.0	6.0	600-800	10	380
	.030	6.4	1.0	6.4	1000	3	330
		6.4	1.0	6.4	800-1000	6	490
Tungsten	0.015	7.5	0.9	6.7	500-900	12	130
	.020	7.5	1.0	7.5	700-900	3	175
		7.5	1.2	9.0	700-900	4	130
	.030	7.5	1.5	11.3	700-1100	11	215
		7.5	2.0	15.0	900-1000	7	235
		7.5	2.5	18.8	900	2	230
		6.5	2.0	13.0	900	1	310

The energy and clamping-force levels for the bi-metal investigation are given in Table 34; tensile-shear strength values for these dissimilar material welds are also included in this table.

The weld characteristics were evaluated on the basis of tensile-shear strength measurements in an Instron Testing Machine, microscopic surface inspection, and metallographic study.

Because of the low ductility of tungsten and Mo-0.5Ti, welded coupons of these materials were joined to aluminum support strips (by means of quick-setting epoxy adhesive) before shear-strength measurements could be made. The cross-sectional area of the aluminum backing plates was larger than that of the welded tungsten and Mo-0.5Ti coupons to compensate for the disparity in moduli. The weld specimens of the four remaining materials were tested in shear by tensioning the welded assemblies directly with an Instron Testing Machine at a cross-head rate of 0.5 inches/minute. The strength values were recorded by means of an automatic strip-chart.

Table 34

BI-METAL WELDS: WELDING CONDITIONS AND TENSILE-SHEAR STRENGTH

WELDMENT MATERIAL									
Material	Gage (inch)	Material	Gage (inch)	Power (kilowatts)	Weld Interval (second)	Weld Energy (kw-sec)	Clamping Force (pounds)	Number of Measure-ments	Tensile Strength (lb/spot)
Cb(D-31)	0.025	Inconel X-750	0.040	6.3	1.0	6.3	900	1	680
					1.5	9.4	700	1	680
		Mo-0.5Ti	0.032	7.0	1.0	7.0	700	2	700
		PH15-7Mo	0.030	6.3	0.6	3.8	800	2	1240
					0.8	5.0	800	1	1100
					1.0	6.3	600-1000	4	1110
					1.5	9.4	800	1	960
		René 41	0.030	7.0	1.0	7.0	900	1	750
					1.5	10.5	900	1	900
		Tungsten	0.030	6.3	1.0	6.3	700	1	90
Inconel X-750	0.040	Mo-0.5Ti	0.032	6.3	1.5	9.4	800-1000	3	533
		PH15-7Mo	.030	6.3	0.6	3.8	800	2	820
					0.7	4.4	800	1	1560
					1.0	6.3	800	5	1120
		René 41	.030	6.3	0.8	5.0	800-1000	3	1750
		Tungsten	.030	7.0	1.5	10.5	900	1	180
Mo-0.5Ti	0.032	PH15-7Mo	0.030	7.0	0.8	5.6	800	1	550
				7.0	1.0	7.0	800	1	750
		René 41	.030	6.3	1.5	9.4	600-800	2	330
		Tungsten	.030	6.3	1.0	6.3	700	1	115
PH15-7 Mo	0.030	René 41	.030	6.3	0.7	4.4	800	2	1025
					1.0	6.3	800	9	1525
René 41	0.030	Tungsten	0.030	6.3	1.0	6.3	700	2	115

APPENDIX III

TRANSDUCER MATERIAL STUDIES

BACKGROUND

The power handling capacity of an ultrasonic welder, in general, is limited by the efficiency with which vibratory energy is transmitted by critical elements in the acoustical system. The efficiency of these elements, i.e. transducer, coupler and tip, in turn is affected by such factors as design variables, material properties, fabrication methods, etc. In order to develop the high power equipment required in this program, transducers of both magnetostrictive and electrostrictive materials were evaluated to ensure the selection of a transducer element of maximum efficiency.

Laminated nickel-type magnetostrictive transducers are commonly used in ultrasonic welding because these materials are relatively easy to fabricate and possess good mechanical properties, which enables the core to withstand induced stresses at high power levels. The operating efficiency of these units is generally between 20 and 25 percent, which is considerably less than that associated with the newer, electrostrictive ceramic transducers. With the newer ceramic materials, such as lead zirconate titanate (PZT-4), electromechanical coupling and ultimate power conversion efficiency is reported to be much higher than that for any other type of transducer material. Although Whymark (82) recently proposed a method for increasing the energy conversion efficiency of nickel transducers to very high levels, considerable work will be required to reduce his proposal to practical application.

In order to evaluate these newer ceramic materials and compare their efficiencies with that of the magnetostrictive, nickel-type, transducer, a method was devised to measure the performance of both types of transducer units under load conditions similar to those induced during welding operations.

TEST UNITS

Test specimens consisted of a preloaded sandwich-type arrangement of electrostrictive ceramic wafers wherein the compression load was produced by three geometric arrangements, see Figure 9D in Section IV.

These arrangements to provide compression on the ceramic elements included peripheral tension bolts, a center tension bolt, and a tension shell design, see Figure 9, Section IV. On the advice of specialists*, the units were prestressed at approximately 7000 psi and electrically driven at a strain level delineated by tan $\delta < 0.04$.

EXPERIMENTAL PROCEDURE

The ceramic units were coupled to the energy sink, or load, which involved a lead billet (Figure 17). Electrical input power to the ceramic unit was supplied at a 600-watt level by a 2-kilowatt electronic power source. The input power was monitored and maintained at the proper level by means of a VAW** in the line between the power source and the transducer. To drive the power source, a General Radio oscillator was used. Optimum frequency for the system was maintained by vibration pick-up probes, located along the coupling element, and a Hewlett Packard-type VTVM.

As the vibratory energy delivered into the lead billet degraded into heat, the temperature rise in the billet was measured by thermocouples and recorded on strip-charts. The energy conversion efficiency was calculated from these temperature measurements.

SUMMARY OF EXPERIMENTAL WORK

During the course of this work, four ceramic transducer units were studied, as shown in Table 35. In this initial evaluation, tuning and impedance characteristics were determined at relatively low-power levels. Later, units 1A and 4 were subjected to more rigorous testing at high-power levels and the performance of each unit was compared with that of a standard nickel transducer under the same load conditions.

The temperature measurements for each unit were converted into energy values by computing the ratio of vibratory energy delivered into the lead billet to initial electrical energy input (input power (watts) x test period (minutes)). These data are summarized in Table 36 and curves of the temperature distribution in the lead billet after 8 minutes are given in Figure 18 for ceramic units 1A and 4 as well as for the standard nickel transducer.

---

* Brush Development Company.

** Fluke VAW Model 101, J. Fluke Company, Seattle, Washington.

Figure 17 : TRANSDUCER EVALUATION EQUIPMENT

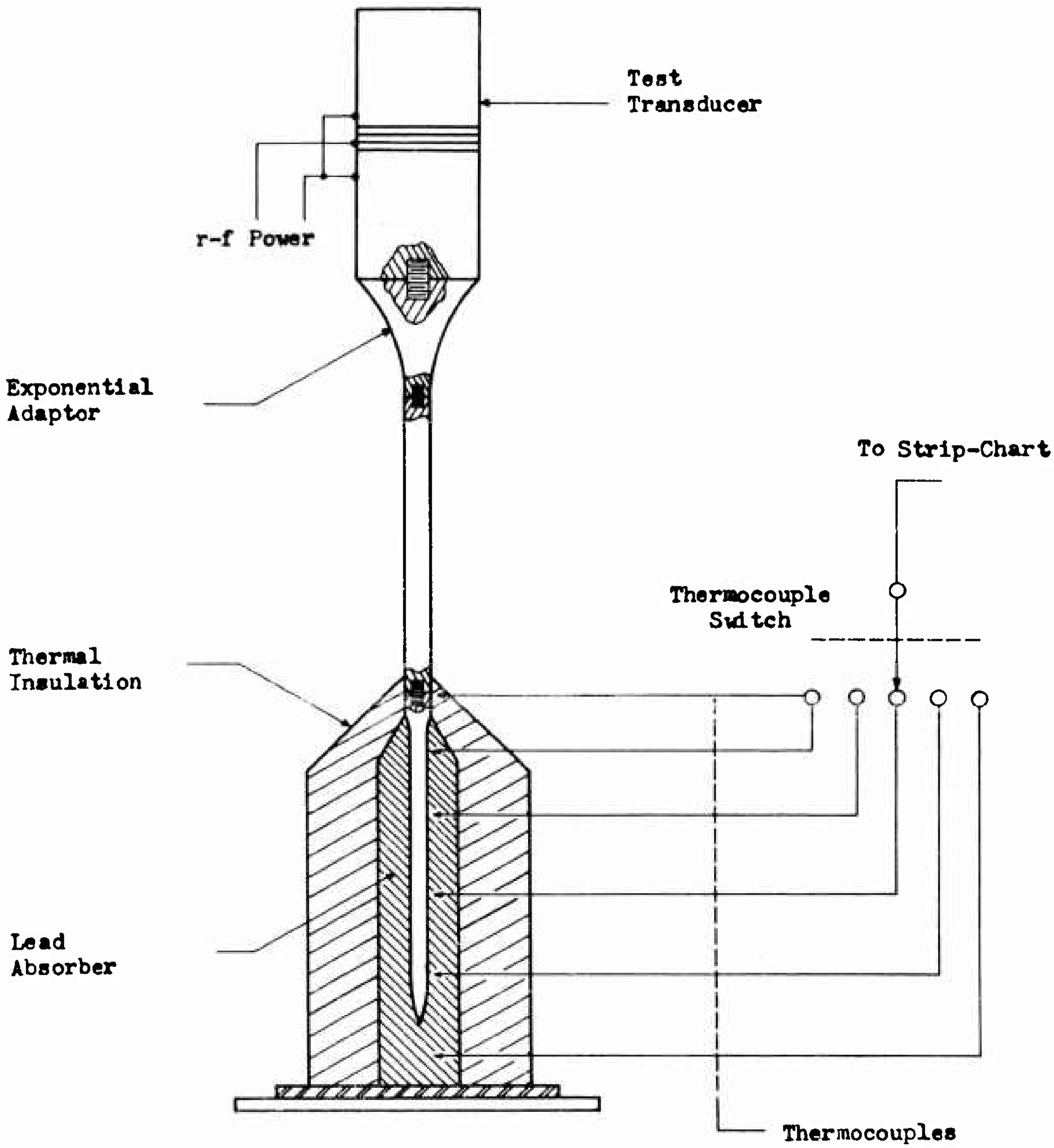

Table 35

CERAMIC TRANSDUCER ELEMENTS: OPERATING CHARACTERISTICS

Unit No.	Transducer Element	Operating Characteristics
1	Peripheral Tie-Bolt	Spurious, plate-type resonance observed on end-sections.
1A	Unit 1 plus 1/2-wavelength stub on end plate	Unit easily driven and very active. Performance satisfactory.
2	Center-bolt	Unit not symmetrical; both torsional and bell-type vibration observed. Difficult to drive in longitudinal mode.
3	Shell	Plate-type vibrations on rear support plate, peristaltic vibrations on compression noted in harmony with longitudinal vibratory mode.
4	Unit 2 plus 1/2-wavelength stub on end plate	Performance satisfactory.

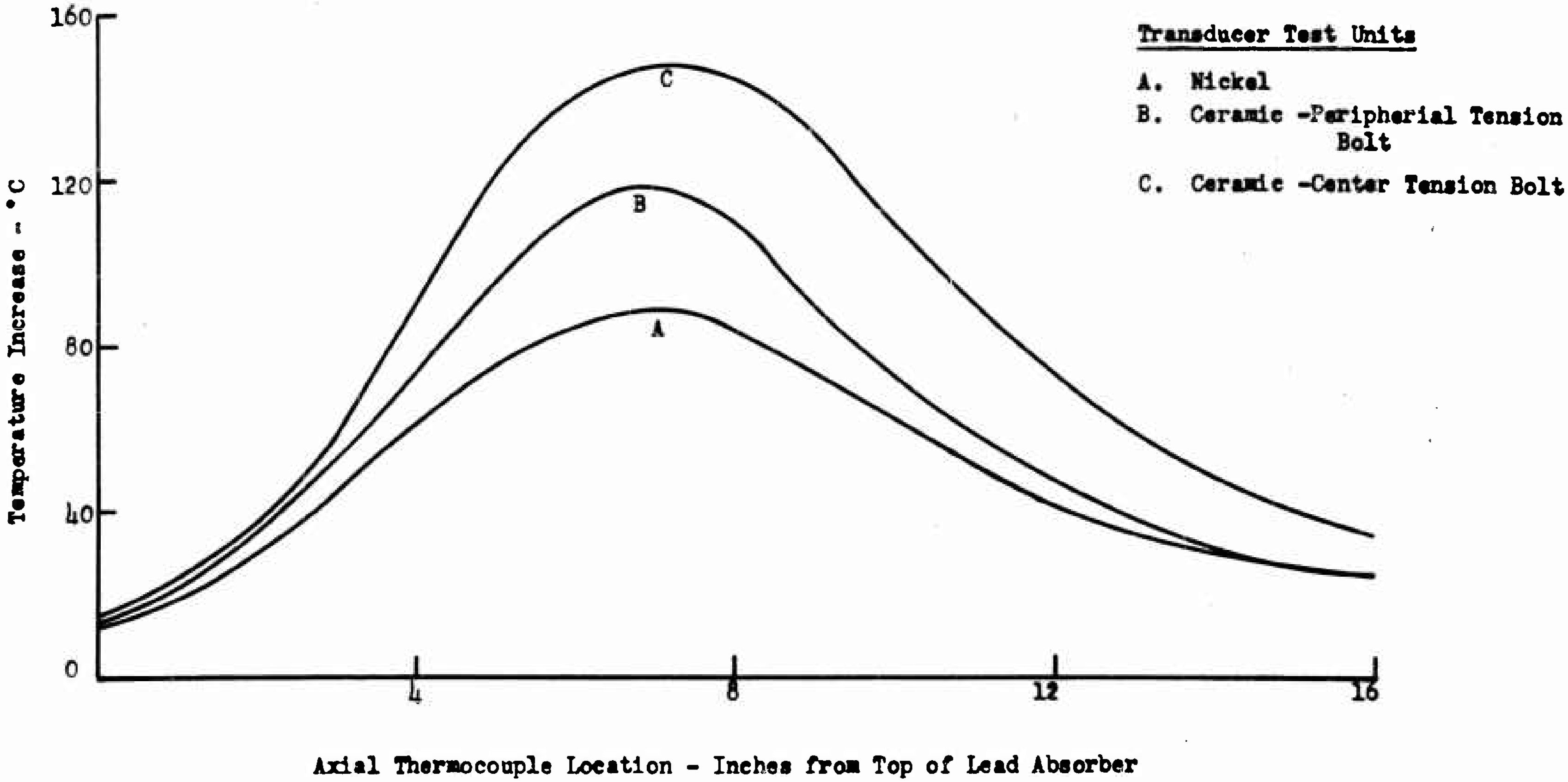

Figure 18: TEMPERATURE DISTRIBUTION IN LEAD ABSORBER AFTER 8-MINUTE TEST PERIOD

Table 36

TRANSDUCER ASSEMBLIES: RELATIVE ENERGY CONVERSION EFFICIENCY
(Input Power - 600 watts)

Transducer	Test Period (min)	Energy Input (kilowatt-seconds)	Energy Output (kilowatt-seconds)	Conversion Efficiency (percent)
Nickel	15	540	119	21
Ceramic:				
Unit 1A	15	540	140	26
Unit 4*	8	288	95	33

* Section of test unit broke after 8 minutes.

As shown in Figure 18, the relative energy conversion efficiency of both ceramic units is superior to that of the standard nickel transducer. While the efficiency of unit 4 is greater than that of 1A, this difference is attributed to the improved design of ceramic element 4.

A review of the electrical information derived from this work disclosed that both the drive voltage and the operating strain were higher than recommended. The desirability of making further modifications in the design of the ceramic elements was also indicated.

Specialists at Brush Development Company have been cooperative and will assist in the development of ceramic transducer assemblies with which system efficiencies of 50 percent or higher can be achieved.

APPENDIX IV

COUPLER MATERIAL STUDIES

EXPERIMENTAL EQUIPMENT

A schematic diagram of the equipment used in the resonant-element method for evaluating candidate coupler materials is given below:

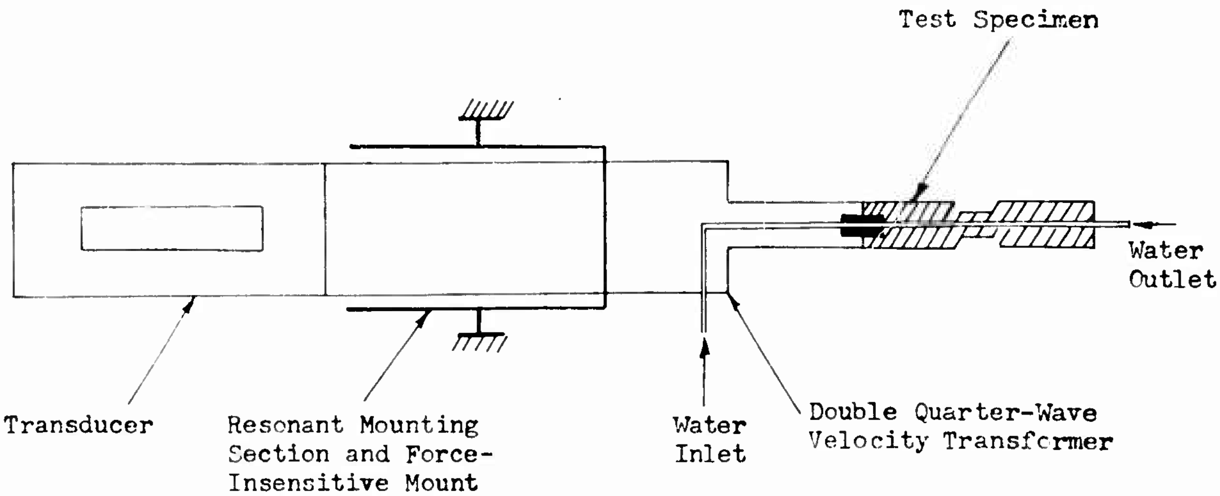

Electrical energy at a frequency of 15 kilocycles is delivered by a standard ultrasonic electronic generator to a transducer, where it is converted into mechanical vibrations. The transducer, a standard laminated nickel stack is attached to a combination resonant half-wavelength coupler and force-insensitive mount. Mechanical transformers of (several types (74, 135) are easily fabricated) were used to achieve the necessary strain levels. These consisted of a resonant double quarter-wavelength cylindrical element (to drive the test specimen) and the test specimen which was so designed as to amplify the strain.

TEST SPECIMENS

Test specimens in the form of a dumbell with an axial hole (half-wavelength, resonant, cylindrical stub) were designed to give a stress amplification or gain of 2.5 in the central, linearly stressed-section. The dimensions of the individual test units were calculated (after correction for resonance at the precise resonant frequency) from the design equations (given below), are presented in the following table.

Table 37

DESIGN DATA FOR TEST SPECIMENS

Stress gain = 2.5
Frequency = 15 kilocycles

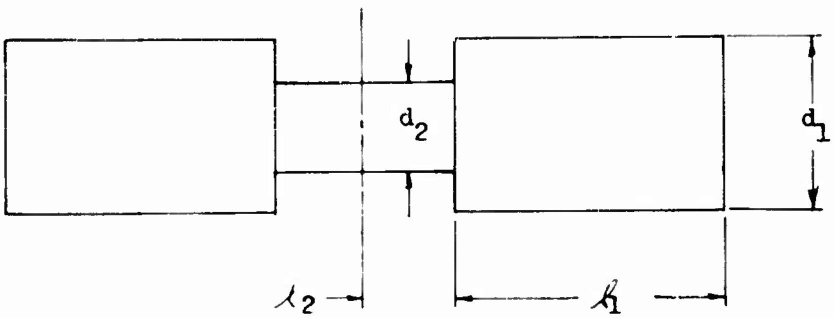

Coupler Material	Wave Length λ (inches)	Impedance ρc	Diameter d_1 (inches)	Diameter d_2 (inches)	Length l_1 (inches)	Length l_2 (inches)
Be-Copper	9.974	3120	1.000	0.575	1.606	0.329
Al-Bronze	10.656	3086	1.000	.575	1.716	.352
K Monel	11.758	3790	0.902	.521	1.893	.388
Ti (6Al-4V)	13.122	2297	1.159	.669	2.113	.433
Steel (303 S.S.)	13.200	3923	1.000	.575	1.870	.430

Evaluation of the candidate coupler materials was thus carried out at essentially the same strain levels as those reported by Neppiras.

BASIC EQUATIONS

Since the frequency equations (79, 131, 135) involved in calculating the dimensions of the resonant, dumbell-shaped specimens are adequately covered in the literature, only the basic design equations are given below:

$$\lambda = c/f \tag{1}$$

where: λ = wavelength of sound in the material

c = velocity of sound

f = frequency

and,

$$k = 2\pi/\lambda \tag{2}$$

$$(d_1/d_2)^2 = (\cot kl_1)(\cot kl_2) \tag{3}$$

$$\text{stress gain} = (\cot kl_1)/(\cot kl_2) \tag{4}$$

where:

d_1 and d_2 = diameters as shown in figure

l_1 and l_2 = length of different portions of test specimen

The strain level can be computed by the standard equations defining the vibration amplitude ξ in terms of its maximum value

$$\xi = \xi_o \sin kx$$

The associated strain is given by

$$\partial\xi/\partial x = k\,\xi_o \cos kx$$

Introducing the boundary conditions (134) associated with the stress amplifications yields the peak value of strain as:

$(\partial \xi/\partial x)$ peak $= k\,\xi_o\,G$ where G represents the strain gain for the dumbell resonant element.

SAMPLE CALCULATIONS

From the above equations, peak strain levels were computed and the power loss-strain curves of Figure 19, were plotted. For example, a peak to peak deflection of 0.78 mils was recorded for a Be-copper test specimen at an input power of 100 watts. Substituting appropriate values into the above equation for peak strain gives:

$$(\partial \xi/\partial x)_{peak} = (2\pi/9.974) \times (0.00078/2) \times 2.5$$

$$= 0.612 \times 10^{-3} \text{ inch/inch.}$$

At this strain level, and at flow rate of 330 cubic centimeters or 2.75 grams/second, the temperature difference between the inflow and outflow stabilized after two minutes -- the temperature difference indicated by the thermocouples was 2.8°C. From this information, the power dissipated, P, was calculated from the equation

$$P = W \times \Delta T \times J$$

where

W = water flow rate in grams/sec (g/sec)

ΔT = temperature difference in degrees centigrade (°C)

J = joules equivalent in joules/calorie.

by substituting the indicated values for W and ΔT,

$$\text{Power loss} = 2.75 \times 2.8 \times 4.8$$

$$= 32.2 \text{ watts.}$$

This value represents the power dissipated internally.

Assuming that the energy dissipated in any part of the system is proportional to the strain in that section and the volume, the power lost in the central linearly strained portion of the test specimen can be computed by considering the geometry and strain distribution along the system (Figure 20). These computations indicated that about 18 percent of the total power loss occurred in the central section. These values are tabulated in the last column of Table 38 and are presented in the form of curves in Figure 21.

Figure 19: POWER LOSS AND STRAIN CHARACTERISTICS OF CANDIDATE COUPLER MATERIALS

(Frequency - 15 kilocycles)

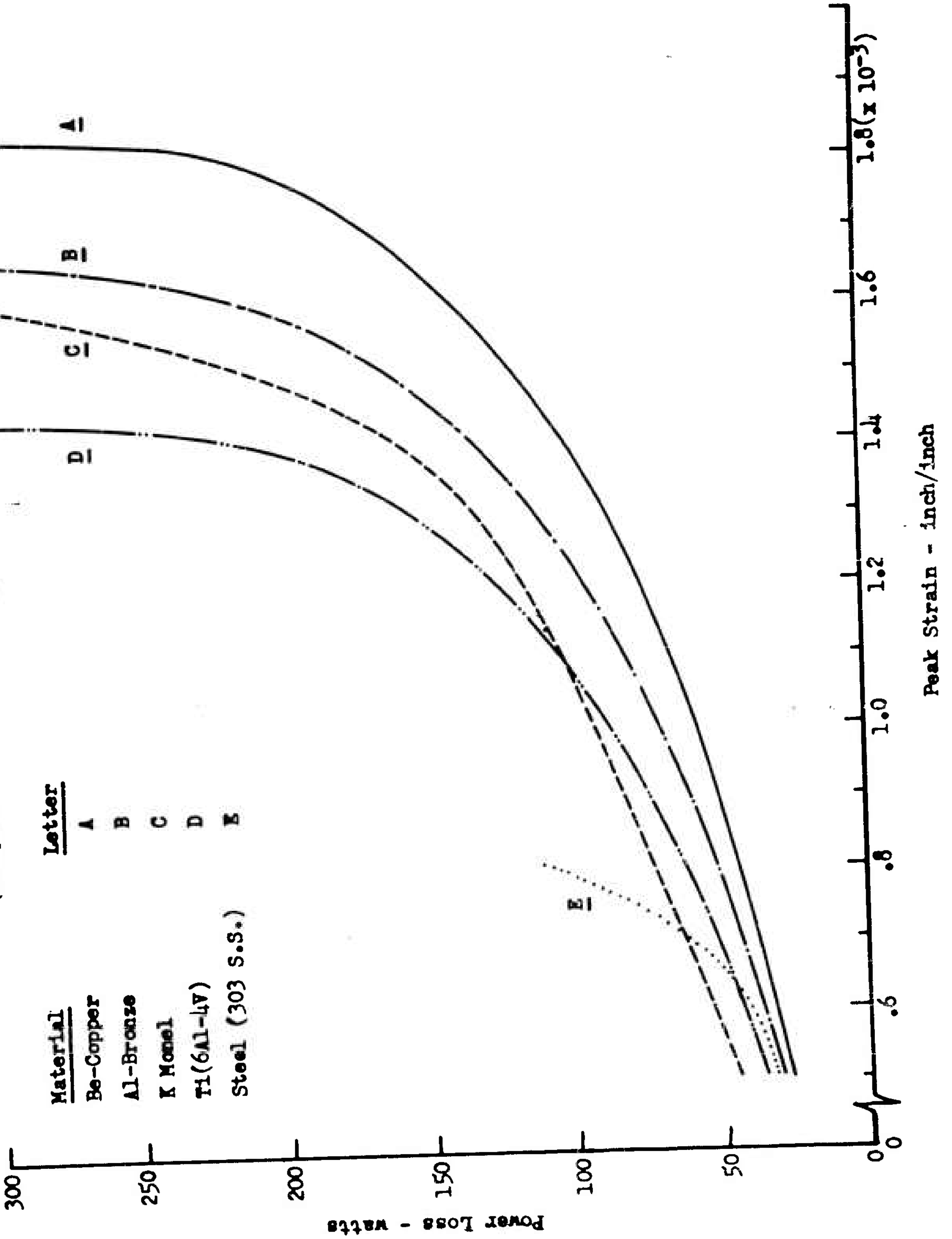

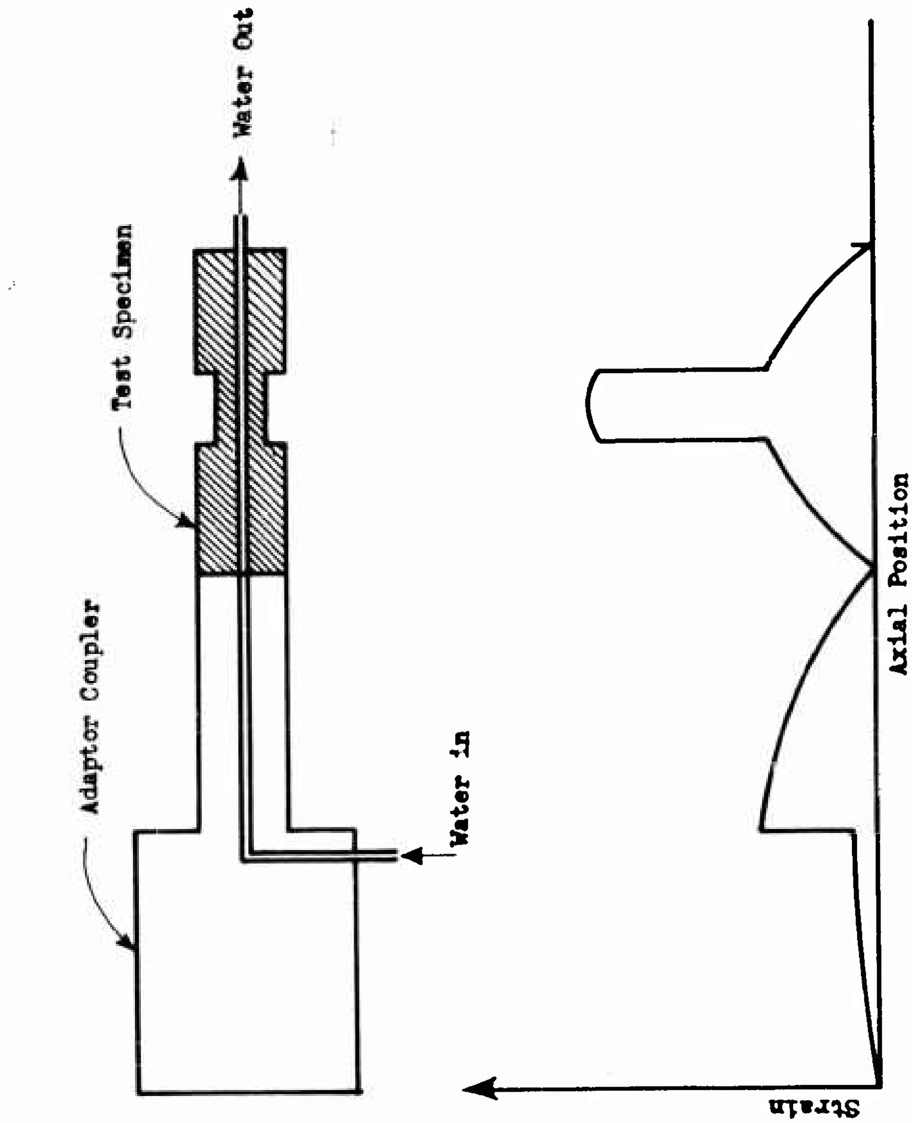

Figure 20: STRAIN DISTRIBUTION ALONG TEST SPECIMEN

Table 38

COUPLER MATERIAL: POWER DISSIPATION AND PEAK STRAIN LEVELS

Material	Input Power (watts)	Deflection ξ_0 (mils)	Water Volume (cm^3)	Time (sec)	Flow (g/sec)	ΔT (°C)	$\partial\xi/\partial x$ 10^{-3} (in./in.)	Power Loss (watts)	Power Diss. Central Sector (watts)
Be-copper	100	0.779	330	120	2.75	2.8	0.61	32.2	5.8
	200	1.112	370	140	2.61	4.6	.88	50.7	9.2
	300	1.446	325	120	2.71	5.4	1.14	61.1	11.0
	500	1.891	420	160	2.63	11.4	1.49	125.2	22.6
	750	2.28	435	160	2.72	16.8	1.79	192.0	34.6
	950	2.34	500	190	2.64	37.0	1.84	408.0	73.4
Al-bronze	55	0.668	441	203	2.17	2.2	0.49	19.7	3.6
	90	.835	400	180	2.22	3.6	.62	33.8	6.0
	100	1.057	513	195	2.63	5.8	.78	63.8	11.4
	160	1.224	500	180	2.78	5.0	.91	58.0	10.4
	200	1.669	316	120	2.63	8.2	1.23	90.0	16.2
	200	1.279	485	180	2.70	5.4	0.94	61.0	11.0
	350	1.669	465	180	2.58	9.5	1.23	102.0	18.4
	500	1.780	220	160	1.38	20.0	1.31	115.0	20.8
	725	2.113	460	170	2.71	15.4	1.55	174.2	31.4
	1050	2.280	830	271	3.06	27.8	1.68	356.0	64.0
K Monel	100	0.779	370	120	3.08	4.0	0.52	50.0	9.0
	100	.830	325	120	2.71	3.4	.55	38.6	7.0
	200	1.224	325	120	2.70	5.6	.81	63.3	11.4
	300	1.500	425	160	2.66	8.0	1.00	89.0	16.0
	380	1.558	330	120	1.375	8.6	1.04	99.0	17.8
	400	1.780	520	180	2.89	8.8	1.19	106.2	19.2
	450	1.890	525	180	2.92	9.8	1.26	119.6	21.6
	500	2.003	601	210	2.86	10.8	1.33	129.2	23.2
	650	2.168	665	240	2.78	15.4	1.44	179.0	32.2
	750	2.336	925	310	2.98	19.0	1.55	237.5	42.8
	900	2.390	890	300	2.97	21.6	1.59	269.0	48.4
Titanium 6Al-4V	100	0.890	711	300	2.37	3.8	0.53	33.7	6.0
	200	1.224	636	300	2.12	7.0	.72	61.6	11.0
	300	1.558	714	300	2.38	6.9	.92	76.3	13.8
	400	1.780	786	300	2.62	7.8	1.05	85.5	15.4
	500	2.113	780	300	2.60	12.0	1.25	130.5	23.4
	700	2.280	960	280	3.43	14.0	1.40	200.5	36.0
	1050	2.336	900	271	3.32	23.2	1.44	322.0	38.0
Stainless Steel 303	120	0.890	201	125	1.61	5.4	0.53	36.0	6.4
	200	1.140	208	120	1.73	7.8	.68	56.5	10.2
	300	1.335	240	120	2.00	13.5	.80	112.6	20.2

Figure 21: POWER LOSS AND STRAIN CHARACTERISTICS OF CANDIDATE COUPLER MATERIALS

(Frequency - 15 kilocycles)

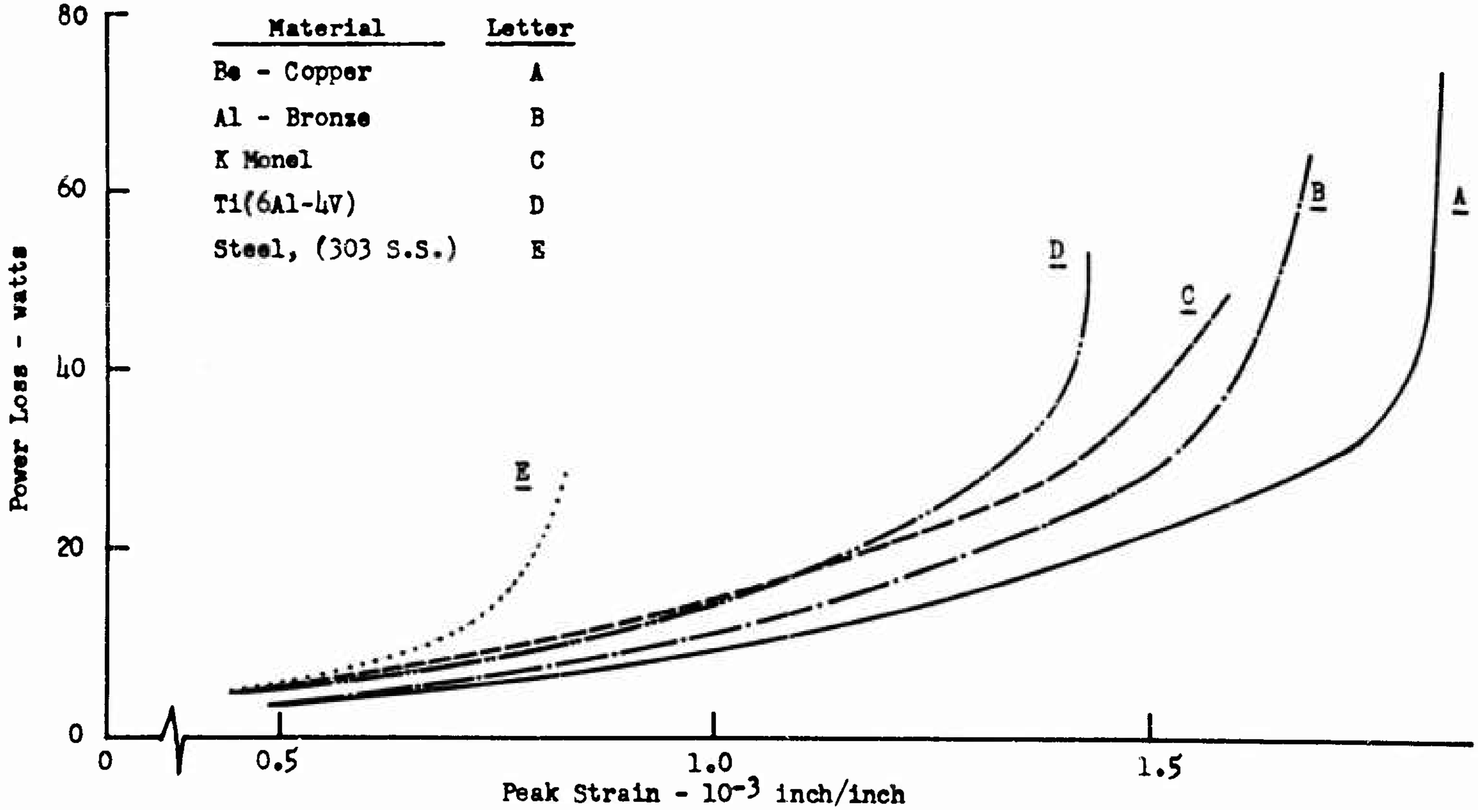

MEASUREMENTS

Water flow through the specimen was monitored and the temperature difference between the inflow and outflow was measured by thermocouples and recorded directly on a strip chart. These measurements were used to determine the energy dissipated in the specimen. The displacement amplitude of the specimen was determined by means of an optical microscope and a capacitive-type displacement probe. The strain level was then computed by substituting the data tabulated in Table 38.

RESULTS AND DISCUSSION

The power losses (or attenuation) and the strain characteristics for the various candidate coupler materials are shown in Figure 19. These losses in the coupler as well as for heat dissipation in the mass ends of the dumbell-shaped specimens to give the curves of Figure 21. The latter curves show only the energy dissipated in the central, linearly-stressed portion of the specimen. The corrections made were similar to the ones reported by Neppiras in his original paper* and confirmed by a recent private communication.

The increased power dissipation at the higher strain levels clearly indicate the rapid rise in internal friction. This phenomena has been observed by others and, as might be expected, is associated with early fatigue. During this work, several specimens failed very rapidly when subjected, for only short time intervals, to the strain levels at which attenuation increases rapidly.

In Table 39, the potential coupler materials are listed in order of decreasing transmissivity (or increasing attenuation) as determined by recent resonant-element type experiments. For comparison purposes, Neppiras work is also included.

Since beryllium copper withstood the high strain levels with the least internal dissipation of energy, it is probably the most suitable coupler material for high-power systems. Before a final selection of a coupler material is made, however, the fatigue life at the anticipated operating strain levels must be determined.

It appears that this equipment material evaluation technique provides an exceedingly fast and convenient method for fatigue and endurance testing as well as an interesting method for studying material characteristics.

---

* As given in detail by Neppiras.

Table 39

COUPLER MATERIALS: RELATIVE ACOUSTIC TRANSMISSIVITY AT HIGH STRAIN LEVELS
(Arranged in Decreasing Order)

Aeroprojects	Neppiras
(Relative Acoustic	Transmissivity)
Be-Copper	
Al-Bronze	Al-Bronze
K Monel	K Monel
Ti (6Al-4V)	
	Brass
Steel (303 S.S.)	Tool Steel
	Phosphorus Bronze

APPENDIX V

THE LIMITATION ON AMPLITUDE SET BY MAXIMUM STRAIN ENERGY IN VIBRATING SYSTEMS

PUBLISHED IN NYO REPORT 9588, "APPLICATIONS OF ULTRASONIC ENERGY" (129)

In many applications of ultrasonics it is desirable to achieve as great an amplitude of oscillation at the work area as is permitted by the elastic properties of the materials constituting the vibrating system. It is assumed in this analysis that a given isotropic material is characterized by a maximum permissible oscillating, elastic, strain-energy density, which can not be exceeded without fatigue failure, regardless of whether the energy density is associated with shear-distortion, simple compression, or a combination of the two. The treatment can be modified later, if it turns out that the fatigue limit depends on the nature of the elastic distortion.

Longitudinal Vibration of a Uniform Bar

Consider first the longitudinal vibration of a slender half-wave rod of uniform section. The strain at any position X, with origin at the center of the rod, is

$$(\partial \xi/\partial x) = (\partial \xi/\partial x)_m \cos K X, \qquad (1)$$

where X has the range $-\lambda/4 \leq X \leq \lambda/4$,

$$K = 2\pi/\lambda = \omega/c , \qquad (2)$$

and $c = \sqrt{E/\rho}$ as usual.

The maximum amplitude at the end of the rod is

$$A_m = (\partial \xi/\partial x)_m \int_0^{\frac{\lambda}{4}} \cos K x \, d X = (\partial \xi/\partial x)_m/K. \qquad (3)$$

The maximum elastic energy density at the center is

$$\mathcal{E}_m = \left[E\,(\partial \xi/\partial x)_m^2\right]/2 \qquad (4)$$

where E is Young's Modulus;

hence,

$$\mathcal{E}_m = (E\,K^2\,A_m{}^2)/2 = (\rho\,\omega^2\,A_m{}^2)/2 \qquad (5)$$

Since the maximum velocity at the end of the rod is $\omega A_m = \dot{\xi}_m$, Eq. 5 can be written

$$\mathcal{E}_m = \rho(\dot{\xi}_m{}^2)/2 \qquad (6)$$

which is the kinetic energy per unit volume of the material at the end of the rod. Whereas the kinetic energy density and velocity is independent of frequency for a given upper limit to $\mathcal{E}_m$, the permissible amplitude varies inversely with frequency.

Lateral Vibration of a Uniform Bar

Next the free-free lateral vibration of a bar of circular section. The following results from Rayleigh, p. 281 et seq., (136) can be used. For the frequency,

$$\omega = \left[(4.73)^2(a/\ell^2\,\sqrt{E/\rho})\right]/2 \qquad (7)$$

For the amplitude at the end, in terms of the amplitude at the center,

$$A(\text{end}) = 1.645\ A(\text{center}). \qquad (8)$$

From the table on p. 282 of Rayleigh (136), by taking second differences,

$$(\partial^2\eta/\partial x^2) = 29.1/\ell^2\ A(\text{center}) = 17.7/\ell^2\ A(\text{end}) \qquad (9)$$

The maximum fiber strain at the center is

$$(\partial \xi/\partial x)_m = a(\partial^2\eta/\partial x^2)(\text{center}) = 17.7\ a/\ell^2\ A(\text{end}) \qquad (10)$$

On combining (7) and (10)

$$(\partial \xi/\partial x)_m = 1.54\ (\sqrt{\rho/E})\ \omega A(\text{end}), \qquad (11)$$

Hence, from Eq. (4)

$$\mathcal{E}_m = 2.37\ \left[\rho\omega^2\ A^2(\text{end})\right]/2 \qquad (12)$$

This result shows that for a given amplitude at the end, the (surface) strain-energy density at the center is nearly two and one-half times as great as for the longitudinal case. It depends on density and frequency as before, a result that is obvious from dimensional considerations.

If the bar is of rectangular section, of thickness 2a, Eq. (7) becomes

$$\omega = 1/\sqrt{3}\ (4.73)^2(a/\ell^2)\ \sqrt{E/\rho} \tag{13}$$

since the radius of gyration of the section is now $a/\sqrt{3}$ instead of a/2. Hence, the value of a/ℓ^2 in Eq. (10) is decreased by the factor $\sqrt{3}/2$ (for a given frequency) and the energy density of Eq. (12) by $(\sqrt{3}/2)^2 = 0.75$. Accordingly, a rod of rectangular section is superior to one of circular section, when as large an amplitude of vibration as possible is desired.

Axial Vibration of a Thin Uniform Disk

It can be shown (137) for one nodal circle with $\sigma = 1/3$ that

$$\omega = 2.615\ (t/a^2)\ \sqrt{E/\rho(1-\sigma^2)} \tag{14}$$

where "a" is the radius and "t", the thickness of the disk. The shape of the disk is given by the function

$$W = J_0\,(kr) + \lambda I_0(kr); \tag{15}$$

with $k^4 = \omega^2/\alpha^4$,

$$\alpha^4 = Et^2/12\rho(1-\sigma^2)$$

$$\lambda = J_1(ka)/I_1(ka)$$

where the "J" and "I" function are ordinary and modified Bessel functions, respectively. For $\sigma = 1/3$, ka = 3.01 and $\lambda = -0.0841$. The amplitude at the edge is 0.74 that at the center.

A calculation based on Eq. (15) shows that the curvature at the center, for a displacement amplitude A(center), is

$$(\partial^2 W/\partial r^2) = \left[(k^2(1-\lambda/1+\lambda)A(\text{center})\right]/2 \tag{16}$$

The strain at the surface is, therefore,

$$(\partial \xi/\partial x)_m = \left[t(\partial^2 w/\partial r^2)\right]/2$$
$$= (t/a^2)(3.01)^2(1.084/0.915)(A(\text{edge})/0.74)\ /4 =$$
$$= 3.62\ (t/a^2)\ A\ (\text{edge}), \tag{17}$$

on introducing the numerical values already quoted for ka, λ and A (edge)/A (center). The strain energy density for a plate stretched uniformly in all directions an amount $\partial\xi/\partial X$ is

$$\mathcal{E} = (E/1-\sigma)(\partial \xi/\partial X)^2 \tag{18}$$

On introducing the value from Eq. (17), for $\partial\xi/\partial X$, the frequency from Eq. (14), and $\sigma = 1/3$,

$$\mathcal{E}_m = (3E/2)\ (3.62)^2 (\rho(1-1/3^2)/E)(\omega^2/(2.615)^2\ A^2(\text{edge})) =$$
$$= \left[5.10(\rho\omega^2\ A^2(\text{edge}))\right]/2 \tag{19}$$

Hence, for a given amplitude at the edge, the maximum strain energy density is slightly more than five times that of the longitudinal case for the same amplitude and frequency.

EXTENSION OF PREVIOUSLY PUBLISHED WORK

Torsional Vibrations of a Uniform Rod

Consider, finally, the torsional vibrations of a uniform half-wave rod of circular section, with origin at the center. If θ is the angular displacement at any section, the angular strain is

$$\partial\theta/\partial X = (\partial\theta/\partial X)_m \cos K X, \tag{20}$$

and the angular amplitude at the end is

$$\theta_m = (\partial\theta/\partial X)_m \int_0^{\lambda/4} \cos K X\ dX = 1/K\ (\partial\theta/\partial X)_m. \tag{21}$$

The linear amplitude at the outer radius "a" is

$$A_m = a\ \theta_m = a/K\ (\partial\theta/\partial X)_m = 1/K\ (\partial\mathcal{J}/\partial X)_m, \tag{22}$$

where $(\partial\mathcal{J}/\partial X)_m$ is the maximum shear strain at the surface of the rod.

Since the strain energy density is

$$\mathcal{E} = \left[\mu \, (\partial \mathcal{J}/\partial x)^2\right]/2, \tag{23}$$

from Eq. (22) and (23), by substituting $K = \omega/c_t$ and $c_t = \sqrt{\mu/\rho}$,

$$\mathcal{E}_m = (\rho\omega^2 \, A_m{}^2)/2 \tag{24}$$

The torsional case, therefore, is identical with the longitudinal case, discussed in the first section, and the longitudinal vibration of a uniform bar, of the original material. All of the results obtained show that $\mathcal{E}_m/\rho$ is a figure of merit for an elastic material, which can be used to estimate the largest possible vibratory amplitude at a given frequency, regardless of the geometry of the vibrator.

APPENDIX VI

EQUIVALENT CIRCUIT OF A VIBRATING DISK SEAM WELDER

The present analysis will consider certain effects in a vibrating disk seam welder. In Fig. 1 is shown a shaped disk coupled at its center to the end of a tapered horn. The center C of the

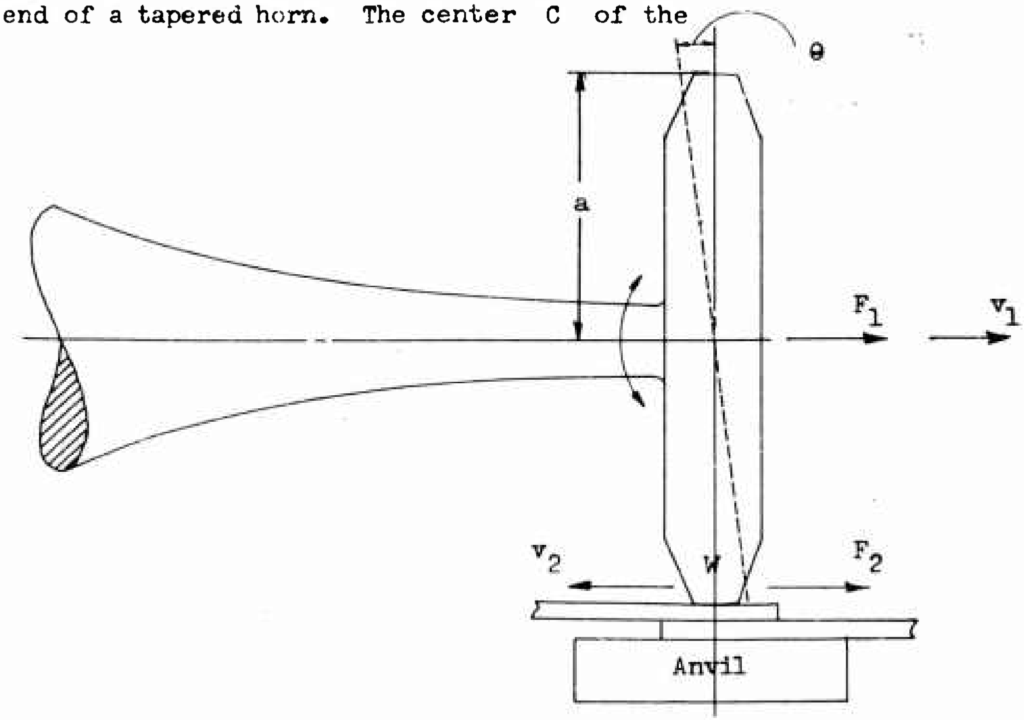

disk has a velocity v_1 and is acted on by the force F_1. It therefore presents the impedance

$$Z_1 = F_1/v_1 \tag{1}$$

to the exponential coupler. The point W on the edge of the disk contacts the weld, and moves with the velocity v_2 in the opposite direction of v_1, if it is assumed that one nodal circle exists in the vibrational mode of the disk. The force F_2 directed as shown acts on the disk at this point, with an equal and opposite force (in the direction

of v_2) acting on the material being welded. The impedance presented by the weld is evidently

$$Z_2 = F_2/v_2 \tag{2}$$

It will be observed that a net force $F_1 + F_2$ acts on the mass M of the disk giving its center of mass an acceleration $a_c = j\omega v_c$ where v_c is the velocity of the center of mass. By Newton's law

$$F_1 + F_2 = j\omega M\, v_c \tag{3}$$

In addition a net torque, $a\, F_2$, acts on the moment of inertia 'I_c' of the disk, about an axis through "C" perpendicular to the drawing. This torque is opposed by a torque supplied by the stiffness of the end of the exponential coupler. If θ is the angle turned through by the disk, as a result of these two torques, the Newton equation of motion is

$$a\, F_2 - N_1\mathring{\theta}/j\omega = j\omega I_c\, \mathring{\theta} \tag{4}$$

where $\mathring{\theta}$ is the angular velocity, and N_1 is the elastic restoring torque per radian supplied by the end of the coupler. (To simplify the calculation, without making much error, the rotary inertia of the end of the coupler is being neglected.)

Let ξ_1 and ξ_2 be the amplitudes of the vibratory motion of the disk at C and W, respectively.

For a disk of given shape, the ratio

$$\xi_2/\xi_1 = A \tag{5}$$

is a constant, for example $A \simeq 0.74$ for a simple disk with parallel faces. If one neglects power losses in the vibration of the disk the power delivered <u>to the disk</u> at the center, $F_1\ \dot{\xi}_1$, must equal the power delivered <u>by the disk</u>, $F_2\ \dot{\xi}_2$. It is thus evident that

$$F_2/F_1 = \dot{\xi}_1/\dot{\xi}_2 = \xi_1/\xi_2 = 1/A \tag{6}$$

The velocity at the center of the disk is

$$V_1 = \dot{\xi}_1 + v_c = j\omega\xi_1 + v_c \tag{7}$$

and at the edge

$$V_2 = \dot{\xi}_2 - v_c - a\mathring{\theta} = j\omega\xi_2 - v_c - a\mathring{\theta} \tag{8}$$

These equations express the fact that the two sorts of motion, governed by Eqs. (3) and (4), contribute to the actual velocities v_1 and v_2, adding v_c to ξ_1, and subtracting v_c and $a\dot{\theta}$ from ξ_2

Let us now obtain an expression for Z_1 in terms of Z_2 and the other parameters of the system by eliminating the seven variables F_1, F_2, ξ_1, ξ_2, V_1, V_2 and $\dot{\theta}$ from the foregoing eight equations. We find that

$$(1/Z_1) = 1/A^2 \left[(1/Z_2) + ((1+A)^2/j\omega M) + (a^2/j\omega I_c + N_1/j\omega) \right] \quad (9)$$

which shows that the weld impedance Z_2 is shunted by two reactances. The first is

$$X_m = j\omega M/(1+A)^2 \quad (9)$$

the reactance of the mass of the disk reduced by the factor $1/(1 + A)^2$ and the second is

$$\bar{X}_I = j\omega I_c/a^2 - j N_1/\omega a^2 \quad (10)$$

the positive reactance associated with rotation about the axis through C in series with the negative reactance arising from the elasticity of the supporting coupler. An equivalent electrical circuit is given in Fig. 2.

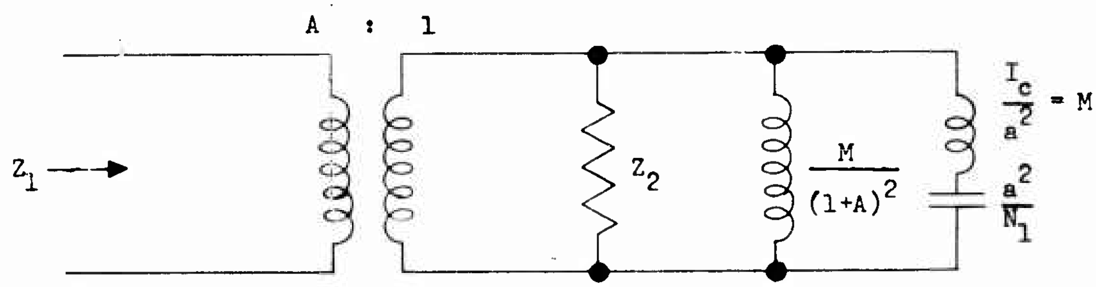

If these reactances are large compared with the weld impedance, their shunting effect will be slight. If, however, they have a magnitude comparable with, or less than the weld impedance, they will considerably reduce power delivery to the weld. Let us estimate their magnitude for a simple disk, first neglecting the presence of N_1.

For a simple disk of thickness $t \ll a$,

$$M = \pi a^2 t . \rho$$

$$M' = I_c/a^2 \doteq M/4$$

$$A = 0.74$$

$$M/(1 + A)^2 \doteq M/3$$

so that Z_2 is shunted by the reactances $j\omega M/4$ and $j\omega M/3$ in parallel, i.e.,

$$\overline{X} = j\omega M/7$$

A typical disk operating at 10 kc may have a mass of about 0.5 kg, so that

$$\overline{X} = j\ 4500 \text{ acoustic ohms.}$$

Instead of comparing this reactance with Z_2, whose value is not presently known with any accuracy, let us take this reactance through the ideal transformer by multiplying it by A^2, and compare the value with the characteristic impedance at the drive end of the exponential coupler. Since $A^2 \approx 0.5$. The reactance load on the coupler is

$$\overline{X}_c = j\ 2250$$

The characteristic impedance of typical coupler (radius 0.469 inches, $\rho = 7.6$ gm/cm^3, c = 4060 m/sec

$$\begin{aligned} Z_o &= S \rho c \\ &= \left[\pi (.469)^2 (2.54)^2 \times 10^{-4}\right] \times 7{,}600 \times 4{,}060 \\ &= 13{,}800 \text{ acoustic ohms.} \end{aligned}$$

The fact that $\overline{X}_c$ has a magnitude of about $Z_o/6$ indicates that the shunting effect of the reactance is very great, and that such a disk tip welder will not be an efficient device at high powers. Stated in other words, the inertia of the disk is nowhere near great enough for it to produce the force that the exponential coupler is capable of supplying by virtue of its characteristic impedance.

The effect of the elastic stiffness of the coupler in holding the disk from moving about the axis through C can be estimated in a qualitative fashion. Examination of Fig. 2 [or of Eq. (8)] shows that as the stiffness is increased from $N_1 = 0$ to a finite value, the early effect is to reduce $\overline{X}_c$ to an even smaller value, making it pass through

zero at series resonance. If the stiffness is increased far beyond that giving resonance, the reactance of the series arm becomes high, and in effect removes its loading effect. Since, however, this arm contributed only slightly more than half the shunting reactance, the improvement is not great. If it is desired to use a disk, or shaped disk, for a seam welder, it is highly desirable to increase the mass of the disk. Since the mass depends on a^2t, whereas the frequency depends on t/a^2, for a given frequency the mass goes up as a^4. Unfortunately, doubling the disk radius requires quadrupling the thickness to keep the same frequency. The disk soon becomes a "thick" disk, and may be subject to relatively greater internal strains for a given amplitude of oscillation. So long as "thin" disk theory applies, this is not the case, as shown in previously reported discussions of this matter.

In conclusion, the present analysis shows that any attempt to deliver high power to a weldment from the edge of a resonant disk, forces the disk to vibrate about a hori ntal diameter. Because of the limited rotary inertia of the disk about this diameter, the amplitude of the horizontal vibration considerably reduces and limits the vibratory power delivery at the weldment.

APPENDIX VII

TORSIONAL VIBRATIONS OF A SHAPED DISK

Consider an axially symmetrical disk whose thickness Z may be a function of the radial distance "r" from the axis. We shall derive the differential equation for the possible radial shear modes of vibration in which the displacements U_r and U_Z vanish and $U_\theta = f(r)$. The shearing strain $e_{r\theta}$ in cylindrical coordinates is (138, p. 56)

$$e_{r\theta} = \partial U_\theta/\partial r - U_\theta/r + 1/R\,(\partial U_r/\partial \theta)$$

and when $U_r = 0$,

$$e_{r\theta} = \partial U_\theta/\partial r - U_\theta/r \qquad (1)$$

The total torque transmitted through a cylindrical surface of radius "r", where the thickness is Z, is

$$N = (2\pi r Z)\,(r\,\mu)\,(\partial U_\theta/\partial r - U_\theta/r) \qquad (2)$$

The net torque accelerating a thin shell of thickness dr, considering Z to be a constant, is

$$dN = 2\pi r^2 Z\mu \left[2/r(\partial U_\theta/\partial r - U_\theta/r) + \partial^2 U_\theta/\partial r^2 + U_\theta/r^2 - 1/r\,(\partial U_\theta/\partial r) \right] dr \qquad (3)$$

The moment of inertia of the shell is

$$dI = 2\pi r^3 Z\, dr\, \rho \qquad (4)$$

and its angular acceleration

$$\alpha = 1/r(\partial^2 U_\theta/\partial t^2) \qquad (5)$$

Since $dN = \alpha\, dI$, we obtain from (3), (4), and (5)

$$\partial^2 U_\theta/\partial r^2 + 1/r\,(\partial U_\theta/\partial r) - U_\theta/r^2 = \rho/\mu\,(\partial^2 U_\theta/\partial t^2) \qquad (6)$$

and for sinusoidal vibrations of angular frequency ω,

$$\partial^2 U_\theta/\partial r^2 + 1/r\,(\partial U_\theta/\partial r) + (\omega^2/c_t^2 - 1/r^2)\,U_\theta = 0 \qquad (7)$$

where $c_t^2 = \mu/\rho$.

Let us now suppose Z in Eq. (2) is a function of r. Eq. (4) and (5) continue to hold, but Eq. (3) becomes

$$dN = 2\pi r^2 Z\mu \left[\partial^2 U_\theta/\partial r^2 + 1/r \ (\partial U_\theta/\partial r) - U_\theta/r^2\right] dr + \\ + 2\pi r^2 \mu \, (\partial U_\theta/\partial r - U_\theta/r) \, (dZ/dr) \, dr \qquad (8)$$

and Eq. (7) becomes

$$d^2U_\theta/dr^2 + \left[(1 + (r/Z) \, dZ/dr)(1/r \, dU_\theta/dr)\right] + \\ + \left[\omega^2/c_t^{\,2} - (1 + (r/Z)dZ/dr) \, 1/r^2\right] U_\theta = 0 \qquad (9)$$

This differential equation appears to have simple solutions (1) when Z = constant, for which $U_\theta = AJ_1 \, (\omega r/c_t) + BN_1(\omega r/c_t)$, where J_1 and N_1 are Bessel functions; and (2) when $(r/Z)(dZ/dr) = -1$, which reduces Eq. (9) to

$$d^2U_\theta/dr^2 + (\omega^2/c_t^{\,2})U_\theta = 0, \qquad (10)$$

the equation for plane waves. For other cases when $(r/Z)(dZ/dr) = a$, (a constant), see Note 1 at the end of this report. When $a = -1$, the disk has the shape

$$rZ = b \text{ (a constant)} \qquad (11)$$

and hence may be termed a hyperbolic disk since its section is that formed by rotating the two hyperbolas $rZ = b/2$ and $rZ = -b/2$ about the Z axis. Since the thickness becomes infinite when $r = 0$, such a disk must always have a hole through its middle in any practical application, for example, in a seam welder.

Let r_o be the inner radius, where the thickness is Z_o. The thickness for larger radii is then given by

$$Z = r_o Z_o / r \qquad (12)$$

Let us now find the outer radius r, such that the disk is resonant with one nodal circle at the angular frequency ω. At both r_o and r, the shearing strain (1) must vanish. The appropriate solution of (10) is

$$U_\theta = A \cos Kr + B \sin Kr = C \sin (kr-\theta) \qquad (13)$$

where $C \equiv \sqrt{A^2 + B^2}$, $\tan \theta \equiv -A/B$ and $K \equiv \omega/c_t$.

The boundary conditions that $e_{r\theta} = 0$ at r_0 and r_1 give

$$\tan \theta = - A/B = (\tan X_o - X_o)/(1 + X_o \tan X_o) =$$

$$= (\tan X_1 - X_1)/(1 + X_1 \tan X_1) \quad (14)$$

where $X_o \equiv Kr_o$ and $X_1 \equiv Kr_1$.

The boundary conditions can only be applied by solving the transcendental equation (14) connecting X_o and X_1. This is most simply done by a graphical means involving a plot of the function

$$f(x) = (\tan X - X)/(1 + X \tan X) \quad (15)$$

in some convenient form. Evidently,

$$f(x) = (\tan X - \tan (\tan^{-1}X)/(1+ \tan(\tan^{-1}X) \tan X) = \tan(X-\tan^{-1}X)X$$

so that, from Eq. (14),

$$\theta (X) = X - \tan^{-1} X \quad (16)$$

where θ, X and $\tan^{-1} X$ are in radians. For computational purposes, let us express angles in degrees. Then (with X in radians)

$$\theta_{deg} = 180X/\pi - (\tan^{-1} X)_{deg} \quad (17)$$

Equation (17) is plotted in Figure 22. Given r_o, ω and c_t one first computes

$$X_o = Kr_o = \omega r_o/c_t,$$

and expresses the result in degrees by multiplying it by $180/\pi = 57.296$ deg/radian. This value is located on the X axis, and the value of θ found from the graph. The same value of θ is now located on the next branch of the curve (for one nodal line), and the value of X_1 read off in degrees, from which value the outer radius

$$r_1 = \pi/180(X_1/K) = \pi/180(c_t X_1/\omega) = c_t X_1/360f \quad (18)$$

is computed.

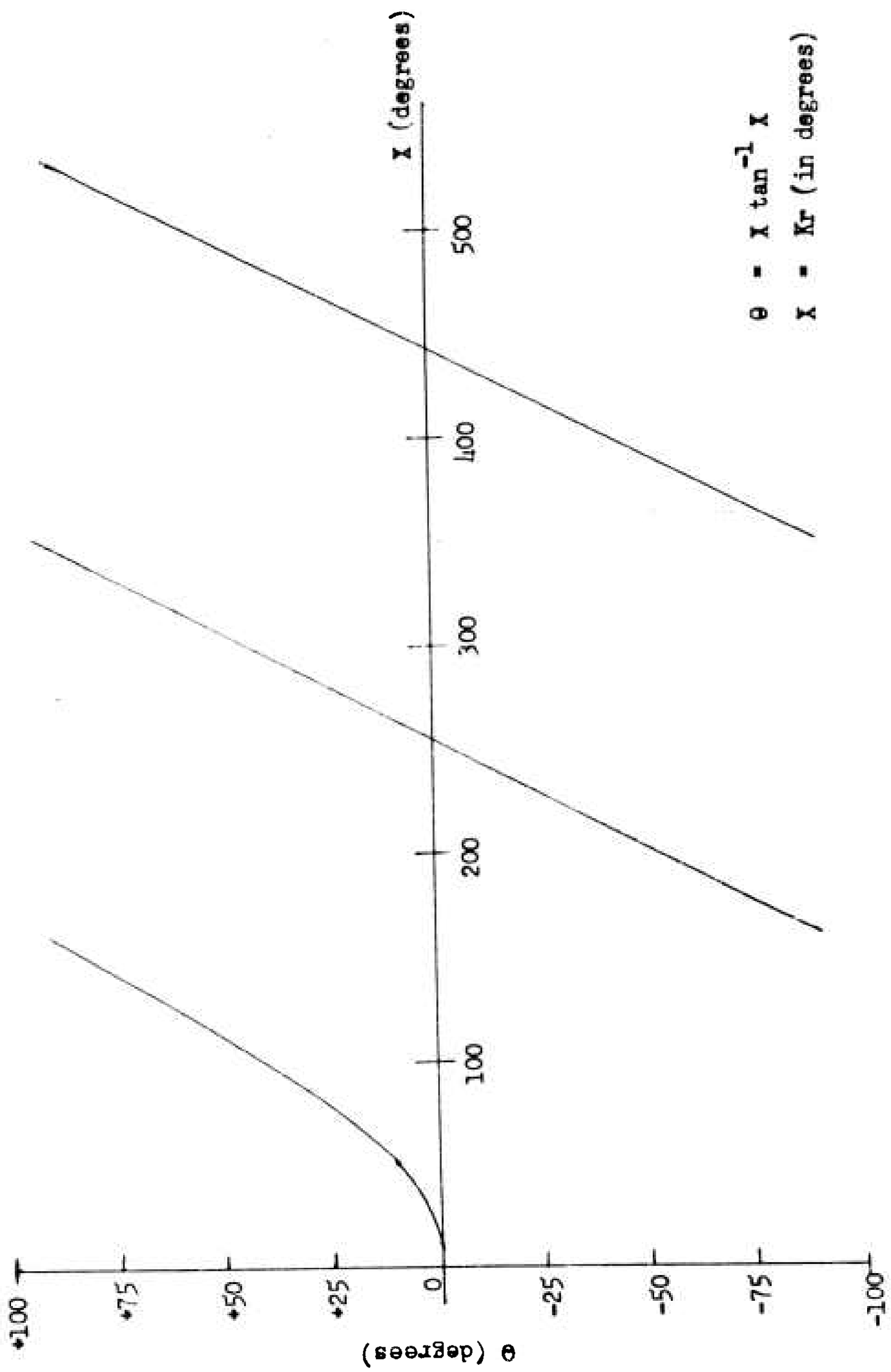

Figure 22: DESIGN CURVES FOR A SHAPED-DISK

The ratio of the amplitudes of oscillation at the two boundaries is

$$\left| U_{\theta_1}/U_{\theta_o} \right| = \sin (X_1 - \theta)/\sin (X_o - \theta) = \sin (\tan^{-1} X_1)/\sin (\tan^{-1} X_o)$$

by using Eqs. (13) and (16). Hence, since $\sin(\tan^{-1}X) = X/\sqrt{1 + X^2}$)

$$\left| U_{\theta_1}/U_{\theta_o} \right| = X_1/X_o \sqrt{1 + X_o^2/1 + X_1^2} =$$

$$= r_1/r_o \sqrt{r_1 + (Kr_o)^2/1 + (Kr_1)^2} \qquad (19)$$

$$= \sqrt{1+(1/(Kr_o)^2)/1+(1/(Kr_1)^2} = 1 + 1/2 \left[(1/Kr_o)^2 - (1/Kr_1)^2 \right] + \ldots \qquad (20)$$

when $Kr_o > 1$ and, a fortiori, $Kr_1 > 1$.

This calculation shows that there is a small increase in amplitude in going from the inner to the outer radius. A load impedance $\overline{Z}_1$ at the outer radius is transformed to the inner radius by the ratio $(U_{\theta_o}/U_{\theta_1})^2$ and hence appears as the impedance

$$\overline{Z}_o = \overline{Z}_1 \left[(1 + (1/(Kr_1)^2) / 1 + (1/(Kr_o)^2) \right] \qquad (21)$$

at the inner radius. In using formulus (19), (20), and (21), the values of Kr, of course, must be expressed in radians.

It is proposed that such a hyperbolically tapered disk be used as the basis for a torsionally driven seam welder. An approximate calculation shows that for a given amplitude of oscillation, the maximum strain energy per unit volume is about the same as for torsional standing waves on a uniform cylindrical rod, which represents an optimal case.

NOTE 1

It should be possible to analyze other shapes of disks, provided

$$(r/Z)(dZ/dr) = a \text{ (a constant)}$$

Such a disk has a thickness given by

$$Z = \text{constant } r^a$$

If $a = -1$, we have the case discussed.

The solution of Eq. (9) for any value of (a) such that $1 + (a/2)$ is not an integer, takes the form

$$U_\theta = (Ar)^{(a/2)} J_{\pm(1+a/2)} (Kr)$$

where $J_{\pm(1+a/2)} (Kr)$ is a Bessel function of order $\pm(1+a/2)$. If $a = -2$, so that $Z = \text{const}/r^2$

then

$$U_\theta = Ar\ J_o(Kr) + Br\ N_o(Kr).$$

As "r" increases, such a disk becomes very thin near the edge; thus, the design of a practical unit with a very large diameter becomes doubtful. Calculations do show, however, that with an outside diameter of about 3 inches, the thickness through the central portion will be about one inch and near the edge approximately 1/4-inch. Accordingly, for a 15-kc torsional disk, an overall diameter of between 3 and 4 inches will probably be satisfactory.

LIST OF REFERENCES

1. Jones, J. B., and Powers, J. J. Jr., "Ultrasonic Welding", Welding J. 36, 761-766, 1956 (August).

2. Jones, J. B., "Progress Report on Ultrasonic Welding", Minutes of the Sixth Annual Meeting of the AEC Welding Committee, Oak Ridge National Laboratory, Oak Ridge, Tenn., Sept. 25-26, 1956.

3. Jones, J. B., "Ultrasonic Welding", Fabrication of Molybdenum, 88-102, Cleveland, Ohio, 1959.

4. McCarthy, D. V., Pirc, V., and Hannahs, W., "Ultrasonic Welded Aluminum-Copper Junctions as Electrical Connections", Reliable Electrical Connections, Third Electronics Industries Association Conference, Engineering Publishers, New York, 1958.

5. "Advances in Fabrication Techniques Revealed at Southern Metals Conference", Metal Progress, 76, 128, 1959 (August).

6. Jones, J. B., and McKaig, H. L. Jr., "Ultrasonic Welding and Improved Structural Efficiency". Presented at the 28th Annual Meeting of the Inst. of Aeronautical Sciences, New York, N. Y., Jan. 25-27, 1960.

7. Collins, F. R., "Ultrasonic Welding", Aluminum Company of America Report No. 2-57-5, New Kensington, Pa., 1957 (February).

8. "Ultrasonic Welding", 235-237, 133, Kaiser Aluminum Sheet and Plate Product Information, Chicago, Ill. Sec. Ed., 1958 (January).

9. Collins, F. R., "Properties of Aeroprojects Ultrasonic Seam Welds", Aluminum Company of America Report No. 2-59-14, Process Metallurgy Division, Alcoa Research Laboratories, New Kensington, Pa., 1959 (August).

10. "Ultrasonic Welding of Titanium", (Crucible Steel Company of America), Titanium Review 8, 5-7, 1950 (March).

11. Fabel, G., "Ultrasonic Welding: Optimizing the Variables", Assembly and Fastener Engineering, 3, 32-36, 1960 (November).

12. Terrill, J. R., Collins, F. R., and Dowd, J. D., "Applications for Ultrasonic Welding of Aluminum", Paper No. 60-WA-322, Presented at Annual Winter Meeting of the ASME, New York, N. Y., Nov. 27-Dec. 2, 1960.

13. Alden, J. H., "Ultrasonic Sealing of Foil", Modern Packaging, 34, 129-133, 1961 (July).

14. Koziarski, J., and Dick, P., "Ultrasonic Welding Joins Stainless to Aluminum in Nuclear Power Plant", Materials in Design Engineering, 53, 146-147, 1961 (May).

15. Weare, N. E., and Antonevich, J. N., et al., "Research and Development of Procedures for Joining Similar and Dissimilar Heat-Resisting Alloys by Ultrasonic Welding", Battelle Memorial Institute, ASTIA Document 208323, WADC Tech. Report 58-479 on Contract AF 33(616)-5342, Project No. 7-(8-7351), 1959 (February).

16. "Current Welding Research Problems", Welding Research Council, Welding Journal, 37, Research Supplement, 379-s to 384-s, 1958 (August).

17. Koziarski, J., "Some Considerations on Design for Fatigue in Welded Aircraft Structures", Welding J., 38, 565-575, 1959 (June).

18. "Summary Report of the Committee on Refractory Metals", National Research Council, (Materials Advisory Board, National Academy of Sciences), Report MAB-154-M, 1, Washington, D. C., 1959, (October 15).

19. "Ultrasonic Welding", American Welding Society, Welding Handbook, Section Three, Chapter 52, Fourth Edition, New York, N. Y., 1960.

20. "Current Welding Research Problems", Welding Research Council, Welding Journal, 39, Research Supplement, 547-s to 552-s, 1960 (December).

21. "Joining of Refractory Sheet Metals", National Research Council (Materials Advisory Board, National Academy of Sciences), Report No. MAB-171-M, Washington, D. C., 1961, (March).

22. Koziarski, J., "Ultrasonic Welding", Welding Journal 40, 349-358, 1961 (April).

23. Jones, J. B., Maropis, N., Thomas, J. G., and Bancroft, D., "Phenomenological Considerations in Ultrasonic Welding", Welding Journal, 40, Research Supplement, 289-s to 305-s, 1961 (July).

24. Neville, S. W., "Ultrasonic Welding", British Welding Journal, 8, 177-187, 1961 (April).

25. Kitaigorodskii, Yu. I., Kogan, M. G. et al., "Joining of Metals in the Solid State by Ultrasonic Vibrations", Izvestiya Adademii Nauk SSSR, Otdelenie Tekhnicheskikh Nauk, 88-90, 1958 (August).

26. Ainbinder, S. B., "Certain Problems in Ultrasonic Welding", Svarochnoe Proizvodstvo, 32, 4-6, 1959 (December).

27. Silin, L. L., Kuznetsov, V. A., and Sysolin, G. V., "The Ultrasonic Welding of Aluminum and Its Alloys", Svarochnoe Proizvodstvo, 33, 42-44, 1960 (April).

28. Garber, R. I., Polyakov, L. M. and Malik, G. N., "Ultrasonic Welding of Copper", Fizika Metallov i Metallovedeniye, 10, 1960, (October).

29. Makarov, L. O., "Ultrasonic Welding", Akusticheskiy Zhurnal, 6, 507-508, 1960.

30. Miller, Fred, ASRCTF, Manufacturing Technology Laboratory, Fabrication Branch, AFSC, Aeronautical Systems Division, Wright-Patterson Air Force Base, Ohio.

31. "Properties and Selection of Metals," Metals Handbook, 8th Edition, 1, American Society for Metals.

32. Hampel, Clifford A., (ed.), Rare Metals Handbook, Reinhold, N. Y., 1954.

33. Grabecker, D. W. (ed.), Metals for Supersonic Aircraft and Missiles, Am. Soc. for Metals, Cleveland, 1958.

34. Roberts, D. A., Roach, D. B., and Hall, A. M., "Physical and Mechanical Properties of Nine Commercially Precipitation-Hardenable Stainless Steels". DMIC Report 112, 1959, (May).

35. Ludwigson, D. C. and Hall, A. M., "The Physical Metallurgy of Precipitation-Hardenable Stainless Steels," DMIC Report 111, 1959 (April).

36. "Semi-Austenitic Precipitation-Hardening Stainless Steels" (Tentative). DMIC Report (in preparation).

37. "DuPont Columbium Alloy D-31," E. I. du Pont de Nemours and Co., Technical Bulletin, 1960 (April).

38. Bartlett, E. S. and Houck, J. A., "Physical and Mechanical Properties of Columbium and Columbium-Base Alloys". DMIC Report 125, 1960, (February).

39. Jahnke, L. P., Frank, R. G. and Redden, T. K., "Columbium Alloys Today," Metal Progress, 77, 1960, (June and July).

40. Columbium (D-31) Alloy, Heat No. 31-048-02, E. I. du Pont de Nemours and Co., Order No. KZ-1915, August 29, 1961.

41. "Engineering Properties of Inconel," Technical Bulletin T-7, Huntington Alloy Products Division, The International Nickel Company, N. Y., 1959 (September).

42. Freeman, Robert R., and Briggs, J. Z., "Molybdenum for High Strength at High Temperatures". Jet Propulsion, 27, No. 2, Part 1, 1957 (February).

43. "Molybdenum + 0.5% Titanium Sheet", Universal-Cyclops Steel Corp., (Refractomet Division), Spec. No. MTS-59-9, 1959, (September).

44. Houck, J. A., "Physical and Mechanical Properties of Commercial Molybdenum-Base Alloys". DMIC Report 140, 1960 (November).

45. Molybdenum-0.5 Titanium, Universal-Cyclops Corporation, Mill Order No. RW8-0387-G, July 14, 1961.

46. "René 41", The Alloy Specialist, Series No. 86. Cannon-Muskegon Corp., Muskegon, Michigan.

47. "René 41, Engineering Data", VM107, Metallurgical Products Division, General Electric Company, Detroit, Michigan.

48. Barth, V. D., "Physical and Mechanical Properties of Tungsten and Tungsten-Base Alloys", DMIC Report 127, 1960 (March).

49. "Tungsten at a Glance". Series 1000, General Electric Company, Cleveland, Ohio.

50. "Tungsten Sheet and Ribbon", Series 1400, General Electric Company, Cleveland, Ohio.

51. Tungsten, Fansteel Metallurgical Corporation, Metals and Fabrication Division, Chicago, Illinois.

52. Carruthers, M. E., Burns, R. S., "PH15-7Mo Steel", Armco Steel Corp., Middletown, Ohio.

53. Olson, C. M., Columbium (D-31) Alloy, Pigments Department, Experimental Station Laboratory, E. I. du Pont de Nemours and Company, Wilmington, Delaware.

54. Buck, M. P., Stevens, W., Inconel X-750, The International Nickel Company, Inc., 67 Wall Street, New York 5, New York.

55. Richmond, F. M., Molybdenum-0.5 Titanium Alloy, Universal-Cyclops Steel Corporation, Bridgeville, Pennsylvania.

56. Pohlman, M. A., René 41, Cannon-Muskegon Corporation, P. O. Box 506, Muskegon, Michigan.

57. Michael, A. B., Tungsten, Fansteel Metallurgical Corp., North Chicago, Illinois.

58. Lewis, W. J., Metals Joining Division, Battelle Memorial Institute, 505 King Avenue, Columbus 1, Ohio.

59. Ludwigson, David C., AM-355 Steel, Battelle Memorial Institute, 505 King Avenue, Columbus 1, Ohio.

60. MacLeary, Donald L., Columbium (D-31) Alloy, Metal Products, E. I. du Pont de Nemours and Company, Pigments Department, Wilmington 98, Delaware.

61. Lund, Carl H., René 41 and Inconel X-750, Battelle Memorial Institute, 505 King Avenue, Columbus 1, Ohio.

62. Wrobleski, Paul A., René 41, Speciality Alloys Section, General Electric Company, Metallurgical Products Department, Box 237, R. P. A. Detroit 32, Michigan.

63. Wall, Robert W., Molybdenum-0.5 Titanium Alloy, Refractory Metals Section, National Aeronautics and Space Administration, Lewis Research Center, 21000 Brookpark Road, Cleveland 35, Ohio.

64. Freeman, Robert R., Molybdenum-0.5 Titanium Alloy, Refractory Metal Division, Climax Molybdenum Company of Michigan, 1270 Avenue of the Americas, New York 20, New York.

65. Semchyshen, M., Molybdenum-0.5 Titanium Alloy, Metallurgical Section, Climax Molybdenum Company, 14410 Woodrow Wilson, Detroit 38, Michigan.

66. Ingram, Albert C., Molybdenum-0.5 Titanium Alloy, Tungsten, and Columbium (D-31) Alloy, Battelle Memorial Institute, 505 King Avenue, Columbus 1, Ohio.

67. Kubaschewski, O. and Hopkins, B. E., Oxidation of Metals and Alloys, Butterworth Scientific Publications, London, 1953.

68. Gurklis, J. A. and McGraw, L. D., "Pickling and Descaling of High-Strength, High-Temperature Metals and Alloys." DMIC Memorandum 85, Defense Metals Information Center, Battelle Memorial Institute, Columbus, Ohio, 1961 (February).

69. Jones, J. Byron, Maropis, N., Thomas, J. G., and Bancroft, D., "Fundamentals of Ultrasonic Welding, Phase I, RR-59-105, Final Report on Navy Contract NOas-58-108-c, 1959, (May). Available from OTS as PB 161677.

70. Jones, J. Byron, Maropis, N., Thomas, J. G., and Bancroft, D., "Fundamentals of Ultrasonic Welding, Phase II, RR-60-89, Final Report on Navy Contract NOas-59-6070-c, 1960 (August).

71. McKaig, H. L., and Jones, J. B., RR-60-94, Final Report on Navy Contract NOrd-18779(FBM), 1960 (July).

72. Jones, J. B., et.al., "Investigation of the Ultrasonic Weldability of Beryllium Metal Sheet," RR-61-68, Final Report on Contract No. AF 33(616)-7065, 1961.

73. Jones, J. B. and Barrett, L. D., "Ultrasonic Welding of Aluminum Alloys for Missile Use", Final Report RR-59-100, Contract No. DA-36-034-ORD-2424, 1959, (August).

74. Gretter, R. and Wilks, L., "Research Investigation of Magnetostrictive Techniques for Obtaining High Frequency Vibrations", WADC Tech. Report 54-382, 1954, (June).

75. Heuter, T., and R. H. Bolt, Sonics, J. Wiley & Sons, 1955.

76. Mason, W. P., Piezoelectric Crystals and Their Application to Ultrasonics, D. Van Nostrand Co., 1950.

77. Am. Inst. of Physics, Physics Handbook, McGraw-Hill, N. Y., 1957.

78. Crawford, A. E., Ultrasonic Engineering, Academic Press Inc., London, 1955.

79. "The Design and Constriction of Magnetostriction Transducers", National Defense Research Committee, Summary Tech. Report of Div. 6, 13, 1946.

80. Berlincourt, D., Jaffe, B., Jaffe, H., and Krueger, H. H. A., "Transducer Properties of Lead Titanate Zirconate Ceramics", IRE Transactions, UE7, No. 1, 1960, (February).

81. Oshry, H. I. and Oshry, J. M., "Physical Properties of Piezoelectric Ceramics", RP 30004, 1953.

82. Whymark, R. R., "Magnetostrictive Transducers with Mechanical Loads", Acoustica, 6, No. 3, 1956.

83. Dobelli, A. C., "Piezoelectric Transducers", Acoustica, 6, 1956.

84. Nachman and Buehler, Naval Ordnance Laboratory, Tech. Report Navord 4130.

85. Davis and Ferebee, Naval Ordnance Laboratory, Tech. Report Navord 3947.

86. "Design of Nickel Magnetostrictive Transducer", International Nickel Co., Technical Publication, 1955.

87. Klingsberg, Sy, Office of Naval Research, Washington, D. C.

88. Casavant, Raymond A., Munitions Building Bureau of Naval Weapons, Washington, D. C.

89. Rabun, E. D., Munitions Building, Bureau of Naval Weapons, Washington, D. C.

90. Arndt, J. P., Clevite Electronics Components, Div. Clevite Corporation, 232 Forbes Road, Bedford, Ohio.

91. Kullin, Mel, Clevite Electronics Components, Div. Clevite Corporation, 232 Forbes Road, Bedford, Ohio.

92. Belford, John F., Clevite Electronics Components, Div. Clevite Corporation, 232 Forbes Road, Bedford, Ohio.

93. Salzberg, L. F., Directorate of Materials and Processes, Wright-Patterson Air Force Base, Ohio.

94. Cooke, Isadore, Bureau of Ships, Washington 25, D. C.

95. Berlincourt, D. A., Electronic Research Division, Clevite Corporation, 540 East 105th Street, Cleveland 8, Ohio.

96. Marin, Joseph, Dept. of Engineering Mechanics, Pennsylvania State University, University Park, Pennsylvania.

97. Huggins, Robert, Dept. of Metallurgical Engineering, Stanford University, Stanford, California.

98. Lazan, B. J., Dept. of Aeronautics and Engineering Mechanics, University of Minnesota, Minneapolis, Minnesota.

99. Nowick, A. S. and Berry, B. S., International Business Machines Corp., Research Center, P. O. Box 218, Yorktown Heights, New York.

100. Manson, S. S. and Stearns, C. A., NASA, Lewis Research Center, 21000 Brook Park Road, Cleveland 35, Ohio.

101. Mason, Warren P., Bell Telephone Laboratories, Inc., Murray Hill, New Jersey.

102. Sack, H. S., Dept. of Engineering Physics, Cornell University, Ithica, New York.

103. Mebs, Russell W., Metallurgy Division, National Bureau of Standards, Dept. of Commerce, Washington 25, D. C.

104. Truell, Rohn, Division of Applied Mathematics, Brown University, Providence, Rhode Island.

105. Maringer, Robert E., Battelle Memorial Institute, 505 King Avenue, Columbus 1, Ohio.

106. Duwez, Pol Edgard, California Technical Institute, 1201 E. California St., Pasadena 4, California.

107. Promisel, N. E., Bureau of Naval Weapons, Department of the Navy, Washington 25, D. C.

108. Harwood, Julius, Metallurgical Research Division, Ford Motor Company, American Road, Dearborn, Michigan.

109. Office of Naval Research, Washington 25, D. C.

110. American Society for Metals, Metals Park, Novelty, Ohio.

111. Mason, W. P., "Internal Friction, Plastic Strain, and Fatigue in Metals and Semiconductors", Symposium on Basic Mechanism of Fatigue, 36-50, ASTM Annual Meeting, Boston, Mass., 1958 (June).

112. Lazan, B. J., "Fatigue Under Resonant Vibrations Considering Both Material and Slip Damping." University of Minnesota, Minneapolis, Minn.

113. Barker, J. F., et al, "Astroloy - A Superalloy for 1900°F Use", Metal Progress, 77, 1960 (December).

114. Mason, W. P., Physical Acoustics and the Properties of Solids, D. Van Nostrand Company, New York, 1958.

115. Castings and Forgings, Philadelphia Bronze and Brass Corp., Philadelphia, Pa.

116. Ampco Alloy Specification, Ampco Metals, Inc., Milwaukee 46, Wisc.

117. "The Machining of Ampco Metal", Ampco Metals, Inc., Bulletin 66b, Milwaukee, Wisc.

118. Aluminum Bronze, Heat No. 33647, Philadelphia Bronze & Brass Corporation, Order No. 3169, Special No. 4040, July, 1961.

119. Beryllium Copper, General Copper and Brass Company, Philadelphia, Pa., Order No. 17368, November, 1961.

120. Inconel X-750, Somers Brass Co., Inc., Order No. P-5472, Waterbury, Connecticut, August, 1961.

121. "Brazing and Soldering Nickel and High-Nickel Alloys", International Nickel Co., Tech. Bulletin T-34.

122. "Inconel X: Age-Hardenable Nickel Chromium Alloy", International Nickel Co., Tech. Bulletin T-38.

123. K Monel, Heat No. M-8819K, Whitehead Metals Inc., Cambridge, Mass., Order No. PH-02318, August, 1961.

124. "Engineering Properties of K Monel and R Monel", International Nickel Co., Tech. Bulletin T-9.

125. Camp, J. M. and Francis, C. B., Carnegie Illinois Steel Corp., The Making, Shaping, and Treating of Steel, Fifth Ed., Pittsburgh, Pa.

126. Titanium(6Al-4V), Heat M-9422, Titanium Metals Corp. of America, Invoice No. 511808, August, 1961.

127. Titanium Engineering Bulletin No. 1, Titanium Metals Corp. of America, New York 7, N. Y.

128. Randall, R. H., An Introduction to Acoustics, Addison Wesley Press, Inc., 1951.

129. "Applications of Ultrasonic Energy", NYO-9588, Aeroprojects Incorporated, First Quarterly Report on Task 5 of AEC Contract AT(30-1)-1836, 1961, (February).

130. Kolsky, H., Stress Waves in Solids, Oxford Press, 1953.

131. Von Heydekampf, Part 2-157 of Proc. of ASTM, 1931.

132. Hanstock, R. F., and A. Murray, "Damping Capacity and the Fatigue of Metals", J. Inst. Metals (London), 72, 97, 1946.

133. Thompson, N., Wadsworth, N., and Lociat, N., "The Origin of Fatigue Fracture in Copper", Philosophical Mag., 1, Serial 8, 113, 1956.

134. Neppiras, E. A., "Techniques and Equipment for Fatigue Testing at Very High Frequencies." Proceedings of the American Society for Testing Materials, 59, 691-709, 1959.

135. Balamuth, L., "Mechanical Impedance Transformers in Relation to Ultrasonic Machining", 47th Meeting, Acoustical Society of America, June, 1954.

136. Rayleigh, Lord, Theory of Sound, 1, Dover Publications.

137. Lamb, Horace, The Dynamical Theory of Sound, Edward Arnold, London, 1910.

138. Love, A. E. H., "A Treatise on the Mathematical Theory of Elasticity," Dover Publications, New York, 1944.

DISTRIBUTION LIST

1 Accoustica Associates, Inc.
Attn: R. J. Hurley, General Manager
10400 Aviation Boulevard
Los Angeles 45, California

2 Aerojet-General Corp.
Attn: Kenneth F. Mundt, Vice Pres. Mfg.
6352 Irwindale Avenue
Azusa, California

1 Aeronca Mfg. Corp.
Attn: L. C. Wolfe, Chief Engineer
1712 Germantown Road
Middletown, Ohio

1 AiResearch Manufacturing Co.
Attn: Chief Engineer
4851 Sepulveda Blvd.
Los Angeles 45, California

1 American Machine & Foundry Co.
Government Products Group
Alexandria Division
Attn: J. D. Graves, General Manager
1025 North Royal St.
Alexandria, Virginia

1 Armour Research Foundation
Illinois Institute of Technology
Technology Center
Attn: Director, Metals
10 West 35th Street
Chicago 16, Illinois

1 Avco Corporation
Nashville Division
Attn: Mr. W. F. Knowe, Mgr. Design Eng.
Nashville 1, Tennessee

1 Avco Corporation
Nashville Division
Attn: Mr. F. A. Truden, Mfg. Dev.
Nashville 1, Tennessee

1 Avco Corporation
Research and Advanced Development Division
Attn: Director of Research
Wilmington, Massachusetts

1 Beech Aircraft Corp.
Attn: Mr. E. Utter, Chief Structures
Wichita 1, Kansas

1 Bell Aerosystems Company
Attn: R. W. Varrial, Manager
Production Engineering
P. O. Box 1
Buffalo 5, New York

1 B. M. Harrison Electrosonics, Inc.
Attn: Bertram M. Harrison, President
80 Winchester Street
Newton Highlands 61, Massachusetts

1 Bendix Products Division
Missiles Department
Attn: Chief, Airframe Design Group
400 S. Reiger St.
Mishawaka, Indiana

2 Boeing Company
Attn: Boyd K. Bucey, Asst to Vice Pres-Mfg.
P. O. Box 3707
Seattle 24, Washington

2 Boeing Company
Attn: C. C. Lacy, Manager
Research & Development
Aero-Space Division
P. O. Box 3707
Seattle 24, Washington

1 Boeing Company
Attn: Fred P. Laudan, Vice Pres.
Manufacturing-Headquarters Office
P. O. Box 3707
Seattle 24, Washington

1 Boeing Company
Wichita Division
Attn: W. W. Rutledge, Mfg. Mgr.
Wichita, Kansas

1 Cessna Aircraft Company
Attn: R. L. Lair, Vice Pres & Gen Mgr
Prospect Plant
Wichita, Kansas

1 Chesapeake Instrument Corporation
Attn: Director, Research & Developent
Shadyside, Maryland

1 Chrysler Missile Division
Chrysler Corporation
Attn: Chief Design Engineer
P. O. Box 1919
Detroit 31, Michigan

1 Circo Ultrasonic Corporation
Attn: Benson Carlin, Vice President
51 Terminal Avenue
Clark, New Jersey

1 Convair Division of General Dynamics Corp
Attn: R. K. May, Chief, Mfg Res & Dev Engrg
P. O. Box 5907
Fort Worth, Texas

1 Convair Div. of General Dynamics Corp
Attn: A. T. Seeman, Chief of Mfg-Engr.
P. O. Box 1011
Pamona, California

1 Convair (Astronautics) Division
General Dynamics Corporation
Attn: J. H. Famme, Dir. of Mfg. Dev.
P. O. Box 1128 (Zone 20-00
San Diego 12, California

1 Curtiss-Wright Corp.
Propeller Division
Attn: J. H. Sheets, Works Manager
Fairfield Road
Caldwell, New Jersey

1 Curtiss-Wright Corp.
Attn: H. Hanink, New Process Mfg.
Woodridge, New Jersey

1 Douglas Aircraft Co., Inc.
Attn: C. B. Perry, Plant Supv.
3855 Lakewood Boulevard
Long Beach 8, California

1 Douglas Aircraft Co., Inc.
Attn: C. H. Shappell, Works Mgr.
3000 Ocean Park Blvd.
Santa Monica, California

2 Douglas Aircraft Co., Inc.
Attn: J. L. Jones, Vice Pres, Gen. Mgr.
2000 N. Memorial Drive
Tulsa, Oklahoma

1 Fairchild Aircraft & Missile Div.
Fairchild Engine & Airplane Corp.
Attn: E. E. Morton, Mfg. Technical Analysi
Hagerstown, Maryland

1 General Electric Company
Attn: Manufacturing Engineering Res Lab.
Cincinnati 15, Ohio

1 General Motors Corp.
Allison Division
Attn: N. F. Bratkovich, Supv. Joining Processes
P. O. Box 894
Indianapolis 6, Indiana

1 Gulton Industries, Inc.
Attn: Walter Welkowitz
Director, Research & Development
212 Durham Avenue
Metchen, New Jersey

1 Harris ASW Division
General Instrument Corp.
Attn: Frank David, Chief Engineer
33 Southwest Park
Westwood, Massachusetts

2 Lockheed Aircraft Corp
California Division
Attn: J. B. Wassall, Dir. of Engineering
Burbank, California

1 Lockheed Aircraft Corp.
Missiles and Space Division
Attn: Mr. Don McAndrews
Supv. Manufacturing Research
P. O. Box 504
Sunnyvale, California

2 McDonnell Aircraft Corp.
Attn: E. G. Szabo, Mgr. Production Eng.
Lambert-St. Louis Municipal Airport
P. O. Box 516
St. Louis 3, Missouri

1 Marquardt Aircraft Co.
Attn: J. M. Norris, Factory Mgr.
Box 670
Ogden, Utah

1 Marquardt Aircraft Co.
Attn: John S. Liefeld, Dir. of Mfg.
16555 Saticoy Street
Van Nuys, Calif.

1 The Martin Company
Attn: Chief Engineer
P. O. Box 179
Baltimore 3, Maryland

1 The Martin Company
Attn: Chief Librarian, Eng. Lib.
Baltimore 3, Maryland

1 The Martin Company
Attn: L. J. Lippy, Dir. Fabrication Div
Denver, Colorado

1 North American Aviation, Inc.
Attn: Chief Engineer
Port Columbus Airport
Columbus 16, Ohio

1 North American Aviation, Inc.
Attn: Latham Pollock, Gen. Supv. Mfg. Eng
International Airport
Los Angeles 45, Calif.

1 Northrop Aircraft, Inc.
Attn: R. R. Nolan, Vice Pres. Mfg.
1001 E. Broadway
Hawthorne, Calif.

1 Northrop Aircraft, Inc.
Norair Division
Attn: Ludwig Roth, Dir., Research Engineering Department
1001 E. Broadway
Hawthorne, California

1 Pratt & Whitney Aircraft Div.
United Aircraft Corporation
Attn: L. M. Raring
Chief, Metallurgical & Chemical Lab
P. O. Box 611
Middletown, Conn.

1 Republic Aviation Corp.
Attn: Adolph Kastekowits, Chief Mfg. Engr.
Farmingdale, Long Island, New York

2 Commanding General
Redstone Arsenal
Rocket & Guided Missile Agency
Attn: Chief, Space Flight Structure Design
Redstone Arsenal, Alabama

1 Rocketdyne Division
North American Aviation, Inc.
Attn: R. J. Thompson, Jr., Dir. Research
6633 Canoga Avenue
Canoga Park, Calif.

1 Rocketdyne Division
North American Aviation, Inc.
Attn: Mr. J. P. McNamara, Plant Mgr.
P. O. Box 511
Neosho, Missouri

1 Rohr Aircraft Corporation
Attn: Chief Structures Engr.
P. O. Box 878
Chula Vista, Calif.

1 Rohr Aircraft Corp.
Attn: Burt F. Raynes, Vice Pres. Mfg.
P. O. Box 878
Chula Vista, Calif.

1 Ryan Aeronautical Company
Attn: Robert L. Clark, Mfg. Works Mgr.
Lindbergh Field
San Diego, California

1 Sciaky Bros., Inc.
4915 W. 57th Street
Chicago 38, Illinois

10 Armed Services Technical Info. Agency
Attn: Document Service Center (TICSCP)
Arlington Hall Station
Arlington 12, Virginia

6 & 1 repro Aeronautical Systems Division
Attn: Manufacturing Technology Lab(ASRCT)
Wright-Patterson Air Force Base, Ohio

1 Air Force Systems Command
Attn: Mr. C. W. Kniffin (RDRAE-F)
Andrews Air Force Base, Maryland

1 Aeronautical Systems Division
Attn: ASRKCB
Wright-Patterson Air Force Base, Ohio

2 Aeronautical Systems Division
Attn: Metals & Ceramics Lab (ASRCM)
Wright-Patterson Air Force Base, Ohio

1 Aeronautical Systems Division
Attn: Applications Lab (ASRCE, Mr. Teres)
Wright-Patterson Air Force Base, Ohio

2 Aeronautical Systems Division
Attn: Flight Dynamics Lab
Structures Branch (ASRMDS)
Wright-Patterson Air Force Base, Ohio

1 Battelle Memorial Institute
Defense Metals Information
Attn: Mr. C. S. Dumont
505 King Ave.
Columbus, Ohio

1 Ballistic Missile Systems Division
Attn: Industrial Resources
P. O. Box 262
AF Unit Post Office
Inglewood, Calif.

1 Chief, Bureau of Naval Weapons (PID-2)
Department of the Navy
Washington 25, D. C.

1 Frankford Arsenal
Research Institute, 1010 (110-1)
Attn: Mr. E. R. Rechel, Deputy Director
Philadelphia 37, Pa.

1 Solar Aircraft Company
Attn: Engineering Library
2200 Pacific Highway
San Diego, California

1 Temco Aircraft Corp.
Attn: D. T. Brooks, Mfg. Mgr.
P. O. Box 6191
Dallas, Texas

1 Southwest Research Institute
Attn: Glenn Damewood, Dir. A
8500 Culebra Road Dep
San Antonio 6, Texas

1 Union Ultra-sonics Corporatio
Attn: John Zotos, Chief Proj
111 Penn Street
Quincy 69, Massachusetts

1 Vought Aeronautics Division
Chance-Vought Aircraft, Inc.
Attn: George Gasper, Mfg. Eng
P. O. Box 5909
Dallas, Texas

1 Vought Aeronautics Division
Chance-Vought Aircraft, Inc.
Attn: Chief Librarian, Eng. Libr
Dallas, Texas

1 Vought Aeronautics Division
Chance-Vought Aircraft, Inc.
Attn: J. A. Millsap, Chief Engr.
Manufacturing Research Dev
P. O. Box 5907
Dallas, Texas

1 G. C. Marshall Space Flight Cente
National Aeronautics & Space Admin
Attn: William A. Wilson,
Chief, MR & D Branch
Huntsville, Alabama

2 Langley Research Center
National Aeronautics & Space Admin
Attn: Technical Director
Langley, Virginia